ISSN 1881-7815 Online ISSN 1881-7823

BST BioScience Trends

Volume 8, Number 1
February, 2014

IRCA BSSA

IACMHR

www.biosciencetrends.com

BST
BioScience Trends

ISSN: 1881-7815
Online ISSN: 1881-7823
CODEN: BTIRCZ
Issues/Year: 6
Language: English
Publisher: IACMHR Co., Ltd.

BioScience Trends is one of a series of peer-reviewed journals of the International Research and Cooperation Association for Bio & Socio-Sciences Advancement (IRCA-BSSA) Group and is published bimonthly by the International Advancement Center for Medicine & Health Research Co., Ltd. (IACMHR Co., Ltd.) and supported by the IRCA-BSSA and Shandong University China-Japan Cooperation Center for Drug Discovery & Screening (SDU-DDSC).

BioScience Trends devotes to publishing the latest and most exciting advances in scientific research. Articles cover fields of life science such as biochemistry, molecular biology, clinical research, public health, medical care system, and social science in order to encourage cooperation and exchange among scientists and clinical researchers.

BioScience Trends publishes Original Articles, Brief Reports, Reviews, Policy Forum articles, Case Reports, News, and Letters on all aspects of the field of life science. All contributions should seek to promote international collaboration.

Editorial Board

Editorial Office

Pearl City Koishikawa 603,
2-4-5 Kasuga, Bunkyo-ku,
Tokyo 112-0003, Japan
Tel: +81-3-5840-8764
Fax: +81-3-5840-8765
E-mail: office@biosciencetrends.com

BioScience Trends

Editorial and Head Office

Pearl City Koishikawa 603, 2-4-5 Kasuga, Bunkyo-ku,
Tokyo 112-0003, Japan

Tel: +81-3-5840-8764, Fax: +81-3-5840-8765
E-mail: office@biosciencetrends.com
URL: www.biosciencetrends.com

Editorial Board Members

CONTENTS

Volume 8, Number 1, 2014

Reviews

Original Articles

CONTENTS (*Continued*)

Case Report

Guide for Authors

Copyright

Review

DOI: 10.5582/bst.8.1

Transient receptor potential (TRP) channels, promising potential diagnostic and therapeutic tools for cancer

Jianpeng Chen[1,*], Yi Luan[2,*], Ruofei Yu[3], Zheng Zhang[1], Jinbiao Zhang[4,], Weibo Wang[1,**]**

[1] *Department of Oncology, Provincial Hospital Affiliated with Shandong University, Ji'nan, Shandong, China;*
[2] *Center for Disease Control, Ji'nan Command of the People's Liberation Army, Ji'nan, Shandong, China;*
[3] *Department of Oncology, Nanfang Hospital, Southern Medical University, Guangzhou, Guangdong, China;*
[4] *Department of Oncology, the 148th Hospital of the People's Liberation Army, Zibo, Shandong, China.*

Summary **Despite the advances in detection of and therapies for various tumors, high rates of treatment failure and mortality still exist throughout the world. These high rates are mainly due to the powerful capability of tumor cells to proliferate and migrate. Recent studies regarding the transient receptor potential (TRP) have indicated that TRP channels are associated with tumors and that TRP channels might represent potential targets for cancer treatment. TRP channels are important calcium-selective ion channels in many different tissues and cell types in mammals and are crucial regulators of calcium and sodium. TRP were first discovered in the photoreceptors of Drosophila with gene defects or mutations. TRP channels can be divided into seven subfamilies: TRPC (canonical), TRPV (vanilloid), TRPM (melastatin), TRPML (mucolipin), TRPP (polycystin), TRPA (ankyrin transmembrane protein), and TRPN (NomPC-like). TRPC proteins are conserved across organisms since they are most homologous to Drosophila TRP. TRP superfamilies have been linked to many physiological and pathological functions, including cell differentiation, proliferation, apoptosis, and ion homeostasis. This review focuses on the properties of TRP in oncogenesis, cancer proliferation, and cell migration.**

Keywords: Ion channels, transient receptor potential (TRP), cancer, proliferation, migration

1. Introduction

Most of life's activities cannot function properly without ion channels (*1*). Likewise, many studies have found that tumor proliferation, invasion, and metastasis are always accompanied by changes in ion channels, and particularly changes in the expression of transient receptor potential (TRP) channels. TRP channels are Ca^{2+} entry channels. They are ubiquitously expressed in a wide variety of tissues and have an extraordinarily diverse set of functions. Tumor formation and metastasis are complex processes involving multiple genes and multiple steps, including oncogenesis, basement membrane degradation, matrix permeability, cell adhesion, and vessel formation. During these processes, many genetic alterations induce changes in TRP channels expression, and the abnormal expression of these channels may promote the growth, proliferation, and metastasis of tumor cells (*2*). A growing amount of evidence from both *in vitro* and *in vivo* studies has implicated TRP channels in these processes. For example, TRPM8 is highly expressed in prostate cancer (*3*) and TRPM7 channels influence the growth and proliferation of head and neck tumor cells (*4*).

2. TRP

TRP genes were first described in *Drosophila melanogaster* in studies related to the fruit fly's visual system, but the genes were not recognized until Montell and Rubin's work in 1989 (*5*). As their research progressed, TRP channels were further understood, but the original study did not go far enough. About thirty TRP channels have currently been identified, and they are grouped into seven main

* Both contributed equally to this work.
***Address correspondence to:*
Dr. Jinbiao Zhang, Department of Oncology, the 148th Hospital of the People's Liberation Army, Zibo, 255300, China.
E-mail: 1018426999@qq.com
Dr. Weibo Wang, Department of Oncology, Provincial Hospital Affiliated with Shandong University, Ji'nan, 250021, China.
E-mail: wbwb1620@163.com

subfamilies depending on their homology and channel function: TRPC (canonical), TRPV (vanilloid), TRPM (melastatin), TRPML (mucolipin), TRPP (polycystin), TRPA (ankyrin transmembrane protein), and TRPN (NomPC-like). With the exception of TRPN proteins, the other TRP proteins have been detected in mammals; TRPN proteins have been detected in fruit flies and zebra fish (*6,7*). According to in silico sequence analysis, all of the TRP proteins contain six transmembrane segments (S1-S6) and a pore-forming loop between segments S5 and S6. The major differences between TRP channel subfamilies are found in the N- and C-terminal cytosolic domains, which contain putative protein interaction and regulatory motifs (*8*) (Figure 1). Most TRP channels are non-selective cation channels, and they are widely expressed in almost all tissues and cell types. These channels also perform various functions, including taste transduction, temperature sensation, muscle contraction, and cell death (*9,10*).

3. TRP channels and cancer

TRP channels are increasingly recognized as playing roles in the growth, proliferation, migration, and invasion of cancer cells (Table 1 and Figure 2).

3.1. *TRP channels and lung cancer*

Of all cancers, lung cancer has the highest mortality rate. It is a major public health problem and causes death worldwide. More than 1.3 million new lung cancer cases and over one million deaths due to lung cancer occur every year (*11*). In 2013, the US had approximately 228,190 new lung cancer cases and approximately 159,480 deaths due to lung cancer-related disease (*12*). The median survival time for patients with advanced lung cancer is only 8-12 months (*13,14*). Invasion, metastasis, and recurrence are common biological characteristics of lung cancer, and they are also the major obstacles hampering therapeutic interventions and prognosis.

Recent studies have implicated TRPC1, TRPC3, TRPC4, TRPC6, TRPM7, and TRPM8 as playing a role in lung cancer.

TRPC1 regulates cell proliferation and migration. In non-small cell lung cancer cell lines, siRNA-mediated TRPC1 depletion inhibits cell proliferation and induces G_0/G_1 cell cycle arrest, resulting in a dramatic decrease in cell growth. TRPC1 might mediate these processes *via* epidermal growth factor receptor (EGFR) phosphorylation and the activation of EGF-induced signaling pathways (*15*). Jiang *et al.* found that the expression of TRPC1, TRPC3, TRPC4, and TRPC6 was correlated with the grade of NSCLC differentiation; no correlation was observed between TRP channel expression and age, sex, smoking history, or cell type. The blocking of TRPC channels inhibited A549 cell proliferation, while over-expression of TRPCs led to increased proliferation. Additionally, all-trans-retinoic acid (ATRA) induced the up-regulation of TRPC3,

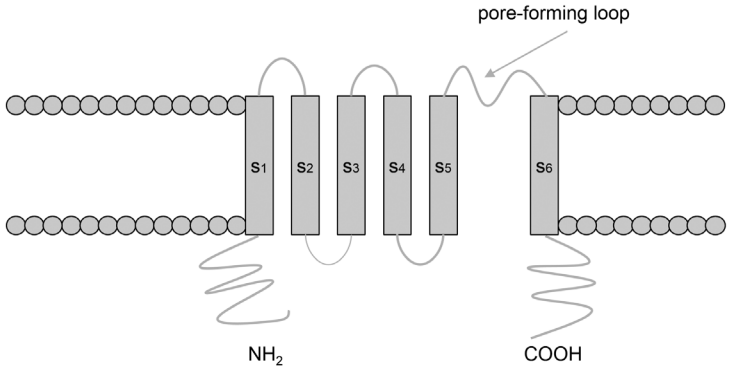

Figure 1. TRP channels contain six transmembrane segments and a pore-forming loop between S5 and S6.

Table 1. TRP channels involved in cancer proliferation and migration

Cancer	Proliferation		Migration		*Ref.*
	Positive correlation	Negative correlation	Positive correlation	Negative correlation	
Lung cancer	TRPC1,C4,C6	--	TRPC1,M7	--	*15-20*
Breast cancer	TRPC1,C3,C6,V6,M7,M8	--	TRPM7,V6	--	*22-31*
Prostate cancer	TRPM8,V2,V6,M2,C6	--	TRPM8,V1,V2	--	*3,33-46*
Ovarian cancer	TRPC1,C3,C4,C6	--	--	--	*48-49*
Gastric cancer	TRPC6,M7,V6	--	--	--	*53-57*
Liver cancer	TRPC1,C3,C6,M4,M7	--	TRPV1,V4	--	*60-64*
Nasopharyngeal cancer	TRPM7	--	TRPC1,M7	--	*4,68-70*
Glioblastoma	TRPC1,C3,C4,C5,C6	TRPV1,V2	TRPV4	--	*73-76*
Melanoma	TRPM2,M8	TRPV2,M7	--	TRPM1	*78-86*

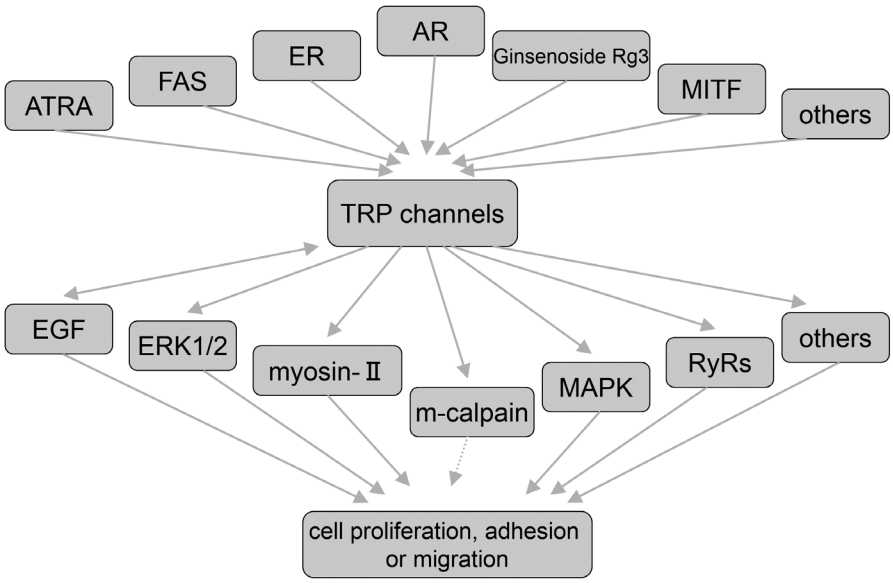

Figure 2. TRP channels mediated signal transduction pathways and cellular behaviors. ATRA can stimulate TRPC3, 4, and 6. EGF and some TRP channels may interact with each other. Stimulation of Fas receptors could induce TRPM7 to regulate apoptosis and may induce the negative control of TRPV2. ER could affect the expression of TRPM8 and TRPV6. AR changes could lead to the expression of changes in TRPM8. Ginsenoside Rg3 could block TRPM7 to induce cell death. The up-regulation or down-regulation of MITF could cause corresponding changes in TRPM1. Some TRP channels may induce cell proliferation, adhesion, or migration *via* ERK1/2, myosin-II, MAPK, RyRs, and unknown signaling pathways while other TRP channels may inhibit those processes *via* pathways such as m-calpain. ATRA, all-trans-retinoic acid; EGF, epidermal growth factor; ER, estrogen receptor; MITF, microphthalmia transcription factor; ERK1/2, extracellular signal-regulated kinases 1 and 2; MAPK, mitogenactivated protein kinase; RyRs, ryanodine receptors.

TRPC4, and TRPC6 expression and enhanced Ca^{2+} influx in A549 cells (*16*). Conversely, Saito *et al.* suggest that TRPC3 expression is related to the progression and the clinicopathological characteristics of lung cancer (*17*). The 5-year overall survival (OS) and disease-free survival (DFS) rates for patients with higher levels of TRPC3 mRNA expression are significantly higher than the rates for patients with lower levels of TRPC3 mRNA. Higher levels of TRPC3 expression in tumor cells are an independent predictor of a better prognosis for patients with lung adenocarcinoma.

In A549 lung cancer cells, the depletion of TRPM7 expression *via* RNA interference inhibited cell migration, and TRPM7 is positively correlated with EGF expression (*18*). TRPM8 is the predominant thermoceptor for cellular and behavioral responses following exposure to cold temperatures (*19*). This thermoceptor has been studied in different contexts, including breast adenocarcinoma, lung adenocarcinoma, melanoma, and prostate cancer (*20*).

3.2. *TRP channels and breast cancer*

Breast cancer is the most frequently diagnosed cancer (excluding skin cancers) and has the second highest mortality rate of all cancers, following lung cancer, in the US. An estimated 39,510 deaths were expected to occur in the US in 2012. Notably, the incidence of breast cancer has increased in developing countries; about half of the new breast cancer cases and 60% of breast cancer-associated deaths occur in developing countries (*21*).

TRPC1, TRPC3, TRPC6, TRPM7, TRPM8, and TRPV6 expression are correlated with breast cancer. Dhennin-Duthille *et al.* observed high levels of TRPC1, TRPC6, TRPM7, TRPM8, and TRPV6 expression in human breast ductal adenocarcinoma (hBDA) tissue in comparison to adjacent non-tumor tissue. A study reported that TRPC1, TRPM7, and TRPM8 expression a strongly correlated with the Scarff-Bloom-Richardson (SBR) grade, Ki67 proliferation index, and tumor size (*22*). Moreover, the activation of TRPC1 enhanced the proliferation of MCF-7 cells, a human breast cancer cell line with low metastatic potential, by stimulating phosphorylation of extracellular signal-regulated kinases 1 and 2 (ERK1/2) and Ca^{2+} entry (*23*).

Previous studies reported that TRPC3 and TRPC6 are involved in the control of the growth of polarized epithelial cells (*24*). Recently, TRPC6 was found to be expressed and to be the predominant TRPC channel in biopsied breast cancer tissue, and TRPC3 appears to be significantly up-regulated in breast cancer tissue (*25*).

The level of TRPV6 expression is higher in invasive tissue compared to corresponding non-invasive tissue and TRPV6 expression has been assessed using laser capture microdissection. TRPV6 silencing can inhibit MDA-MB-231 migration and invasion in addition to MCF-7 cell migration (*22*). Moreover, limited estrogen receptor (ER) signaling reportedly leads to lower levels of TRPV6 expression, and the antitumor effect of Tamoxifen may be related to the inhibition of TRPV6 expression (*26*).

TRPM7 plays an important role in breast cancer. TRPM7 is both an ion channel and a protein kinase that is ubiquitously expressed in various tissues; these proteins are also called "channels plus enzymes" or "chanzymes". Studies have found that the TRPM7 channel regulates breast cancer cell proliferation, and TRPM7 is over-expressed in breast carcinoma tissue and is positively correlated with the Ki67 mitosis marker (*27*). Some studies have found that TRPM7 influences cell adhesion and migration *via* the regulation of myosin-IIA filament stability and that it influences protein localization by phosphorylating the heavy chain (*28*). However, one study found that mitogen-activated protein kinase (MAPK) signaling pathways are involved in the TRPM7-mediated migration and invasion of MDA-MB-435 breast cancer cells. Silencing of TRPM7 caused a significant reduction in the migration and invasion potential of MDA-MB-435 breast cancer cells in addition to a decrease in the levels of phosphorylated Src and MAPK (*29, 30*).

TRPM8 channels are highly expressed at both the mRNA and protein levels in the MCF-7 breast cancer cell line. These channels are over-expressed in breast adenocarcinomas and are correlated with estrogen receptor positive (ER^+) tumors according to immunohistochemical analysis (*31*).

3.3. *TRP channels and prostate cancer*

Prostate cancer is the second leading cause of internal malignancy in men worldwide, and approximately 29,720 men die from the disease each year in the US (*12*). Furthermore, data indicate that prostate cancer mortality is increasing in Asia, and particularly in China and Japan (*32*).

A number of TRP channels have been implicated in prostate cancer, including TRPV1, TRPV2, TRPV6, TRPM8, TRPM2, and TRPC6. Among these, TRPV6 and TRPM8 are the most studied and characterized.

The expression of TRPV6 may be a predictor for prostate cancer progression because levels of TRPV6 mRNA and protein are both substantially elevated in prostate carcinoma compared to normal tissue or cells. Lehen *et al.* first found that Ca^{2+} entry *via* the TRPV6 channel controls proliferation directly and promotes apoptosis resistance in prostate cancer cells (*33*). TRPV6-targeted siRNA has been reported to effectively inhibit the transcription of TRPV6 mRNA, inhibit the proliferation of human prostate cancer LnCaP cells, arrest the LnCaP cell cycle in the G0 and G1 phases, and induce LnCaP apoptosis (*34*). Moreover, the expression of TRPV6 in lymph node metastases and androgen-insensitive tumors is markedly and significantly decreased in comparison to untreated tumors. Furthermore, TRPV6 expression is significantly correlated with the Gleason score, the pathological stage, and extraprostatic extensions (*35*).

Tsaveler *et al.* originally identified TRPM8 in 2001 by screening a prostate cDNA library; the gene was described as a novel prostate-specific gene with expression that increased during the transformation of prostate cancer (*20*). In normal prostate cells, there is a slight level of TRPM8 expression. In prostate cancer, however, the expression of TRPM8 increases dramatically (*36*). A similar result has been reported by Fuessel *et al.*, who analyzed multiple tumor markers in primary prostate cancers *via* quantitative real-time PCR (*37*). One potential mechanism for the action of TRPM8 in prostate carcinoma is through the inhibition of the migration of prostate cancer cells by inactivating focal adhesion kinase. Furthermore, the over-expression of TRPM8 is independent of changes in the level of androgen receptor (AR) mRNA expression (*38*). Henshall *et al.* found that the expression of TRPM8 decreased markedly following anti-androgen therapy. They also showed that TRPM8 expression decreased when prostate cancer cells became androgen-independent, supporting the hypothesis that TRPM8 is regulated by androgens (*39*). Indeed, the androgen dependence of TRPM8 expression is related to the stage of differentiation of prostate epithelial cells. Affymetrix gene chip experiments have been conducted to determine whether TRPM8 expression was correlated with the Gleason grade or the TNM stage. Results of those experiments indicated that TRPM8 mRNA expression increases with the Gleason score and TNM stage (*40*).

TRPC6 is also up-regulated in prostate cancer and is associated with the histological grade, Gleason score, and extra-prostatic cancer extension. However, there is no significant difference between androgen-independent and androgen-dependent tumors (*41*). In addition, TRPV1 and TRPV2 are up-regulated in patients with metastatic cancer (*42-44*). Levels of TRPM2 mRNA are elevated in both prostate cancer tissue and in LnCaP and PC3 cell lines (*45,46*). This suggests that these channels could play an important role in the diagnosis and treatment of prostate carcinoma.

3.4. *TRP channels and ovarian cancer*

Ovarian cancer (OC) is one of the most common gynecological cancers. It poses a great challenge because it is a heterogeneous, rapidly progressing, and highly lethal group of malignancies (*47*). According to estimates, approximately 22,240 women will be diagnosed with OC and 14,030 women will die from this disease in 2013 in the US (*12*). The etiology of OC is still poorly understood.

TRPC1, TRPC3, TRPC4, and TRPC6 channels were identified by Western blotting and immunostaining in human ovarian adenocarcinoma tissue and in ovarian adenocarcinoma-derived SKOV3 cells. In 2009, Yang *et al.* found that the protein expression of TRPC3 increased markedly in human OC tissue compared to

normal ovarian tissue (*48*). The down-regulation of TRPC3 expression in SKOV3 cells led to a reduction in proliferation, suppression of epidermal growth factor-induced Ca^{2+} influx, dephosphorylation of Cdc2 and CaMKIIα, and prolonged M phase progression in these cells. Furthermore, decreased expression of TRPC3 suppressed tumor formation when SKOV3 cells were injected into nude mice. A 2013 study by Zeng *et al.* reached similar conclusions with RT-PCR, whole-cell patch recording, Western blotting, and immunostaining (*49*). Additionally, they also found that several spliced variants of TRPC1, TRPC3, TRPC4, and TRPC6 were expressed in ovarian cancer. TRPC channel activity was blocked using 2-APB, SKF-96365, or TRPC isoform-specific functional antibodies or by transfecting cells with TRPC siRNAs; blocking of the channel significantly inhibited cancer cell proliferation. Furthermore, the level of TRPC expression is reportedly correlated with the grade of cancer differentiation, and the over-expression of *TRPC* genes could also increase ovarian cancer colony growth. An interesting fact is that the expression of *TRPC* genes in undifferentiated human ovarian cancer is significantly lower than their level in normal ovarian tissue. Further study is required to elucidate the role of TRPC channels in ovarian cancer.

3.5. *TRP channels and gastric cancer*

Gastric cancer continues to be a leading cause of cancer death worldwide (*50*). In East Asia, including South Korea, Japan, and China, the morbidity due to gastric cancer is the second highest among common cancers while and the mortality due to that cancer is the third highest among common cancers. In more than half of gastric cancer cases, cancer recurs after curative surgery, and the median survival time for these patients is only 6-9 months (*51,52*). The prognosis for these patients is poor mainly because there are limited diagnostic measures for early detection and because of the clonal hyperplasia that is characteristic of gastric cancer cells. The discovery of TRP channels may help to improve the diagnosis and treatment of gastric cancer.

TRPC6, TRPM7, and TRPV6 are the main TRP channels associated with gastric cancer. TRPC6 is not only associated with lung cancer, breast cancer, prostate cancer, and ovarian cancer as mentioned earlier, but it also over-expressed in gastric cancer epithelial cells compared to normal gastric epithelial cells. When the TRPC6 channel was inhibited with SKF96365, the growth of gastric cancer cells was suppressed and cells were arrested in the G2/M phase. Cai *et al.* found that the histamine-mediated Ca^{2+} elevation in MKN45 human gastric cells was inhibited by SKF96365 and DNC6, and that inhibition of TRPC6 suppressed the formation of gastric tumors in nude mice (*53*).

The activation of TRPM7 is associated with the growth and survival of human gastric adenocarcinoma cells. Kim *et al*. examined the expression and potential role of TRPM7 channels in the growth and survival of AGS cells, the most commonly used line of human gastric adenocarcinoma cells (*54*). Abundant expression of TRPM7 messenger RNA and protein were observed in AGS gastric cancer cells. Transfection of AGS cells with TRPM7 siRNA significantly reduced the expression of TRPM7 mRNA and protein levels as well as the amplitude of the TRPM7-like currents. Blocking of TRPM7 channels with La^{3+} and 2-APB or suppression of TRPM7 expression with siRNA inhibited the growth and survival of these cells. Kim *et al*. later found that TRPM7 channels are over-expressed in HEK 293 cells undergoing Rg3-induced cell death. Ginsenoside Rg3 inhibits the growth and survival of gastric cancer cells, which occurs due to the blocking of TRPM7 channel activity (*55,56*).

Moreover, the up-regulation of TRPV6 levels has been observed in gastric cancer cells. Over-expression of TRPV6 in normal cells increased capsaicin-induced apoptosis, and knockdown of TRPV6 in cancer cells suppressed this activity (*57*).

3.6. *TRP channels and liver cancer*

Liver cancer (696,000 deaths, 9.2% of all cancer deaths) is the third most common cause of cancer death after lung cancer (1.38 million, 18.2% of all cancer deaths) and gastric cancer (738,000 deaths, 9.7% of all cancer deaths) worldwide (*58*). There are two common types of cancer affecting the liver, hepatocellular carcinoma (HCC) and liver metastases from colorectal cancer (LM-CRC). Liver cancer greatly impacts people's health, and this is particularly true in China (approximately 350,000 incident cases per year) (*59*).

Numerous studies have shown that several TRP channels are present in liver cancer tissue, including TRPC1, TRPC3, TRPC6, TRPV1, TRPV2, TRPV4, TRPM4, and TRPM7.

TRPC1, TRPC3, TRPC6, TRPM4, and TRPM7 mRNAs are expressed in both rat hepatocytes and in H4-IIE cells (derived from rat liver tumor cells); immunofluorescence was used to directly compare these cells to hepatocytes isolated from normal rat liver (*60*). TRPC6 is very weakly expressed in hepatocytes isolated from healthy patients and is expressed at much higher levels in human liver tumor tissue. Over-expressing TRPC6 or silencing TRPC6 *via* siRNA revealed that increased expression of TRPC6 is associated with increased thapsigargin-initiated Ca^{2+} entry and an increased rate of cell proliferation (*61*).

TRPV1 and TRPV4 are reported to be involved in modulating cell migration (*62*). In addition, high levels of TRPV1 expression have been noted in hepatocarcinoma tissue in comparison to normal liver tissue. Clinicopathologic examination indicated a

significant correlation between TRPV1 expression and histopathologic differentiation. Moreover, univariate analysis revealed that low levels of TRPV1 expression were associated with increased disease-free survival (*63*).

Quantitative PCR, Western blotting, and immunofluorescence analyses revealed increased levels of TRPV2 mRNA and protein expression in moderately and well-differentiated human hepatocarcinoma tissues compared to poorly differentiated tumors. Clinicopathologic assessment suggested a significant association between TRPV2 expression and portal vein invasion and histopathologic differentiation (*64*).

3.7. *TRP channels and nasopharyngeal carcinoma*

Compared to the malignant cancers mentioned earlier, nasopharyngeal carcinoma (NPC) is a rare malignancy in most parts of the world. However, the incidence of NPC is relatively high in Asian countries, and China accounts for almost 80% of all NPC cases. An annual incidence of more than 20 cases per 100,000 has been reported in southern China. Men are twice as likely to develop NPC as women (*65*). NPC is a confusing, misdiagnosed, and poorly understood disease. Radiotherapy is a primary treatment for nasopharyngeal carcinoma and has significantly improved clinical outcomes. The median survival time for patients receiving radiotherapy is approximately 52 months, and the 5-year survival rate is 50-80% (*66,67*). Although many patients with NPC had a good clinical prognosis, some still died of recurrence or metastatic disease. Furthermore, related risk factors play an important role during the development of the tumor type.

TRPM7 warrants mention when considered the relationship between NPC and TRP channels. TRPM7 is a bifunctional protein consisting of a Ca^{2+} and Mg^{2+} permeable TRP channel that is fused to a C-terminal α-kinase domain, and this channel plays an important role in regulating cell adhesion and directional migration. A pro-migratory role of TRPM7 was noted in NPC cells, in which impaired TRPM7 channel function significantly reduced cellular migratory potential. Conversely, increased TRPM7 activity promoted migration. Moreover, activation of TRPM7 resulted in a global increase in $[Ca^{2+}]_i$ (intracellular calcium influx) due to both Ca^{2+} entry and calcium-induced calcium release (CICR) involving ryanodine receptors (RyRs) (*68*).

Jiang *et al.* studied TRPM7 expression in the FaDu and SCC25 human head and neck tumor cell lines (*69*). They suggested that activation of the TRPM7 channel was critical to the growth and proliferation of human head and neck carcinoma cells. Additionally, low levels of extracellular Ca^{2+} induced the TRPM7 current, which was inhibited by Gd^{3+}, 2-APB, or intracellular Mg^{2+}.

Recently, the current authors have provided evidence demonstrating that TRPM7 plays a role in NPC cell migration by mediating Ca^{2+} influx. This role of TRPM7 in potential migration was examined in 5-8F and 6-10B human nasopharyngeal carcinoma cells using RT-PCR, Western blotting, immunofluorescence, calcium imaging, siRNA silencing, and a transwell chamber migration assay. The migratory potential of 5-8F cells was significantly reduced by the addition of an extracellular Ca^{2+} chelator (EGTA), TRPM7 inhibitors (La^{3+} and 2-APB), and TRPM7 knockdown. Conversely, addition of a TRPM7 activator (Bradykinin) and overexpression of TRPM7 promoted the migration of 5-8F and 6-10B cells. Furthermore, the sustained Ca^{2+} influx regulated by TRPM7 activated release of Ca^{2+} stores *via* RyRs and a calcium-induced mechanism of calcium release (*4*).

In addition, studies by colleagues have indicated that TRPC1 is involved in nasopharyngeal carcinoma cell migration. Those researchers used RNAi technology or the addition of 2-APB, an inhibitor of the inositol 1,4,5-trisphosphate (IP3) receptor and store-operated Ca^{2+} channel-mediated Ca^{2+} entry, to down-regulate TRPC1 in CNE2 cells. Down-regulation of TRPC1 significantly attenuated the adhesive and invasive abilities of NPC cells (*70*).

3.8. *TRP channels and glioblastoma*

Glioblastoma is the most common malignant primary brain tumor, and it accounts for almost 80% of all primary brain tumors. Despite advances in surgical and adjuvant radiation and chemotherapy strategies, glioblastoma continues to be associated with a poor prognosis (*71*). Patients with glioblastoma multiforme have a median survival of approximately 12 months. Approximately 10,000 new cases are diagnosed each year in the US (*72*).

Only two factors have thus far been shown to conclusively affect glioma risk: exposure to high doses of ionizing radiation and inherited mutations in highly penetrant genes associated with rare syndromes. Therefore, additional factors that correlate with glioblastoma occurrence and development should be studied (*71*).

Different studies have suggested that TRP channels (*e.g.*, TRPC1, TRPC3, TRPC4, TRPC5, TRPC6, TRPV1, TRPV2, TRPV4, TRPM2, and TRPM8) are likely to play a role in glioma progression, growth and/or invasion.

The TRPC1 channel is associated with lipid rafts and is essential for glioma chemotaxis in response to stimuli such as epidermal growth factor (EGF). Gliomas are attracted to EGF in a chemotactic manner. Stimulation with EGF results in TRPC1 channel localization at the leading edge of migrating D54MG glioma cells. Chemotaxis toward EGF was lost when TRPC channels were pharmacologically inhibited or

knocked down with TRPC1-specific shRNA (*73*).

The TRPC6 channel is involved in the growth of glioblastoma. Some studies suggest that TRPC6 is more abundant at both the protein and mRNA levels in human glioma tissue. The increased expression of TRPC6 is also associated with the grade of glioma malignancy. Inhibition of TRPC6 activity or decreased expression of the channel led to an increase in intracellular Ca^{2+} *via* platelet-derived growth factor, which suppressed cell growth and clonogenic ability and induced cell cycle arrest in the G2/M phase (*74*).

Moreover, TRPV1 has been implicated in the capsaicin-induced apoptosis of glioma cells. TRPV2 negatively controls glioma cell survival and proliferation and protects the cells from Fas-induced apoptosis in an ERK-dependent manner (*75,76*).

3.9. *TRP channels and melanoma*

Among skin diseases, malignant melanoma is the leading cause of death and accounts for approximately 75% of deaths attributed to skin disease due to its propensity to metastasize. Localized melanoma is curable by surgical techniques and immunotherapy, whereas there are limited therapeutic options for metastatic melanoma or melanoma with metastatic potential. Once diagnosed with metastatic melanoma, most patients will die from the disease within 2 years (*77*). Moreover, current diagnostic methods are limited in their ability to diagnose early disease and to accurately predict an individual's risk of disease progression and outcome (*78*). Thus, melanoma diagnosis and therapy are great clinical challenges.

TRPM1 (also called melastatin) is known to be involved in melanoma, and TRPM2, TRPM7, TRPM8 (also known as Trp-p8), and TRPV2 also play a role. TRPM1 was first discovered by differential display analysis in the B-16 mouse melanoma cell line. The gene is steadily lost during the progression of primary cutaneous and vertical growth phase melanomas (*79*). Many studies suggest that the *TRPM1* gene is a tumor suppressor. TRPM1 mRNA is partially absent or completely absent in approximately 80% of invasive primary melanomas (*78*).

In their study involving murine cell lines, Duncan *et al.* reported that TRPM1 was expressed at high levels in poorly metastatic variants of the B16-F1 melanoma cell line and expressed at very low levels in the highly metastatic B16-F10 melanoma cell line (*80*).

In similar human melanomas experiments, Deeds *et al*. examined TRPM1 mRNA expression in nevi, primary melanoma, and melanoma metastases. They found high levels of TRPM1 mRNA in melanocytic nevi, but radioactive *in situ* hybridization was unable to detect levels of TRPM1 mRNA in melanoma metastases (*81*). Decreased expression of TRPM1 has been shown to correlate with the melanoma cell transition from a low to a high metastatic phenotype (*80*). Moreover, TRPM1 mRNA is reported to correlate with patient prognosis. Patients with American Joint Committee on Cancer stage I tumors diffusely expressing TRPM1 mRNA have an 8-year disease-free survival rate of 100% while patients with stage I tumors with no TRPM1 expression have an 8-year disease-free survival rate of 77 ± 15%. Furthermore, patients with stage II disease in which tumors diffusely express TRPM1 mRNA have an 8-year disease-free survival rate of 90 ± 7% while patients with stage II disease with no TRPM1 expression have an 8-year disease-free survival rate of 51 ± 8% (*82*). Some studies suggest that TRPM1 transcription is regulated by the binding of microphthalmia transcription factor (MITF), which is an essential transcription factor for the development of melanoma. Levels of MITF and TRPM1 mRNA are high in several human melanoma cell lines. Endogenous TRPM1 expression may be regulated by MITF up- or down-regulation, and TRPM1 promoter-driven reporters yielded similar patterns (*83*).

The TRPM8 channel is expressed in the G-361 human melanoma cell line, and the channel is activated by menthol, a naturally occurring ligand for TRPM8. Menthol-induced activation caused prolonged increases in both the intracellular Ca^{2+} concentration and the amplitude of the current in melanoma cells. The most interesting finding is that exposure to menthol drastically reduced the survival of melanoma cells (*84*). TRPV2 mRNA is found in benign astrocyte tissues, and its expression progressively decreased in high-grade glioma tissues as the histological grade increased (*76*).

Moreover, TRPM2 is cited as a factor that can induce melanoma apoptosis and necrosis, while TRPM7 is regarded as a protector and detoxifier in both melanocyte physiology and in melanoma cells (*85,86*).

3.10. *TRP channels and other cancers*

Several TRP channels have been identified in other cancers. For example, TRPC6 has been observed in esophageal carcinomas, and TRPM7 and TRPM8 have been identified in pancreatic adenocarcinoma (PDAC). TRPV1, TRPV3, and TRPV6 have been noted in colon cancer, and TRPC1, TRPC4, TRPC6, and TRPC7 have been observed in renal cell carcinoma.

4. Conclusion

In summary, cancer continues to be a public health problem worldwide. Different TRP channels exist in normal tissues and tumors, and some play important roles in the processes of tumorigenesis, migration, and metastasis. Differences in expression of TRP channels may provide a new basis for tumor diagnosis and might be a new target for cancer therapy. Tumor treatment may become more diverse and more accurate. Although

many studies have examined TRP channels and cancer, this area of research is still in its infancy. Current data are not sufficient to ascertain the specific action of TRP since there are no highly selective inhibitors or agonists of TRP. Not all TRP channels have been investigated, and most of the completed research is still inadequate. An inspiring fact is that associations between TRP proteins and various cancers are still being discovered thanks to rapid advances in molecular biology, genetics, and other disciplines. TRP channels may play an important role in the diagnosis and targeted treatment of tumors.

Acknowledgements

This work was supported by the National Nature Science Foundation of China (grant No. 81102052). The authors wish to thank their colleagues for the helpful comments and suggestions.

References

1. Huber, SM. Oncochannels. Cell Calcium. 2013; 53:241-255.
2. Brooks SA, Lomax-Browne HJ, Carter TM, Kinch CE, Hall DM. Molecular interactions in cancer cell metastasis. Acta Histochem. 2010; 112:3-25.
3. Bidaux G, Roudbaraki M, Merle C, Crépin A, Delcourt P, Slomianny C, Thebault S, Bonnal JL, Benahmed M, Cabon F, Mauroy B, Prevarskaya N. Evidence for specific TRPM8 expression in human prostate secretory epithelial cells: Functional androgen receptor requirement. Endocr Relat Cancer. 2005; 12:367-382.
4. Chen JP, Luan Y, You CX, Chen XH, Luo RC, Li R. TRPM7 regulates the migration of human nasopharyngeal carcinoma cell by mediating Ca^{2+} influx. Cell Calcium. 2010; 47:425-432.
5. Montell C, Rubin GM. Molecular characterization of the Drosophila trp locus: A putative integral membrane protein required for phototransduction. Neuron.1989; 2:1313-1323.
6. Pan Z, Yang H, Reinach PS. Transient receptor potential (TRP) gene superfamily encoding cation channels. Hum Genomics. 2011; 5:108.
7. Wu LJ, Sweet TB, Clapham DE. International Union of Basic and Clinical Pharmacology. LXXVI. Current progress in the mammalian TRP ion channel family. Pharmacol Rev. 2010; 62:381-404.
8. Gaudet R. TRP channels entering the structural era. J Physiol. 2008; 586:3565-3575.
9. Nilius B, Owsianik G. The transient receptor potential family of ion channels. Genome Biol. 2011; 12:218-228.
10. Tano JY, Lee RH, Vazquez G. Macrophage function in atherosclerosis: Potential roles of TRP channels. Channels. 2012; 6:141-148.
11. Sun Y, Shi YK. Handbook of Clinical Medical Oncology. People's Medical Publishing House, Beijing, China, 2007; pp. 388-403. (in Chinese)
12. Siegel R, Naishadham D, Jemal A. Cancer Statistics, 2013. CA Cancer J Clin. 2013; 63:11-30.
13. Ramalingam S, Belani CP. State-of-the-art chemotherapy for advanced non-small cell lung cancer. Semin Oncol. 2004; 31:68-74.
14. Ohe Y, Ohashi Y, Kubota K, Tamura T, Nakagawa K, Negoro S, Nishiwaki Y, Saijo N, Ariyoshi Y and Fukuoka M. Randomized phase III study of cisplatin plus irinotecan versus carboplatin plus paclitaxel, cisplatin plus gemcitabine, and cisplatin plus vinorelbine for advanced non-small-cell lung cancer: Four-Arm Cooperative Study in Japan. Ann Oncol. 2007; 18:317-323.
15. Tajeddine N, Gailly P. TRPC1 protein channel is major regulator of epidermal growth factor receptor signaling. J Biol Chem. 2012; 287:16146-16157.
16. Jiang HN, Zeng B, Zhang Y, Daskoulidou N, Fan H, Qu JM, Xu SZ. Involvement of TRPC channels in lung cancer cell differentiation and the correlation analysis in human non-small cell lung cancer. PLoS One. 2013; 8:e67637.
17. Saito H, Minamiya Y, Watanabe H, Takahashi N, Ito M, Toda H, Konno H, Mitsui M, Motoyama S, Ogawa J. Expression of the transient receptor potential channel C3 correlates with a favorable prognosis in patients with adenocarcinoma of the lung. Ann Surg Oncol. 2011; 18:3377-3383.
18. Gao H, Chen X, Du X, Guan B, Liu Y, Zhang H. EGF enhances the migration of cancer cells by up-regulation of TRPM7. Cell Calcium. 2011; 50:559-568.
19. Knowlton WM, McKemy DD. TRPM8: From cold to cancer, peppermint to pain. Curr Pharm Biotechnol. 2011; 12:68-77.
20. Tsavaler L, Shapero MH, Morkowski S, Laus R. Trp-p8, a novel prostate-specific gene, is up-regulated in prostate cancer and other malignancies and shares high homology with transient receptor potential calcium channel proteins. Cancer Res. 2001; 61:3760-3769.
21. Jiemin M, Ahmedin J. Breast Cancer Statistics. In: Breast Cancer Metastasis and Drug Resistance (Ahmad A, ed.). Springer, New York, USA, 2013; pp. 1-18.
22. Dhennin-Duthille I, Gautier M, Faouzi M, Guilbert A, Brevet M, Vaudry D, Ahidouch A, Sevestre H, Ouadid-Ahidouch H. High expression of transient receptor potential channels in human breast cancer epithelial cells and tissues: Correlation with pathological parameters. Cell Physiol. Biochem. 2011; 28:813-822.
23. EI Hiani Y, Lehen'kyi V, Ouadid-Ahidouch H, Ahidouch A. Activation of the calcium-sensing receptor by high calcium induced breast cancer cell proliferation and TRPC1 cation channel over-expression potentially through EGFR pathways. Arch Biochem Biophys. 2009; 486:58-63.
24. Bandyopadhyay BC, Swaim WD, Liu X, Redman RS, Patterson RL, Ambudkar IS. Apical localization of a functional TRPC3/TRPC6-Ca^{2+}-signaling complex in polarized epithelial cells: Role in apical Ca^{2+} influx. J Biol Chem. 2005; 280:12908-12916.
25. Aydar E, Yeo S, Djamgoz M, Palmer C. Abnormal expression, localization and interaction of canonical transient re-ceptor potential ion channels in human breast cancer cell lines and tissues: A potential target for breast cancer diagnosis and therapy. Cancer Cell Int. 2009; 9:23.
26. Bolanz KA, Hediger MA, Landowski CP. The role of TRPV6 in breast carcinogenesis. Mol Cancer Ther. 2008; 7:271-279.
27. Guilbert A, Gautier M, Dhennin-Duthille I, Haren N, Sevestre H, Ouadid-Ahidouch H. Evidence that TRPM7 is required for breast cancer cell proliferation. Am J Physiol Cell Physiol. 2009; 297:C493-502.
28. Clark K, Middelbeek J, Lasonder E. TRPM7 regulates

myosin-IIA filament stability and protein localization by heavy chain phosphorylation. J Mol Biol. 2008; 378:788-801.
29. Meng X, Cai C, Wu J. TRPM7 mediates breast cancer cell migration and invasion through the MAPK pathway. Cancer Lett. 2013; 333:96-102.
30. Quadid-Ahidouch H, Dhennin-Duthille I, Gautier M, Sevestre H, Ahidouch A. TRP calcium channel and breast cancer: Expression, role and correlation with clinical parameters. Bull Cancer. 2012; 99:655-664.
31. Chodon D, Guilbert A, Dhennin-Duthille I, Gautier M, Telliez MS, Sevestre H, Ouadid-Ahidouch H. Estrogen regulation of TRPM8 expression in breast cancer cells. BMC Cancer. 2010; 10:212.
32. Hsing AW, Devesa SS. Trends and patterns of prostate cancer: What do they suggest? Epidemiol Rev. 2001; 23:3-13.
33. Lehen'Kyi V, Flourakis M, Skryma R and Prevarskaya N. TRPV6 channel controls prostate cancer cell proliferation *via* Ca^{2+}/NFAT-dependent pathways. Oncogene. 2007; 26:7380-7385.
34. Zhao XZ, Guo HQ, Liu GX. Inhibitory effect of TRPV6 silencing on prostate cancer cell line LNCaP *in vitro*. Zhonghua Nan Ke Xue. 2010; 16:423-427. (in Chinese with English abstract)
35. Fixemer T, Wissenbach U, Flockerzi V, Bonkhoff H. Expression of the Ca^{2+}-selective cation channel TRPV6 in human prostate cancer: A novel prognostic marker for tumor progression. Oncogene. 2003; 22:7858-7861.
36. Zhang L and Barritt GJ. TRPM8 in prostate cancer cells: A potential diagnostic and prognostic marker with a secretory function? Endocr Relat Cancer. 2006; 13:27-38.
37. Fuessel S, Sickert D, Meye A, Klenk U, Schmidt U, Schmitz M, Rost AK, Weigle B, Kiessling A, Wirth MP. Multiple tumor marker analyses (PSA, hK2, PSCA, trp-p8) in primary prostate cancers using quantitative RT-PCR. Int J Oncol. 2003; 23:221-228.
38. Bai VU, Murthy S, Chinnakannu K, Muhletaler F, Tejwani S, Barrack ER, Kim SH, Menon M, Veer Reddy GP. Androgen regulated TRPM8 expression: A potential mRNA marker for metastatic prostate cancer detection in body fluids. Int J Oncol. 2010; 36:443-450.
39. Henshall SM, Afar DE, Hiller J, *et al*. Survival analysis of genome-wide gene expression profiles of prostate cancers identifies new prognostic targets of disease relapse. Cancer Res. 2003; 63:4196-4203.
40. Gkika D, Flourakis M, Lemonnier L and Prevarskaya N. PSA reduces prostate cancer cell motility by simulating TRPM8 activity and plasma membrane expression. Oncogene. 2010; 29:4611-4616.
41. Yue D, Wang Y, Xiao JY, Wang P, Ren CS. Expression of TRPC6 in benign and malignant human prostate tissues. Asian J Androl. 2009; 11:541-547.
42. Gabriella C, Varga A, Nyeste K, Marincsák R, Tóth BI, Kovács I, Kovács L, Bíró T. Increased expressions of cannabinoid receptor-1 and transient receptor potential vanilloid-1 in human prostate carcinoma. J Cancer Res Clin Oncol. 2009; 135:507-514.
43. Monet M, Lehen'kyi V, Gackiere F *et al*. Role of cationic channel TRPV2 in promoting prostate cancer migration and progression to androgen resistance. Cancer Res. 2010; 70:1225-1235.
44. Henshall SM, Afar DE, Hiller J, *et al*. Survival analysis of genome-wide gene expression profiles of prostate cancers identifies new prognostic targets of disease relapse. Cancer Res. 2003; 63:4196-203.
45. Zeng X, Sikka SC, Huang L, Sun C, Xu C, Jia D, Abdel-Mageed AB, Pottle JE, Taylor JT and Li M. Novel role for the transient receptor potential channel TRPM2 in prostate cancer cell proliferation. Prostate Cancer Prostatic Dis. 2009; 13:195-201.
46. Zhang W, Chu X, Tong Q, Cheung JY, Conrad K, Masker K, Miller BA. A novel TRPM2 isoform inhibits calcium influx and susceptibility to cell death. J Biol Chem. 2003; 278:16222-16229.
47. Kisielewski R, Tołwińska A, Mazurek A, Laudański P. Inflammation and ovarian cancer-current views. Ginekol Pol. 2013; 84:293-297.
48. Yang SL, Cao Q, Zhou KC, Feng YJ, Wang YZ. Transient receptor potential channel C3 contributes to the progression of human ovarian cancer. Oncogene. 2009; 28:1320-1328.
49. Zeng B, Yuan C, Yang X, Atkin SL, Xu SZ. TRPC Channels and their splice variants are essential for promoting human ovarian cancer cell proliferation and tumorigenesis. Curr Cancer Drug Targets. 2013; 13:103-116.
50. Jemal A, Center MM, DeSantis C, Ward EM. Global Patterns of Cancer Incidence and Mortality Rates and Trends. Cancer Epidemiol Biomarkers Prev. 2010; 19:1893-1907.
51. Yang L. Incidence and mortality of gastric cancer in China. World J Gastroenterol. 2006; 12:17-20.
52. Verdecchia A, Corazziari I, Gatta G, Lisi D, Faivre J, Forman D. Explaining gastric cancer survival differences among European countries. Int J Cancer. 2004; 109:737-741.
53. Cai R, Ding X, Zhou K, Shi Y, Ge R, Ren G, Jin Y, Wang Y. Blockade of TRPC6 channels induced G2/M phase arrest and suppressed growth in human gastric cancer cells. Int J Cancer. 2009; 125:2281-2287.
54. Kim BJ, Park EJ, Lee JH, Jeon JH, Kim SJ, So I. Suppression of transient receptor potential melastatin 7 channel induces cell death in gastric cancer. Cancer Sci. 2008; 99:2502-2509.
55. Kim BJ, Nah SY, Jeon JH, So I, Kim SJ. Transient Receptor Potential Melastatin 7 Channels are Involved in Ginsenoside Rg3-Induced Apoptosis in Gastric Cancer Cells. Basic Clin Pharmacol Toxicol. 2011; 109:233-239.
56. Kim BJ, Kim SY, Lee S, Jeon JH, Matsui H, Kwon YK, Kim SJ, So I. The role of transient receptor potential channel blockers in human gastric cancer cell viability. Can J Physiol Pharmacol. 2012; 90:175-186.
57. Chow J, Norng M, Zhang J, Chai J. TRPV6 mediates capsaicin-induced apoptosis in gastric cancer cells-Mechanisms behind a possible new "hot" cancer treatment. Biochim Biophys Acta. 2007; 1773:565-576.
58. Ferlay J, Shin HR, Bray F, Forman D, Mathers C, Parkin DM. Estimates of worldwide burden of cancer in 2008: GLOBOCAN 2008. Int J Cancer. 2010; 127:2893-2917.
59. Chen JG, Zhang SW. Liver cancer epidemic in China: Past, present and future. Semin Cancer Biol. 2011; 21:59-69.
60. Reuber MD. Transplantable Bile-Secreting Hepatocellular Carcinoma in the Rat. J Natl Cancer Inst. 1961; 26:891-899.
61. El Boustany C, Bidaux G, Enfissi A, Delcourt P, Prevarskaya N, Capiod T. Capacitative calcium entry and transient receptor potential canonical 6 expression control human hepatoma cell proliferation. Hepatology. 2008; 47:2068-2077.

62. Rychkov GY, Barritt GJ. Expression and Function of TRP Channels in Liver Cells. Adv Exp Med Biol. 2011; 704:667-686.
63. Rychkov GY, Litjens T, Roberts ML, Barritt GJ. Arachidonic acid inhibits the store-operated Ca^{2+} current in rat liver cells. Biochem J. 2005; 385:551-556.
64. Liu G, Xie C, Sun F, *et al*. Clinical significance of transient receptor potential vanilloid 2 expression in human hepatocellular carcinoma. Cancer Genet Cytogenet. 2010; 197:54-59.
65. Yu MC, Yuan JM. Epidemiology of nasopharyngeal carcinoma. Semin Cancer Biol. 2002; 12:421-429.
66. Chien CR, Lin HW, Yang CH, Yang SN, Wang YC, Kuo YC, Chen SW, Liang JA. High case volume of radiation oncologists is associated with better survival of nasopharyngeal carcinoma patients treated with radiotherapy: A multifactorial cohort analysis. Clin Otolaryngol. 2011; 36:558-565.
67. Kong F, Cai BZ, Chen XZ, Zhang J, Wang YM. Prognostic factors for survival of patients with nasopharyngeal carcinoma following conventional fractionation radiotherapy. Exp Ther Med. 2013; 6:57-60.
68. Wei C, Wang X, Chen M, Ouyang K, Song LS, Cheng H. Calcium flickers steer cell migration. Nature. 2008; 457:901-905.
69. Jiang J, Li MH, Inoue K, Chu XP, Seeds J, Xiong ZG. Transient receptor potential melastatin 7-like current in human head and neck carcinoma cells: Role in cell proliferation. Cancer Res. 2007; 67:10929-10938.
70. He B, Liu F, Ruan J, Li A, Chen J, Li R, Shen J, Zheng D, Luo R. Silencing TRPC1 expression inhibits invasion of CNE2 nasopharyngeal tumor cells. Oncol Rep. 2012; 5:1548-1554.
71. Schwartzbaum JA, Fisher JL, Aldape KD, Wrensch M. Epidemiology and molecular pathology of glioma. Nat Clin Pract Neurol. 2006; 2:494-503.
72. Ahluwalia MS, Gladson CL. Progress on antiangiogenic therapy for patients with malignant glioma. J Oncol. 2010; 2010:689018.
73. Bomben VC, Turner KL, Barclay TT, Sontheimer H. Transient receptor potential canonical channels are essential for chemotactic migration of human malignant gliomas. J Cell Physiol. 2011; 226:1879-1888.
74. Ding X, He Z, Zhou K, Cheng J, Yao H, Lu D, Cai R, Jin Y, Dong B, Xu Y, Wang Y. Essential Role of TRPC6 Channels in G2/M Phase Transition and Development of Human Glioma. J Natl Cancer Inst. 2010; 102:1052-1068.
75. Amantini C, Mosca M, Nabissi M, Lucciarini R, Caprodossi S, Arcella A, Giangaspero F, Santoni G. Capsaicin-induced apoptosis of glioma cells is mediated by TRPV1 vanilloid receptor and requires p38 MAPK activation. J Neurochem. 2007; 102:977-990.
76. Nabissi M, Morelli MB, Amantini C, Farfariello V, Ricci-Vitiani L, Caprodossi S, Arcella A, Santoni M, Giangaspero F, De Maria R, Santoni G. TRPV2 channel negatively controls glioma cell proliferation and resistance to Fas-induced apoptosis in ERK-dependent manner. Carcinogenesis. 2010; 31:794-803.
77. Jones V, Katiyar SK. Emerging phytochemicals for prevention of melanoma invasion. Cancer Lett. 2013; 335:251-258.
78. Markovic SN, Erickson LA, Rao RD, *et al*. Malignant melanoma in the 21st century, part 1: Epidemiology, risk factors, screening, prevention, and diagnosis. Mayo Clin Proc. 2007; 82:364-380.
79. Duncan LM, Deeds J, Hunter J, Shao J, Holmgren LM, Woolf EA, Tepper RI, Shyjan AW. Down-regulation of the novel gene melastatin correlates with potential for melanoma metastasis. Cancer Res. 1998; 58:1515-1520.
80. Fang D, Setaluri V. Expression and up-regulation of alternatively spliced transcripts of melastatin, a melanoma metastasis-related gene, in human melanoma cells. Biochem Biophys Res Commun. 2000; 279:53-61.
81. Deeds J, Cronin F, Duncan LM. Patterns of melastatin mRNA expression in melanocytic tumors. Hum Pathol. 2000; 31:1346-1356.
82. Duncan LM, Deeds J, Cronin FE, *et al*. Melastatin expression and prognosis in cutaneous malignant melanoma. J Clin Oncol. 2001; 19:568-576.
83. Miller AJ, Du J, Rowan S, Hershey CL, Widlund HR, Fisher DE. Transcriptional Regulation of the Melanoma Prognostic Marker Melastatin (TRPM1) by MITF in Melanocytes and Melanoma. Cancer Res. 2004; 64:509-516.
84. Yamamura H, Ugawa S, Ueda T, Morita A, Shimada S. TRPM8 activation suppresses cellular viability in human melanoma. Am J Physiol Cell Physiol. 2008; 295:C296-301.
85. Nazıroğlu M. TRPM2 cation channels, oxidative stress and neurological diseases: Where are we now? Neurochem Res. 2011; 36:355-366.
86. McNeill MS, Paulsen J, Bonde G, Burnight E, Hsu MY, Cornell RA. Cell death of melanophores in zebrafish trpm7 mutant embryos depends on melanin synthesis. J Invest Dermatol. 2007; 127:2020-2030.

(Received November 24, 2013; Revised December 29, 2013; Re-revised February 18, 2014; Accepted February 25, 2014)

Review

DOI: 10.5582/bst.8.11

Prediction of response to preoperative chemoradiotherapy in patients with locally advanced rectal cancer

Xiangjiao Meng[1], Zhaoqin Huang[2], Renben Wang[1], Jinming Yu[1,*]

[1] *Department of Radiation Oncology and Key Laboratory of Radiation Oncology of Shandong Province, Department of Radiation Oncology of Shandong Cancer Hospital and Institute, Ji'nan, Shandong, China;*
[2] *Department of Radiology, Provincial Hospital Affiliated to Shandong University, Ji'nan, Shandong, China.*

Summary **Preoperative chemoradiotherapy (CRT) combined with surgery has become a standard treatment strategy for patients with locally advanced rectal cancer (LARC). The pathological response is an important prognostic factor for LARC. The variety of tumor responses has increased the need to find a useful predictive model for the response to CRT to identify patients who will really benefit from this multimodal treatment. Magnetic resonance imaging (MRI), positron emission tomography-computed tomography (PET-CT), serum carcinoembryogenic antigen (CEA), molecular biomarkers analyzed by immunohistochemistry and gene expression profiling are the most used predictive models in LARC. The majority of predictors have yielded encouraging results, but there is still controversy. Diffusion-weighted MRI may be the best model to detect the dynamic changes of rectal cancer and predict the response at an early stage. Gene expression profiling and single nucleotide polymorphisms hold considerable promise to unveil the underlying complex genetics of response to CRT. Because each parameter has its own inherent shortcomings, combined models may be the future trend to predict the response.**

Keywords: Rectal cancer, preoperative chemoradiotherapy, prediction, response

1. Introduction

Rectal cancer is one of the leading causes of cancer related deaths in the world (*1*). Over the last two decades, advances in new treatment strategies have contributed significantly to the improvement of the outcome of patients with locally advanced rectal cancer (LARC). Compared with postopertive chemoradiotherapy (CRT), preoperative CRT (pre-CRT) reduced toxicity, improved local recurrence control and disease free survival (*2,3*). For the true benefits, pre-CRT combined with surgery has been implemented as a standard treatment strategy for patients with LARC (*3,4*). The pathological complete response (pCR) is associated with a high 5-year overall survival rate and disease-free survival (DFS) rate (*5-7*), but there is a wide spectrum of responses to preoperative CRT, ranging from none to complete. The variety of tumor responses increased the need to find a useful predictive model for the response to preoperative CRT, which may be helpful in the design of individualized treatment for rectal cancer and allow an early surgery in nonresponders. In this review, we will discuss the current predictive models of the response to pre-CRT in patients with LARC.

2. Functional or molecular imaging techniques

2.1. *Magnetic resonance imaging (MRI)*

With the advancement of MRI techniques, recent studies are no longer only reliant on staging rectal cancer patients, but also on prognostic and predictive functions (*8,9*). Diffusion-weighted MRI (DW-MRI) provides information about microscopic structures through the detection of water proton mobility in biologic tissues (*9,11*). In DW-MRI, the apparent diffusion coefficient (ADC) provides a tool for absolute

**Address correspondence to:*
Dr. Jinming Yu, Department of Radiation Oncology and Key Laboratory of Radiation Oncology of Shandong Province, Department of Radiation Oncology of Shandong Cancer Hospital and Institute. No.440 Jiyan Road, Ji′nan 250117, Shandong, China.
E-mail: sdyujinming@126.com

quantitative image analysis. The ADC is related to tissue cellularity, tissue organization, extracellular space tortuosity, tumor proliferation, tumor grade, and tumor necrosis (*9-11*). With respect to ADC as a quantitative biomarker in rectal cancer, several investigations have reported promising results for the prediction and monitoring of therapeutic responses (*10-18*) (Table 1).

Concerning the pre-CRT ADC value (ADC-pre) as a predictor for response, Sun *et al*. observed that the mean ADC-pre value in the T-downstaged group was lower than that in the T-non-downstaged group (p = 0.013) (*10*). Based on the tumor regression grade (TRG), ADC-pre showed a positive predictive value of 42% for pCR and 67% for a good response (GR, pCR, and near-pCR) (*11*). Lambrecht *et al*. confirmed a low ADC-pre value was significantly correlated with pCR yielding a sensitivity of 100% and specificity of 86% (*12*). In a recent study, ADC for predicting response was confirmed using the area under the receiver-operating characteristic (ROC) curve analysis with a sensitivity of 75% and specificity of 48% (*13*). Despite the promising results, there is no consensus whether low ADC-pre value should be used as a predictor for response to CRT because in some studies the ADC-pre value could not reliably discriminate CR from non-CR (*14,15*). Therefore, relying on ADC-pre seems to be insufficient to select in advance poor responders who might need to undergo early surgery.

Regarding the post-CRT ADC value (ADC-post) as a predictor for response, several studies showed that it could differentiate patients with pCR from those without (*14,15,17*). Moreover ADC-post value measurements are reliable and reproducible (*17*). It might be used as a non-invasive tool to evaluate response to CRT as an ADC-post value presenting good performance to select good responders.

The percentage change in the ADC (ΔADC) was also a useful predictor for pCR. Sun *et al*. observed that the ΔADC was significantly higher in the T-downstaged group than that in the nondownstaged group ($p < 0.001$) (*10*). An increase of ADC had a high positive predictive value for pCR (*11,15*). During treatment, the mean percentage of ADC increase was significantly greater in the responders than nonresponders ($p < 0.0001$) and a > 23% ADC increase had a negative predictive value of 96.3% for TRG4 (*18*). For dynamic observation ΔADC during (ΔADC-during) and after CRT (ΔADC-post) showed a significantly higher value in patients

Table 1. Recent studies of ADC as a predictor for response to CRT of patients with LARC

Ref.	No.	Parameters	Cut-off value ($\times 10^{-3}$ mm^2/s)	*p* value	Conclusion
Sun *et al*. (*10*)	37	ADC-pre ADCchange	1.07 23%	0.013 < 0.0001	Early increase of mean ADC and low mean ADC-pre correlate with good response to CRT.
Intven *et al*. (*11*)	59	ADC-pre ΔADC	0.97 41%		Low ADC-pre and high ΔADC correspond to pCR.
Lambrecht *et al*. (*12*)	20	ADC-pre ΔADC-during ΔADC-post ΔV-during ΔV-post	0.94 ± 0.12 72 ± 14% 88 ± 35% -62 ± 16% -86 ± 12%	0.003 0.0006 0.0011 0.015 0.012	ADC-pre, ΔADC-during, and ΔADC-post may be useful for prediction and early assessment of pathologic response to pre-RCT, with higher accuracy than volumetric measurements.
Barbaro *et al*. (*13*)	49	ADC-pre	0.833		Low ADC-pre may be an early biomarker for predicting treatment response.
Kim *et al*. (*14*)	76	ADC-pre ADC-post ADCchange	0.85 ± 0.10 1.43 ± 0.10 70.0 ± 23.5%	0.409 < 0.0001 < 0.0001	ADC-post alone can reliably differentiate pCR from non-pCR.
Genovesi *et al*. (*15*)	28	ADC-pre ADC-post % ADC	1.01 ± 0.061 1.79 ± 0.51 29.5%	0.33 0.003 0.001	The mean % ADC increase appears to be a reliable tool to differentiate CR from non-CR.
Kim *et al*. (*16*)	40	Mean ADC-post	1.62 +/- 0.36	< 0.0001	The mean ADC-post value of the CR group was significantly higher than that of the non-CR group.
Monguzzi *et al*. (*17*)	31	ADC-post	1.294	AUC of 0.833	Post-CRT ADC measurements are reliable and reproducible to evaluate response to therapy.
Elmi *et al*. (*18*)	62	ADC-pre ΔADC	< 1.0 > 23%	0.0011 < 0.001	Low ADC-pre was correlated with TRG 4, the increase in ADC was greater in the responders.

ADC: apparent diffusion coefficient; CRT: chemoradiotherapy; LARC: locally advanced rectal cancer; pCR: pathological complete response; ADC-pre: pre-CRT ADC values; ADC-post: post-CRT ADC;ΔADC :change in the ADC;ΔV-during: volume reduction during CRT; ΔV-post: volume reduction after CRT. ADC% = (ADC-post−ADC-pre)/ADC-pre×100%.

with pCR than those without, yielding a sensitivity and specificity of 100% for the ΔADC-during and, respectively, 100% and 93% for the ΔADC-post (*12*).

With its great development, MRI has potential to assess and predict the response to pre-CRT. First, most studies provided promising results to confirm the predictive value with high sensitivity and specificity. Second, tumors appear hypointense on ADC maps for the diffusion restriction of proton motion which can help differentiate tumorous lesions from non-tumorous lesions such as radiation-induced fibrosis and inflammation. Furthermore, MRI is known to enable the most accurate and useful assessment of tumor (T) staging before CRT (*19*). So it is convenient to acquire an ADC value. Despite some inconsistent results, ADC values hold great potentiality to be a useful predictor for response. However, all previous studies suffer the same issue that the sample size was too small and lack of standardization in ADC acquisition. Therefore, before ADC can be used as a predictor clinically, large cohort studies are needed.

2.2. *Positron emission tomography-computed tomography (PET-CT)*

PET-CT has become increasingly used for staging and evaluating therapeutic response in oncology (*20*). Over the past decades, lots of studies have implemented PET-CT to assess the response to CRT in LARC. Various PET-CT parameters have been investigated: mean standardized uptake value (SUVmean), maximum SUV (SUVmax), ΔSUVmax (SUVmax-pre – SUVmax-post), response index [RI, $(SUV_{pre} - SUV_{post})/SUV_{pre}$), metabolic tumor volume (MTV), ΔMTV% ($MTV_{pre} - MTV_{post})/MTV_{pre}$, visual response assessment (VRA), and total lesion glycolysis (TLG, SUVmean × MTV) (Table 2) (*19-32*). These studies were able to establish a correlation between PET-CT results and CRT response (*22-30*). Most studies used several parameters but found just one or two parameters correlated with CRT response (*21-27*). Kim *et al*. used SUVmax-pre, SUVmax-post, ΔSUVmax and RI to assess tumor response. Univariate and multivariate analysis revealed

Table 2. Recent studies of SUV as a predictor for response to CRT of patients with LARC

Ref.	No.	Parameters	Sensitivity (%)	Specificity (%)	Cut-off value	Conclusion
Amthauer *et al*. (*21*)	22	ΔSUVmax	93%	100%	36%	ΔSUVmax was significantly greater in responders than in non-responders.
Hur *et al*. (22)	37	SUVmean-post	84.6	79.2	3.35	SUV-post and RR were significantly associated with pathological treatment response, especially in pCR.
Shanmugan *et al*. (*23*)	70	SUVmax-post SUV decrease	58 60	78 84	4.0 63%	SUVpost and %SUV decrease correlate with pCR.
Melton *et al*. (*24*)	21	ΔSUV	86	85	75%	Tumor downstaging and CR are associated with greater RI.
Capirci *et al*. (*25*)	87	RI	84.5	80	65%	RI seems the best predictor to identify CRT response.
Martoni *et al*. (*26*)	80	SUVmax-post RI	88 94	34 31	5.0 66%	SUVmax-post supplies limited predictive information.
Chennupati *et al*. (*27*)	35	ΔSUVmax	93	19	64%	SUVmax, MTV and ΔMTV are not correlated with TRG.
Kim *et al*. (*28*)	151	SUVmax-post	73.7	63.7	3.55	SUVmax-post independently predicts pCR.
Maffione *et al*. (*29*)	69	SUVmax-post MTVpost TLGpost RI ΔMTV% ΔTLG VRA	85.7 65.3 85.7 83.7 69.4 69.4 86	80 80 75 70 80 80 55	5.1 2.1 cm^3 23.4 cm^3 61.8% 81.4% 94.2%	SUVmax ,MTV and TLG after CRT, RI, ΔMTV% and ΔTLG% parameters were significantly correlated with pathological treatment response. SUVmax-post demonstrated the highest AUC, sensitivity and specificity.
Everaert *et al*. (*32*)	45	%ΔSUVmax %ΔSUVmean	90 80	60 72	39% 24.5%	%ΔSUVmax and %ΔSUVmean correlate with histopathologic response.

SUV: standardized uptake value; CRT: chemoradiotherapy; LARC: locally advanced rectal cancer; pCR: pathological complete response; SUVmean: mean SUV; SUVmax: maximum SUV; SUVmean-post: SUVmean of post CRT; SUVmax-post: SUVmean of post CRT; ΔSUVmax: SUVmax-pre-SUVmax-post; RI: response index $(SUV_{pre} - SUV_{post})/SUV_{pre}$); MTV: metabolic tumor volume; ΔMTV%($MTV_{pre} - MTV_{post})/MTV_{pre}$; TLG: total lesion glycolysis (SUVmean × MTV); VRA: visual response assessment;%ΔSUVmax: the percentage differences (%Δ) between SUVmax-pre and SUVmax-post; %ΔSUVmean: the percentage differences (%Δ) between SUVmax-pre and SUVmax-post.

SUVmax-post was a significant factor for prediction of downstaging and pCR (*28*). Maffione *et al*. used 8 parameters to predict TRG and found SUVmax, MTV, TLG-post, RI, ΔMTV%, and ΔTLG% were significantly correlated with pathological treatment response ($p < 0.01$) while SUVmax-post had the highest sensitivity in predicting TRG (*29*). SUVmax is the most commonly studied metabolic parameter for semiquantitative analysis of glucose metabolism with PET-CT. However, SUV can be influenced by the nuclear medicine physicians and acquisition protocols, the reproducibility was poorer than those of RI and the percentage differences. Two studies revealed the mean RI was significantly higher in responders than in nonresponders and concluded that RI may be best for assessing the CRT response (*25,27*). A meta-analysis derived a threshold for RI of 36-52% for predicting response to CRT with a sensitivity and specificity of 86% and 80%, respectively. In the subgroup analysis, the accuracy of the group that underwent PET during therapy (sensitivity 86% and specificity 80%) was statistically higher than that acquired after completion of the therapy (sensitivity 78% and specificity 62%) (*31*). Everaert *et al*. investigated the potential value of sequential PET in assessing the response to radiation therapy (RT). The percentage differences between pre- and post-RT scans in SUVmax (%ΔSUVmax), SUVmean (%ΔSUVmax), %ΔMV, and total glycolytic volume (%ΔtGV) were calculated. Significant differences in %ΔSUVmax and %ΔSUVmean were observed between responders and nonresponders (*32*). However, it remains to be investigated whether these results obtained from patients treated with preoperative RT can be extrapolated to CRT.

Over the past decades lots of PET-CT parameters have been implemented to assess the CRT response in LARC. RI might be the best parameter for response assessment, especially acquired during therapy (*25-27*). The percentage differences in SUV between pre- and post-CRT, especially %ΔSUVmean, can be considered as valuable markers and worth further study (*32*). However, it cannot meet clinical use because of its own limitations. First, up to now the results of the predicting value of PET-CT are still not uniform. Second, PET-CT scans were not successful in determining nodal status (*24*). Third, PET-CT has difficulty in distinguishing between residual cancer and intraluminal or physiologic mucosal activity uptake (*30*). Fourth, the specificity of predictive value is too low to justify modification of the standard treatment protocol for an individual patient.

3. Serum carcinoembryonic antigen (CEA)

Carcinoembryonic antigen (CEA) is the most widely used tumor marker in patients with rectal cancer. Compared with other potential predictive markers, measurement of serum CEA levels are inexpensive, standardized, widely used and easily performed (*33*). In recent years, many studies have focused on the predictive value of CEA levels in patients with rectal cancer receiving pre-CRT (Table 3) (*34-40*). Most studies showed low pre-CRT CEA (CEA-pre) levels with different cut-off values associated with good tumor response or pCR (*34-36*), but concerning the CEA-pre

Table 3. Recent studies of CEA as a predictor for response to CRT of patients with LARC

Ref.	No.	Parameters	Cut-off value	*p* value	Conclusion
Park *et al*. (*34*)	352	CEA-pre	3 ng/mL	< 0.001	CEA-pre levels could be of clinical value as a predictor of response to pre- CRT.
Wallin *et al*. (*35*)	469	CEA-pre	3.4 ng/mL	0.008	Low CEA-pre was significantly associated with pCR.
Lee *et al*. (*36*)	345	CEA-pre	5 ng/mL	0.002	CEA-pre was found to be significant for prediction of pCR.
Perez *et al*. (*37*)	170	CEA-post CEA-pre	5 ng/mL	0.009 (clinical CR) 0.05 (pCR)	Low CEA-pre level was associated with an increased rate of complete clinical response but not with pCR.
		CEA-reduction	5 ng/mL	0.015 (clinical CR) 0.06 (pCR)	There was no correlation between reduction in CEA and CR.
Jang *et al*. (*38*)	109	CEA-post	2.7 ng/mL	0.001	CEA-post was an independent predictor of good tumor regression.
Yang *et al*. (*39*)	138	CEA-post CEA-ratio	2.61 ng/mLl 0.22		CEA-post < 2.61ng/mL predicted pCR (sensitivity 76.0%; specificity 58.4%), CEA ratio predicted pCR (sensitivity 87.5%, specificity 76.7%) for those with CEA-pre ≥ 6 ng/mL.

CEA: Carcinoembryonic antigen; CRT: chemoradiotherapy ; LARC: locally advanced rectal cancer; pCR: pathological complete response; CEA-pre: pretreatment CEA (CEA-pre) level; CEA-post: post-CRT CEA level; CEA ratio: CEA-post divided by CEA-pre; CEA –reduction: CEA-pre-CEA-post.

predictive values, the results were controversial. Perez *et al*. didn't find a correlation between initial CEA-pre level and pCR (*37*).

Recent studies confirmed the predictive value of post-CRT CEA (CEA-post) levels for response to CRT (*37-39*). Perez *et al*. reported that a CEA-post level < 5 ng/mL was associated with increased rates of clinical CR and pCR (*37*). CEA-post with a different cut-off value of 2.7 ng/mL was also proved to be an independent predictor of good tumor regression (p = 0.001) (*38*). In a recent study, CEA-post < 2.61 ng/mL also showed a strong predictive value for pCR with a sensitivity of 76.0% and specificity of 58.4% in patients with a low CEA-pre level or in patients with a high CEA-pre level but normalized CEA-post levels (*39*).

CEA-change as a predictor was first evaluated in a retrospective study, they found patients with a lower CEA-pre level or higher CEA-pre level but CEA reduction ratio ≥ 70% would have a better 5-year DFS. However, it was unknown whether this ratio was related to pCR or not (*40*). To make sure that the CEA ratio (defined as CEA-post divided by CEA-pre) could be used as a predictor for pCR, Yang *et al*. found that when CEA-pre levels ≥ 6 ng/mL, the CEA ratio was a significant predictor for pCR, and the optimal cutoff value of CEA ratio was 0.22 with a sensitivity of 87.5% and specificity of 76.7% (*39*).

Compared with other potential prognostic and predictive markers, measurement of serum CEA levels is inexpensive, widely used and easily performed. There is controversy if CEA-pre could be a predictive marker for pCR or not (*34-39*). CEA change groups were relevant to pCR, but may not be significant enough (*37,38*). CEA-post was an independent predictor for response to CRT (*37-39*), but different studies used different cut-off values and most studies did not mention the sensitivity and specificity of CEA-post as a predictor for CRT response.

4. Molecular markers

Many molecular markers were assessed for response prediction to CRT by immunohistochemistry (IHC) or direct gene sequencing analysis. Recent studies are listed in Table 4.

4.1. *p53*

Several studies assessed the ability of p53 status to predict response to CRT (*41-45*). Of these, some studies found that p53 could significantly predict response (*43-45*). In contrast, with similar sample size and pathological endpoints, some studies found no association between over-expression of the p53 protein and treatment response (*41,45*). Interestingly, one study found p53 genotype but not a p53 IHC result could predict response to preoperative short-term radiotherapy in rectal cancer (*42*). A meta-analysis found the wild-type *p53* gene was significantly associated with complete response (p = 0.003), and low expression of p53 protein was not significantly associated with complete response (p = 0.124) (*46*). Due to inconsistencies in different studies, p53 still cannot be considered a reliable predictor for treatment modalities.

4.2. *p21*

P21 protein has been studied as a response predictor because of the disruption of regulatory networks, in particular those involved in cell death signaling, which may be a causative factor of resistance to radiotherapy (*44*). Rau *et al*. reported that lower p21 expression in pre-treatment biopsies was correlated with poor response (*47*). Another study found p21 and apoptosis together with histologic changes on biopsy specimens obtained 7 days after starting CRT were strong predictors for response to CRT (*48*).

4.3. *K-ras*

K-ras plays an important role in colorectal carcinogenesis. Luna-Perez *et al*. analyzed codons 12, 13, and 61 of K-ras and found that tumors with wild-type K-ras were more likely to be responsive than tumors with mutant K-ras (*49*). In contrast, in two retrospective studies the K-ras mutation status was not found to be correlated with response or TRG (*50,51*).

4.4. *Epidermal growth factor receptor (EGFR) and vascular endothelial growth factor (VEGF)*

EGFR expression is an indicator of poor response to CRT in LARC (*52*). Kim *et al*. found a low level of EGFR expression may be a significant predictive molecular marker for increased tumor downstaging after CRT (*53*). Opposite to the former studies, Zlobec *et al*. found EGFR-positive tumors were six times more likely to undergo pCR compared with EGFR-negative cases (*54*). The conflicting results among different studies might be due to IHC methodological differences and heterogeneity of EGFR expression. Those shortcomings may be overcome by gene polymorphism. The most common single nucleotide polymorphism is Sp1 -216 G/T polymorphism in the EGFR promoter region. Evaluating for EGFR Sp1 -216 G/T polymorphism from blood samples and EGFR expression on primary tumor biopsies simultaneously, the major response rate in patients with Sp1 -216 T containing variants is significantly higher in Sp1 -216 GG homozygote patients, but in regard to EGFR expression by IHC no correlation was observed with response rates (*55*). Low VEGF expression levels also indicated a good pathological response (*56*). Zlobec *et*

Table 4. Recent studies of biomarkers as a predictor for response to CRT of patients with LARC

Ref.	No.	Biomarker	Analysis methods	*p* value	Conclusion
Rebischung *et al*. (*41*)	86	p53	GE	< 0.01	P53 status is an independent prognostic factor of response to radiotherapy.
Kandioler *et al*. (*42*)	64	p53	GE IHC		P53 genotype but not p53 immunohistochemistry is predictive for response to preoperative short-term radiotherapy.
Komuro *et al*. (*43*)	111	p53	IHC	0.045	There was a significant correlation between the expression pattern of p53 and tumor radiosensitivity.
Fu *et al*. (*44*)	49	p53 p21	IHC IHC	0.01	The majority of p53(-) or p21(+) tumors were radiosensitive.
Huh *et al*. (*45*)	123	13 markers	PCR	0.03	Only CD44 expression was found to be significant independent predictive factors for tumor regression grade response.
Chen *et al*. (*46*)	1830	p53	meta-analysis	0.003 0.124	Wild-type p53 gene was significantly associated with CR. Low expression of p53 protein was not significantly associated with CR.
Rau *et al*. (*47*)	66	p53, p21, Ki67	PCR		Lower p21 expression in pre-treatment biopsies correlated to poor response.
Suzuki *et al*. (*48*)	101	p21, apopstosis	IHC	0.04 < 0.01	P21 with tumor regression P21 and apoptosis together obtained 7 days after starting CRT are strong predictors of the response to CRT.
Luna-Perez *et al*. (*49*)	37	K-ras	GE		K-ras mutations is an indicator of tumor response
Bengala *et al*. (*50*)	146	K-ras EGFR	GE		Neither EGFR nor K-ras status was statistically correlated to TRG
Gaedcke *et al*. (*51*)	94	K-ras	GE	> 0.05	The presence of K-ras mutations was not correlated neither with tumor response.
Kim *et al*. (*53*)	183	EGFR	IHC	0.012	The significant predictive factor for increased tumor downstaging was a low level of EGFR expression
Zlobec *et al*. (*54*)	104	EGFR VEGF	IHC	0.01 0.009	Loss of VEGF and positive EGFR are an independent predictor for pCR.
Spindler *et al*. (*55*)	77	EGFR	IHC SNP	> 0.05 0.023	EGFR Sp1-216G/T polymorphism are potential markers for response to CRT.
Kurt *et al*. (*56*)	29	Several markers including VEGF	IHC	0.05	VEGF level was higher in the non-pCR group than the pCR group.
Saigusa *et al*. (*57*)	50	CD133	IHC	< 0.05	The ratio of histopathological responder in cases with CD133 expression was significantly lower than that without it.
Hiroishi *et al*. (*58*)	50	12 biomarkers including CD133	IHC	0.003	CD133 was significantly associated respectively with sensitivity to pre-operative CRT.
Shinto *et al*. (*59*)	96	CD133	IHC	0.002 (uni) 0.003 (multi)	Positivity for CD133 expression was associated with chemoradioresistance on univariate and multivariate analyses.
Sprenger *et al*. (*60*)	126	CD133	IHC	< 0.01	Increased fraction of CD133-expressing cells after preoperative CRT was associated with lower histopathologic tumor regression.
Vaupel *et al*. (*61*)	86	HIF-1α, GLUT-1	IHC		HIF-1α and GLUT-1 expression had no predictive impact regarding response measured by TRG.
Havelund *et al*. (*62*)	50	HIF-1α	IHC		There were no significant differences between the HIF-1α-positive group and HIF-1α-negative group for pathological grading and pCR.

CRT: chemoradiotherapy; LARC: locally advanced rectal cancer; pCR: pathological complete response; GE:gene expression;IHC: immunohistochemistry; PCR: polymerase chain reaction .TRG: tumor regession grade; EGFR: Epidermal growth factor receptor; VEGF: vascular endothelial growth factor; SNP: single nucleotide polymorphisms; HIF-1α:hypoxia-inducible factor 1α ; GLUT-1:glucose transporter-1

al. applied ROC curve derived cut-off scores to VEGF and confirmed VEGF negative tumors were four times more likely to undergo complete tumor regression (*54*). Despite different results, EGFR or VEGF, especially EGFR Sp1-216G/T polymorphism are potential new markers for assessing response to CRT in LARC.

4.5. *Cancer stem cell markers*

CD133, CD44, and CD24 have been described as cancer stem cell markers. Several studies confirmed elevated CD133 expression was associated with resistance to CRT in LARC (*57-60*). The status of CD24 was also found to be significantly associated with response to CRT ($p = 0.029$) (*58*). Huh *et al*. revealed that among 13 molecular markers, only elevated CD44 mRNA levels in pretreatment biopsies might be predictive of poor tumor regression and CD133 level had no significant correlation with the response to CRT (*45*).

4.6. *Markers of tumor hypoxia*

Tumor hypoxia can lead to resistance to radiation and chemotherapy by depriving cells of oxygen essential for the cytotoxic activities of these agents (*61*). Hypoxia-inducible factor 1α (HIF-1α) and glucose transporter-1 (GLUT-1) are intrinsic markers of tumor hypoxia. It has been considered that HIF-1α and GLUT-1 expression may be predictors for poor response. Different from the hypothesis, the HIF-1α and GLUT-1 expressions had no predictive value regarding response to CRT based on TRG in a study carried by Havelund *et al*. (*62*). Shioya *et al*. detected HIF-1α expression in 42.0% of samples but found no significant correlation between the HIF-1α-expression and pathological response (*63*).

Among molecular markers based on tumor tissues, the vast majority of studies have assessed single or multiple markers. A limited number of promising markers have been identified, including p53, p21, EGFR, VEGF, CD133, HIF-1α and so forth. The majority of markers assessed, however, have yielded disappointing results. No specific molecular marker has yet been proven to be a definitive predictor of the response to CRT. The failure of IHC methods as a means of biomarker discovery is that this assesses small numbers of pre-defined protein markers per tissue section.

5. Gene expression profiling

Instead of focusing on specific factors, recent advances in deoxyribonucleic acid (DNA) microarray-based gene expression profiling technology make it possible to analyze a large number of genes simultaneously, and search systematically for molecular markers to predict responses and outcomes (*64*). Consequently, several investigators have used gene expression profiling to analyze the genetics of rectal cancer and their predictive potential in terms of response to CRT (Table 5). Ghadimi *et al*. used two different microarray platforms to analyze pretreatment biopsies and identified 54 genes that were significantly differentially expressed between responders and non-responders based on T-down-staging. The genes were able to predict tumor behavior correctly in 83% of patients (*65*). Using an Affymetrix U95Av2 Gene Chip, 33 novel discriminating genes related to transcription, cell growth, signal transduction and apoptosis were identified based on TRG in another study. Among the 33 genes, 20 genes expression increased and 13 genes expression decreased in responders as compared to nonresponders (*66*). In the following studies, differentially expressed genes related to cell cycle and/or cell signaling were also successfully identified between responders and non-responders (*67-69*). The model based on the identified genes predicted

Table 5. Recent studies using gene expression profiling to analyze the genetics for response to CRT of patients with LARC

Ref.	No.	No. of genes	Accuracy (%)	Conclusion
Ghadimi *et al*. (*65*)	30	54	82.4	Pretherapeutic gene expression profiling may assist in response prediction to preoperative CRT.
Watanabe *et al*. (*66*)	52	33	82.4	Gene expression profiling may be useful in predicting response to radiotherapy.
Kim *et al*. (*67*)	46	95	84	Microarray gene expression analysis was successfully used to predict CR to preoperative CRT.
Rimkus *et al*. (*68*)	43	42	86	Pretherapeutic prediction of response to CRT by gene expression analysis may represent a new valuable and practical tool of therapeutic stratification.
Nishioka *et al*. (*69*)	17	17		Gene expression patterns of diagnostic biopsies can predict pathological response to preoperative CRT.
Supiot *et al*. (*81*)	6	31 (up) 6 (down)		Micro-arrays can efficiently assess early transcriptomic changes during preoperative radiotherapy for rectal cancer.

CRT: chemoradiotherapy; LARC: locally advanced rectal cancer; CR: complete response.

the response to CRT at an accuracy of over 80% (*65-68*).

It seems reasonable to apply microarray gene profiling to identify novel molecular markers to predict response to CRT. Each study generated gene expression classifiers capable of high predictive accuracy (*65-68*), but the use of this microarray data in clinical practice is still limited for several reasons. First, microarray profiling relies on the prompt collection of fresh tissue samples and tumor biopsies consist of varying amounts of stroma, blood vessels and lymphocytes which contribute to the gene expression profiles and thus introduce a potential source of error. Second, the previously reported gene signatures differed considerably in terms of gene composition among different studies which make it difficult to compare the effectiveness of different genes. Third, the numbers of patients in each study were relatively limited. The current reported genes analyzed by microarray technology are not robust enough for clinical utility at this point. However, considering the promising data and usefulness of gene profiling in breast and lung cancer, gene expression profiling holds considerable promise to unveil the underlying complex genetics of response to CRT of rectal cancer if candidate genes are carefully validated in the future.

6. Thymidylate synthase (TYMS)

TYMS is an essential enzyme for cell proliferation and DNA synthesis (*70*). TYMS is considered the indirect target of 5-fluorouracil (5-Fu) and it was evaluated in several studies as a predictor of response to 5-Fu based pre-CRT in LARC (*71-76*), but there is much debate about the results. Saw *et al*. (*71*) observed that pretreatment biopsy specimens negative for TYMS were predictive of tumor down-staging in the CRT group but not in the radiotherapy group. In a contrasting study, patients with high TYMS IHC staining were more likely to achieve complete and partial response in the CRT group only (*72*). Even no correlation between TYMS expression and treatment response was observed in a study carried by Bertolini *et al*. (*73*). All the above studies used the IHC method to determine the TYMS levels, and limitations of IHC (heterogeneity in the TS assay and classification criteria) may contribute partly to the conflicting results. A genetic approach was used to quantify different TYMS genotype activities (2R/2R,2R/3R, and 3R/3R). By evaluating the number of tandem repeats of the *TYMS* gene, patients with either 2R/2R, 2R/3R are more likely to achieve downstaging and pCR than patients with 3R/3R (*74*). According to 2R/3R and 3R/3R tandem repeat polymorphisms in the *TYMS* gene, TYMS polymorphisms were classified into a low expression group (2R/2R, 2R/3RC, or 3RC/3RC) and high expression group (2R/3RG,3RC/3RG, or 3RG/3RG) but no correlation was found between TYMS SNPs and tumor response (*75,76*). However, in a further study, patients in the low-expression group with a G>C SNP exhibited a significantly greater tumor downstaging rate ($p = 0.001$) (*76*). The TYMS gene is complicated and regulation is still not fully understood. The underlying reason for previous contradictory results according to TYMS polymorphisms on the clinical response need to be investigated, and additional novel polymorphisms might be identified to understand the complete role of TYMS genotyping for predicting a 5-Fu based pre-CRT response in rectal cancer.

7. Single-nucleotide polymorphism (SNP) markers

SNP analysis has been used to tailor special gene sites to predict response to CRT (*55,75,76*). Instead of focusing on specific genes, genome-wide association studies were capable of genotyping thousands of SNPs. It is theoretically possible to identify SNP markers predicting a response to pre-CRT in LARC. A quite recent study has implemented a human 3-step genome-wide SNP strategy for the determination of CRT sensitivity in LARC. In the first step, the screening group was performed using the Genome-Wide Human SNP Array with 906,600 probes in 43 patients with LARC. Then the results of the genotyping analysis were associated with the responses to pre-CRT. USP20rs227450, FAM101Ars795574, ZNF281rs424414, OR2T4rs153870, SLC10A7rs41398848, CORO2Ars198585, ASZ1 rs7808424 MED4 rs157125, and CDC42BPA rs192986 were identified as CRT-responsive SNPs. In the second step, the above nine candidate SNPs were genotyped by pyrosequencing for clinical validation in a total of 113 patients. The patients carrying the reference allele(C) of the SNP CORO2A rs1985859 were more likely to obtain a positive response (TRG1-3) than the substitution allele (T) ($p = 0.01$). This was confirmed by the *in vitro* assay of ionizing radiation cytotoxicity and the clonogenic assay in the third step. However, there are controversial findings with respect to FAM101A, no specific genotype or allelotype showing significant CRT sensitivity was identified in the clinical association study, but downregulation of FAM101A reduced early apoptosis, enhanced colony formation and increased cell survival or viability in RKO cells (*77*). Despite the controversial findings in the current study and poor concordance between GWA studies, the finding is novel and SNPs are worth further study.

8. Dynamic analyzing

Increasing evidence shows that the way in which tumors respond to radiation is dynamic by analyzing sequential core biopsies (*78,79*). Recently, the same studies were carried out on rectal cancer. Based on biopsies taken before CRT, after 2, 4, and 6 weeks of CRT and in specimens from the operation, decreasing expressions

of HIF-1α, Bcl-2 and Ki-67 were observed during CRT, but unfortunately no association was seen between the fluctuations of any of the markers and response to CRT (*80*). In another study, based on biopsy specimens obtained 7 days after starting CRT, the expressions of p21 and apoptosis have been proven to be strong predictors of the response to CRT in rectal cancer (*48*). Gene expression changes detected on biopsies after a dose of 7.2 Gy at a median time of 1 hour following irradiation found 31 genes significantly up-regulated and 6 genes down-regulated (*81*). This potentially means that the response may be more accurately predicted after initial treatment cycles rather than only before or after treatment of tissues, but performing serial biopsies is an invasive and unpleasant procedure and has the risk of increasing toxicity from repeated biopsies. As such, a non-invasive means of monitoring early-stage responses would be beneficial. DW-MRI, PET-CT and CEA can detect dynamic changes of rectal cancer during CRT easily and non-invasively. However, the price of PET-CT testing is so high that many patients are unable to afford repeating PET-CT tests and the serum CEA levels of parts of patients are always at a normal level so that CEA detection has no use for them at all. A study including twenty patients underwent MRI before CRT, after 10-15 fractions and 1 to 2 weeks before surgery showed ΔADC-during had a significantly higher value in patients with pCR compared with patients without (*12*). Due to the above evidences, DW-MRI may be the best model to detect the dynamic change of rectal cancer and predict the response at an early stage.

9. Dual or more models combined

As each parameter has its own inherent shortcomings, a combination of dual or more models may improve the accuracy of a response prediction. A prospective study investigated the combination of PET-CT and DW-MRI for the prediction of a pathological response. Twenty two patients had PET-CT before CRT, after 10 to 12 fractions of CRT, 5 weeks after CRT and had DW-MRI before CRT. Both during and after CRT, the number of false positive results were decreased and consequently specificity was increased by the combination of ΔSUV max and ADC. During CRT the combination of ΔSUVmax > 40% and ADC-pre < 1.06×10^3 mm²/s can predict pCR with a sensitivity of 100% and specificity of 94%. Also, the combination of the provided threshold for ΔSUV max after CRT and ADC-pre was able to predict the response in all 22 patients (*82*). In a recently published study, the predictive value of PET-CT and CEA was simultaneously evaluated in terms of downstaging and pCR. SUV-post < 3.7 and CEA-pre < 5.3ng/mL are independent predictors for response to CRT in univariate and multivariate analysis. The combination of SUV-post < 3.7 and CEA-pre < 5.3 ng/mL increased the specificity from 65% and 51.4% to 84.4% for downstaging and the specificity from 63.6% and 81.8% to 91.6% for pCR (*29*).

Despite the small number of patients in the studies, the combination of two modalities provide us with complementary information of the tumor and yielded higher accuracy and specificity than the individual investigations, which holds great potential for response prediction. The integration of functional imaging, CEA, together with the numerous potential molecular markers and identified genes will provide us with a bulk of information on each individual patient and make individualized treatment therapy possible. Combined models may be the future trend to predict a response.

10. Conclusion and prospects

The high level of variation in response to CRT and the potentially toxic side effects increased the need for better patient selection in LARC. A major focus of rectal cancer research has been the identification of predictive factors allowing clinicians to predict responses. However, to be able to base treatment decisions, prediction should be effective and applicable in current clinical practice. From the update of current status, prediction is still in its infancy: First, there is still controversy between different results. Second, until now virtually all biomarkers have been identified in retrospective studies and predictions were not effective enough. Third, the number of patients is naturally limited. Fourth, there is the problem of high dimensionality of the therapy regimens: long or short term radiation and different chemotherapy regimens. Fifth, the histopathological evaluation of tumor response is different, such as complete response, partial response, TRG and downstaging. Differences among studies make a direct comparison of the results impossible. So before any predictor is used clinically, tumor response evaluation should be standardized and large consistent cohort studies are needed.

In this review, we have provided an overview of the different predictive models. The ADC of MRI, SUV of PET-CT, CEA, gene expression profiling and SNPs analysis are the most potential predictors for response to CRT from the evidence today. Due to the evidence that the way in which tumors respond to radiation is dynamic, DW-MRI may be the best model to detect the dynamic change of rectal cancer and predict the response at early stage. Considering the promising data and usefulness of gene profiling in other cancers, gene expression profiling and SNPs analysis hold considerable promise to unveil the underlying complex genetics of response to CRT in rectal cancer. As each parameter has its own inherent shortcomings and a combination of dual or more models may provide us with complementary information, combined models may be the future trend to predict a response. Before any predictor is used clinically, large consistent cohort studies are needed.

Acknowledgments

The work was supported by Shandong province science and technology development program (No. 2012YD18086 and No. 2012YD18053).

References

1. Jemal A, Bray F, Center MM, Ferlay J, Ward E, Forman D. Global cancer statistics. CA Cancer J Clin. 2011; 61:69-70.
2. Sauer R, Becker H, Hohenberger W, Rödel C, Wittekind C, Fietkau R, Martus P, Tschmelitsch J, Hager E, Hess CF, Karstens JH, Liersch T, Schmidberger H, Raab R. Preoperative versus postoperative chemoradiotherapy for rectal cancer. N Engl J Med. 2004; 351:1731-1740.
3. Roh MS, Colangelo LH, O'Connell MJ, Yothers G, Deutsch M, Allegra CJ, Kahlenberg MS, Baez-Diaz L, Ursiny CS, Petrelli NJ, Wolmark N. Preoperative multimodality therapy improves disease-free survival in patients with carcinoma of the rectum: NSABP R-03. J Clin Oncol. 2009; 27:5124-5130.
4. Gérard JP, Conroy T, Bonnetain F, Bouché O, Chapet O, Closon-Dejardin MT, Untereiner M, Leduc B, Francois E, Maurel J, Seitz JF, Buecher B, Mackiewicz R, Ducreux M, Bedenne L. Preoperative radiotherapy with or without concurrent fluorouracil and leucovorin in T3-4 rectal cancers: Results of FFCD 9203. J Clin Oncol. 2006; 24:4620-4625.
5. Rödel C, Martus P, Papadoupolos T, Füzesi L, Klimpfinger M, Fietkau R, Liersch T, Hohenberger W, Raab R, Sauer R, Wittekind C. Prognostic significance of tumor regression after preoperative chemoradiotherapy for rectal cancer. J Clin Oncol. 2005; 23:8688-8696.
6. Eich HT, Stepien A, Zimmermann C, Hellmich M, Metzger R, Hölscher A, Müller RP. Neoadjuvant radiochemotherapy and surgery for advanced rectal cancer: Prognostic significance of tumor regression. Strahlenther Onkol. 2001; 187:225-230.
7. Habr-Gama A, Perez RO. Non-operative management of rectal cancer after neoadjuvant chemoradiation. Br J Surg. 2009; 96:125-127.
8. Smith N, Brown G. Preoperative staging of rectal cancer. Acta Oncol. 2008; 47:20-31.
9. Lambregts DM, Vandecaveye V, Barbaro B, Bakers FC, Lambrecht M, Maas M, Haustermans K, Valentini V, Beets GL, Beets-Tan RG. Diffusion-weighted MRI for selection of complete responders after chemoradiation for locally advanced rectal cancer: A multicenter study. Annals of Surgical Oncology. 2011; 18:2224-2231.
10. Sun YS, Zhang XP, Tang L, Ji JF, Gu J, Cai Y, Zhang XY. Locally advanced rectal carcinoma treated with preoperative chemotherapy and radiation therapy: Preliminary analysis of diffusion-weighted MR imaging for early detection of tumor histopathologic downstaging. Radiology. 2010; 254:170-178.
11. Intven M, Reerink O, Philippens ME. Diffusion-weighted MRI in locally advanced rectal cancer: pathological response prediction after neo-adjuvant radiochemotherapy. Strahlenther Onkol. 2013; 189:117-122.
12. Lambrecht M, Vandecaveye V, De Keyzer F, Roels S, Penninckx F, Van Cutsem E, Filip C, Haustermans K. Value of diffusion-weighted magnetic resonance imaging for prediction and early assessment of response to neoadjuvant radiochemotherapy in rectal cancer: Preliminary results . Int J Radiat Oncol Biol Phys. 2012; 82:863-870.
13. Barbaro B, Vitale R, Valentini V, Illuminati S, Vecchio FM, Rizzo G, Gambacorta MA, Coco C, Crucitti A, Persiani R, Sofo L, Bonomo L. Diffusion-weighted magnetic resonance imaging in monitoring rectal cancer response to neoadjuvant chemoradiotherapy. Int J Radiat Oncol Biol Phys. 2012; 83:594-599.
14. Kim SH, Lee YJ, Lee JM, Han JK, Choi BI. Apparent diffusion coefficient for evaluating tumour response to neoadjuvant chemoradiation therapy for locally advanced rectal cancer. European Radiology. 2011; 21:987-995.
15. Genovesi D, Filippone A, Ausili Cèfaro G, Trignani M, Vinciguerra A, Augurio A, Di Tommaso M, Borzillo V, Sabatino F, Innocenti P, Liberatore E, Colecchia G, Tartaro A, Cotroneo AR. Diffusion-weighted magnetic resonance for prediction of response after neoadjuvant chemoradiation therapy for locally advanced rectal cancer: preliminary results of a monoinstitutional prospective study. Eur J Surg Oncol. 2013; 39:1071-1078.
16. Kim SH, Lee JM, Hong SH, Kim GH, Lee JY, Han JK, Choi BI. LARC: added value of diffusion-weighted MR imaging in the evaluation of tumor response to neoadjuvant chemo-and radiation therapy. Radiology. 2009; 253:116-125.
17. Monguzzi L, Ippolito D, Bernasconi DP, Trattenero C, Galimberti S, Sironi S. Locally advanced rectal cancer: Value of ADC mapping in prediction of tumor response to radiochemotherapy. Eur J Radiol. 2013; 82:234-240.
18. Elmi A, Hedgire SS, Covarrubias D, Abtahi SM, Hahn PF, Harisinghani M. Apparent diffusion coefficient as a non-invasive predictor of treatment response and recurrence in locally advanced rectal cancer. Clin Radiol. 2013; 68:e524-531.
19. Kim DJ, Kim JH, Lim JS, Yu JS, Chung JJ, Kim MJ, Kim KW. Restaging of rectal cancer with MR imaging after concurrent chemotherapy and radiation therapy. Radiographics. 2010; 30:503-516.
20. Shields AF. Positron emission tomography measurement of tumor metabolism and growth: Its expanding role in oncology. Mol Imaging Biol. 2006; 8:141-150.
21. Amthauer H, Denecke T, Rau B, Hildebrandt B, Hünerbein M, Ruf J, Schneider U, Gutberlet M, Schlag PM, Felix R, Wust P. Response prediction by FDG-PET after neoadjuvant radiochemotherapy and combined regional hyperthermia of rectal cancer: Correlation with endorectal ultrasound and histopathology. Eur J Nucl Med Mol Imaging. 2004; 31:811-819.
22. Hur H, Kim NK, Yun MJ, Min BS, Lee KY, Keum KC, Ahn JB, Kim H. 18Fluoro-deoxy-glucose positron emission tomography in assessing tumor response to preoperative chemoradiation therapy for locally advanced rectal cancer. J Surg Oncol. 2011; 103:17-24.
23. Shanmugan S, Arrangoiz R, Nitzkorski JR, Yu JQ, Li T, Cooper H, Konski A, Farma JM, Sigurdson ER. Predicting pathologic response to neoadjuvant chemoradiotherapy in LARC using 18FDG-PET-CT. Ann Surg Oncol. 2012; 19:2178-2185.
24. Melton GB, LavelyWC, Jacene HA, Schulick RD, Choti MA, Wahl RL, Gearhart SL. Efficacy of preoperative combined 18-fluorodeoxyglucose positron emission tomography and computed tomography for assessing primary rectal cancer response to neoadjuvant therapy. J Gastrointest Surg. 2007; 11:961-969.

25. Capirci C, Rubello D, Pasini F Galeotti F, Bianchini E, Del Favero G, Panzavolta R, Crepaldi G, Rampin L, Facci E, Gava M, Banti E, Marano G. The role of dual-time combined 18-fluorodeoxyglucose positron emission tomography and computed tomography in the staging and restaging workup of LARC, treated with preoperative chemoradiation therapy and radical surgery. Int J Radiat Oncol Biol Phys. 2009; 74:1461-1469.
26. Martoni AA, Di Fabio F, Pinto C, Castellucci P, Pini S, Ceccarelli C, Cuicchi D, Iacopino B, Di Tullio P, Giaquinta S, Tardio L, Lombardi R, Fanti S, Cola B. Prospective study on the FDG-PET/CT predictive and prognostic values in patients treated with neoadjuvant chemoradiation therapy and radical surgery for LARC. Ann Oncol. 2011; 22:650-656.
27. Chennupati SK, Quon A, Kamaya A, Pai RK, La T, Krakow TE, Graves E, Koong AC, Chang DT. Positron emission tomography for predicting pathologic response after neoadjuvant chemoradiotherapy for locally advanced rectal cancer. Am J Clin Oncol. 2012; 35:334-339.
28. Kim JW, Kim HC, Park JW, Park SC, Sohn DK, Choi HS, Kim DY, Chang HJ, Baek JY, Kim SY, Kim SK, Oh JH. Predictive value of (18) FDG PET-CT for tumor response in patients with locally advanced rectal cancer treated by preoperative chemoradiotherapy. Int J Colorectal Dis. 2013; 28:1217-1224.
29. Maffione AM, Ferretti A, Grassetto G, Bellan E, Capirci C, Chondrogiannis S, Gava M, Marzola MC, Rampin L, Bondesan C, Colletti PM, Rubello D. Fifteen different 18F-FDG PET/CT qualitative and quantitative parameters investigated as pathological response predictors of LARC treated by neoadjuvant chemoradiation therapy. Eur J Nucl Med Mol Imaging. 2013; 40:853-864.
30. Perez RO, Habr-Gama A, Gama-Rodrigues J, Proscurshim I, Julião GP, Lynn P, Ono CR, Campos FG, Silva e Sousa AH Jr, Imperiale AR, Nahas SC, Buchpiguel CA. Accuracy of positron emission tomography/computed tomography and clinical assessment in the detection of complete rectal tumor regression after neoadjuvant chemoradiation: Long-term results of a prospective trial (National Clinical Trial 00254683). Cancer. 2012; 118:3501-3511.
31. Zhang C, Tong J, Sun X, Liu J, Wang Y, Huang G. F-FDG-PET evaluation of treatment response to neo-adjuvant therapy in patients with locally advanced rectal cancer: A meta-analysis. Int J Cancer. 2012; 131:2604-2611.
32. Everaert H, Hoorens A, Vanhove C, Sermeus A, Ceulemans G, Engels B, Vermeersch M, Verellen D, Urbain D, Storme G, De Ridder M. Prediction of response to neo-adjuvant radiotherapy in patients with locally advanced rectal cancer by means of sequential 18FDG-PET. Int J Radiat Oncol Biol Phys. 2011; 80:91-96.
33. Harrison LE, Guillem JG, Paty P, Cohen AM. Preoperative carcinoembryonic antigen predicts outcomes in node-negative colon cancer patients: A multivariate analysis of 572 patients. J Am Coll Surg. 1997; 185:55-59.
34. Park JW, Lim SB, Kim DY, Jung KH, Hong YS, Chang HJ, Choi HS, Jeong SY. Carcinoembryonic antigen as a predictor of pathologic response and a prognostic factor in locally advanced rectal cancer patients treated with preoperative chemoradiotherapy and surgery. Int J Radiat Oncol Biol Phys. 2009; 74:810-817.
35. Wallin U, Rothenberger D, Lowry A, Luepker R, Mellgren A. CEA - a predictor for pathologic complete response after neoadjuvant therapy for rectal cancer. Dis Colon Rectum. 2013; 56:859-868.
36. Lee JH, Kim SH, Jang HS, Chung HJ, Oh ST, Lee DS, Kim JG. Preoperative elevation of carcinoembryonic antigen predicts poor tumor response and frequent distant recurrence for patients with rectal cancer who receive preoperative chemoradiotherapy and total mesorectal excision: A multi-institutional analysis in an Asian population. Int J Colorectal Dis. 2013; 28:511-517.
37. Perez RO, Sao Juliao GP, Habr-Gama A, Kiss D, Proscurshim I, Campos FG, Gama-Rodrigues JJ, Cecconello I. The role of carcinoembriogenic antigen in predicting response and survival to neoadjuvant chemoradiotherapy for distal rectal cancer. Dis Colon Rectum. 2009; 52:1137-1143.
38. Jang NY, Kang SB, Kim DW, Kim JH, Lee KW, Kim IA, Kim JS. The role of carcinoembryonic antigen after neoadjuvant chemoradiotherapy in patients with rectal cancer. Dis Colon Rectum. 2011; 54:245-252.
39. Yang KL, Yang SH, Liang WY, Kuo YJ, Lin JK, Lin TC, Chen WS, Jiang JK, Wang HS, Chang SC, Chu LS, Wang LW. Carcinoembryonic antigen (CEA) level, CEA ratio, and treatment outcome of rectal cancer patients receiving pre-operative chemoradiation and surgery. Radiat Oncol. 2013; 8:43.
40. Kim CW, Yu CS, Yang SS, Kim KH, Yoon YS, Yoon SN, Lim SB, Kim JC. Clinical significance of pre- to post-chemoradiotherapy s-CEA reduction ratio in rectal cancer patients treated with preoperative chemoradiotherapy and curative resection. Ann Surg Oncol. 2011; 18:3271-3277.
41. Rebischung C, Gerard JP, Gayet J, Thomas G, Hamelin R, Laurent-Puig P. Prognostic value of P53 mutations in rectal carcinoma. Int J Cancer. 2002; 100:131-135.
42. Kandioler D, Zwrtek R, Ludwig C, *et al*. TP53 genotype but not p53 immunohistochemical result predicts response to preoperative short-term radiotherapy in rectal cancer. Ann Surg. 2002; 235:493-498.
43. Komuro Y, Watanabe T, Hosoi Y, Matsumoto Y, Nakagawa K, Saito S, Ishihara S, Kazama S, Tsuno N, Kitayama J, Suzuki N, Tsurita G, Muto T, Nagawa H. Prediction of tumor radiosensitivity in rectal carcinoma based on p53 and Ku70 expression. J Exp Clin Cancer Res. 2003; 22:223-228.
44. Fu CG, Tominaga O, Nagawa H, Nita ME, Masaki T, Ishimaru G, Higuchi Y, Tsuruo T, Muto T. Role of p53 and p21/WAF1 detection in patient selection for preoperative radiotherapy in rectal cancer patients. Dis Colon Rectum. 1998; 41:68-74.
45. Huh JW, Lee JH, Kim HR. Pretreatment expression of 13 molecular markers as a predictor of tumor responses after neoadjuvant chemoradiation in rectal cancer. Ann Surg. 2014; 259:508-515.
46. Chen MB, Wu XY, Yu R, Li C, Wang LQ, Shen W, Lu PH. P53 status as a predictive biomarker for patients receiving neoadjuvant radiation-based treatment: A meta-analysis in rectal cancer. PLoS One. 2012; 7:e45388.
47. Rau B, Sturm I, Lage H, Berger S, Schneider U, Hauptmann S, Wust P, Riess H, Schlag PM, Dörken B, Daniel PT. Dynamic expression profile of p21WAF1/CIP1 and Ki-67 predicts survival in rectal carcinoma treated with preoperative radiochemotherapy. J Clin Oncol. 2003; 21:3391-3401.
48. Suzuki T, Sadahiro S, Tanaka A, Okada K, Kamata

H, Kamijo A, Murayama C, Akiba T, Kawada S. Biopsy specimens obtained 7 days after starting chemoradiotherapy (CRT) provide reliable predictors of response to CRT for rectal cancer. Int J Radiat Oncol Biol Phys. 2013; 85:1232-1238.
49. Luna-Perez P, Segura J, Alvarado I, Labastida S, Santiago-Payán H, Quintero A. Specific c-K-ras gene mutations as a tumor response marker in locally advanced rectal cancer treated with preoperative chemoradiotherapy. Ann Surg Oncol. 2000; 7:727-731.
50. Bengala C, Bettelli S, Bertolini F, Sartori G, Fontana A, Malavasi N, Depenni R, Zironi S, Del Giovane C, Luppi G, Conte PF. Prognostic role of EGFR gene copy number and KRAS mutation in patients with locally advanced rectal cancer treated with preoperative chemoradiotherapy. Br J Cancer. 2010; 103:1019-1024.
51. Gaedcke J, GradeM, Jung K, Schirmer M, Jo P, Obermeyer C, Wolff HA, Herrmann MK, Beissbarth T, Becker H, Ried T, Ghadimi M. KRAS and BRAF mutations in patients with rectal cancer treated with preoperative chemoradiotherapy. Radiother Oncol. 2010; 94:76-81.
52. Giralt J, Eraso A, Armengol M, Rosselló J, Majó J, Ares C, Espin E, Benavente S, de Torres I. Epidermal growth factor receptor is a predictor of tumor response in locally advanced rectal cancer patients treated with preoperative radiotherapy. Int J Radiat Oncol Biol Phys. 2002; 54:1460-1465.
53. Kim JS, Kim JM, Li S, Yoon WH, Song KS, Kim KH, Yeo SG, Nam JS, Cho MJ. Epidermal growth factor receptor as a predictor of tumor downstaging in locally advanced rectal cancer patients treated with preoperative chemoradiotherapy. Int J Radiat Oncol Biol Phys. 2006; 66:195-200.
54. Zlobec I, Vuong T, Compton CC, Lugli A, Michel RP, Hayashi S, Jass JR. Combined analysis of VEGF and EGFR predicts complete tumour response in rectal cancer treated with preoperative radiotherapy. Br J Cancer. 2008; 98:450-456.
55. Spindler KL, Nielsen JN, Lindebjerg J, Brandslund I, Jakobsen A. Prediction of response to chemoradiation in rectal cancer by a gene polymorphism in the epidermal growth factor receptor promotor region. Int J Radiat Oncol Biol Phys. 2006; 66:500-504.
56. Kurt A, Yanar F, Asoglu O, Balik E, Olgac V, Karanlik H, Kucuk ST, Ademoglu E, Yegen G, Bugra D. Low Mmp 9 and VEGF levels predict good oncologic outcome in mid and low rectal cancer patients with neoadjuvant chemoradiation. BMC Clin Pathol. 2012; 12:27.
57. Saigusa S, Tanaka K, Toiyama Y, Yokoe T, Okugawa Y, Kawamoto A, Yasuda H, Morimoto Y, Fujikawa H, Inoue Y, Miki C, Kusunoki M. Immunohistochemical features of CD133 expression: Association with resistance to chemoradiotherapy in rectal cancer. Oncol Rep. 2010; 24:345-350.
58. Hiroishi K, Inomata M, Kashima K, Yasuda K, Shiraishi N, Yokoyama S, Kitano S. Cancer stem cell-related factors are associated with the efficacy of pre-operative chemoradiotherapy for LARC. Exp Ther Med. 2011; 2:465-470.
59. Shinto E, Hashiguchi Y, Ueno H, Kobayashi H, Ishiguro M, Mochizuki H, Yamamoto J, Hase K. Pretreatment CD133 and cyclooxygenase-2 expression as the predictive markers of the pathological effect of chemoradiotherapy in rectal cancer patients. Dis Colon Rectum. 2011; 54:1098-1106.
60. Sprenger T, Conradi LC, Beissbarth T, Ermert H, Homayounfar K, Middel P, Rüschoff J, Wolff HA, Schüler P, Ghadimi BM, Rödel C, Becker H, Rödel F, Liersch T. Enrichment of CD133-expressing cells in rectal cancers treated with preoperative radiochemotherapy is an independent marker for metastasis and survival. Cancer. 2013; 119:26-35.
61. Vaupel P, Harrison L. Tumor hypoxia: Causative factors, compensatory mechanisms and cellular response. Oncologist. 2004; 9:4-9.
62. Havelund BM, Sørensen FB, Lindebjerg J, Spindler KL, Jakobsen A. Pretreatment HIF-1α and GLUT-1 expressions do not correlate with outcome after preoperative chemoradiotherapy in rectal cancer. Anticancer Res. 2011; 31:1559-1565.
63. Shioya M, Takahashi T, Ishikawa H, Sakurai H, Ebara T, Suzuki Y, Saitoh J, Ohno T, Asao T, Kuwano H, Nakano T. Expression of hypoxia-inducible factor 1α predicts clinical outcome after preoperative hyperthermo-chemoradiotherapy for LARC. J Radiat Res. 2011; 52:821-827.
64. Akiyoshi T, Kobunai T, Watanabe T. Predicting the response to preoperative radiation or chemoradiation by a microarray analysis of the gene expression profiles in rectal cancer. Surg Today. 2012; 42:713-719.
65. Ghadimi BM, Grade M, Difilippantonio MJ, Varma S, Simon R, Montagna C, Füzesi L, Langer C, Becker H, Liersch T, Ried T. Effectiveness of gene expression profiling for response prediction of rectal adenocarcinomas to preoperative chemoradiotherapy. J Clin Oncol. 2005; 23:1826-1838.
66. Watanabe T, Komuro Y, Kiyomatsu T, Kanazawa T, Kazama Y, Tanaka J, Tanaka T, Yamamoto Y, Shirane M, Muto T, Nagawa H. Prediction of sensitivity of rectal cancer cells in response to preoperative radiotherapy by DNA microarray analysis of gene expression profiles. Cancer Res. 2006; 66:3370-3374.
67. Kim IJ, Lim SB, Kang HC, Chang HJ, Ahn SA, Park HW, Jang SG, Park JH, Kim DY, Jung KH, Choi HS, Jeong SY, Sohn DK, Kim DW, Park JG. Microarray gene expression profiling for predicting complete response to preoperative chemoradiotherapy in patients with advanced rectal cancer. Dis Colon Rectum. 2007; 50:1342-1353.
68. Rimkus C, Friederichs J, Boulesteix AL, Theisen J, Mages J, Becker K, Nekarda H, Rosenberg R, Janssen KP, Siewert JR. Microarray-based prediction of tumor response to neoadjuvant radiochemotherapy of patients with LARC. Clin Gastroenterol Hepatol. 2008; 6:53-61.
69. Nishioka M, Shimada M, Kurita N, Iwata T, Morimoto S, Yoshikawa K, Higashijima J, Miyatani T. Gene expression profile can predict pathological response to preoperative chemoradiotherapy in rectal cancer. Cancer Genomics Proteomics. 2011; 8:87-92.
70. Kaneda S, Nalbantoglu J, Takeishi K, Shimizu K, Gotoh O, Seno T, Ayusawa D. Structural and functional analysis of the human thymidylate synthase gene. J Biol Chem. 1990; 265:20277-20284.
71. Saw RP, Morgan M, Koorey D, Painter D, Findlay M, Stevens G, Clarke S, Chapuis P, Solomon MJ. p53, deleted in colorectal cancer gene, and thymidylate synthase as predictors of histopathologic response and survival in low, locally advanced rectal cancer treated with preoperative adjuvant therapy. Dis Colon Rectum 2003; 46:192-202.

72. Negri FV, Campanini N, Camisa R, Pucci F, Bui S, Ceccon G, Martinelli R, Fumagalli M, Losardo PL, Crafa P, Bordi C, Cascinu S, Ardizzoni A. Biological predictive factors in rectal cancer treated with preoperative radiotherapy or radiochemotherapy. Br J Cancer. 2008; 98:143-147.
73. Bertolini F, Bengala C, Losi L, Pagano M, Iachetta F, Dealis C, Jovic G, Depenni R, Zironi S, Falchi AM, Luppi G, Conte PF. Prognostic and predictive value of baseline and posttreatment molecular marker expression in locally advanced rectal cancer treated with neoadjuvant chemoradiotherapy. Int J Radiat Oncol Biol Phys. 2007; 68:1455-1461.
74. Villafranca E, Okruzhnov Y, Dominguez MA, García-Foncillas J, Azinovic I, Martínez E, Illarramendi JJ, Arias F, Martínez Monge R, Salgado E, Angeletti S, Brugarolas A. Polymorphisms of the repeated sequences in the enhancer region of the thymidylate synthase gene promoter may predict down staging after preoperative chemoradiation in rectal cancer. J Clin Oncol. 2001; 19:1779-1786.
75. Stoehlmacher J, Goekkurt E, Mogck U, Aust DE, Kramer M, Baretton GB, Liersch T, Ehninger G, Jakob C. Thymidylate synthase genotypes and tumour regression in stage II/III rectal cancer patients after neoadjuvant fluorouracil-based chemoradiation. Cancer Lett. 2008; 272:221-225.
76. Hur H, Kang J, Kim NK, Min BS, Lee KY, Shin SJ, Keum KC, Choi J, Kim H, Choi SH, Lee MY. Thymidylate synthase gene polymorphism affects the response to preoperative 5-fluorouracil chemoradiationtherapy in patients with rectal cancer. Int J Radiat Oncol Biol Phys. 2011; 81:669-676.
77. Kim JC, Ha YJ, Roh SA, Cho DH, Choi EY, Kim TW, Kim JH, Kang TW, Kim SY, Kim YS. Novel single-nucleotide polymorphism markers predictive of pathologic response to preoperative chemoradiation therapy in rectal cancer patients. Int J Radiat Oncol Biol Phys. 2013; 86:350-357.
78. Buchholz TA, Stivers DN, Stec J, Ayers M, Clark E, Bolt A, Sahin AA, Symmans WF, Hess KR, Kuerer HM, Valero V, Hortobagyi GN, Pusztai L. Global gene expression changes during neoadjuvant chemotherapy for human breast cancer. J Cancer. 2002; 8:461-468.
79. Durand RE, Aquino-Parsons C. Predicting response to treatment in human cancers of the uterine cervix: Sequential biopsies during external beam radiotherapy. Int J Radiat Oncol Biol Phys. 2004; 58:555-560.
80. Havelund BM, Sørensen FB, Pløen J, Lindebjerg J, Spindler KL, Jakobsen A. Immunohistological expression of HIF-1α, GLUT-1, Bcl-2 and Ki-67 in consecutive biopsies during chemoradiotherapy in patients with rectal cancer. APMIS. 2013; 121:127-138.
81. Supiot S, Gouraud W, Campion L, Jezéquel P, Buecher B, Charrier J, Heymann MF, Mahé MA, Rio E, Chérel M. Early dynamic transcriptomic changes during preoperative radiotherapy in patients with rectal cancer: a feasibility study. World J Gastroenterol. 2013; 19:3249-3254.
82. Lambrecht M, Deroose C, Roels S, Vandecaveye V, Penninckx F, Sagaert X, van Cutsem E, de Keyzer F, Haustermans K. The use of FDG-PET/CT and diffusion-weighted magnetic resonance imaging for response prediction before, during and after preoperative chemoradiotherapy for rectal cancer. Acta Oncol. 2010; 49:956-963.

(Received October 30, 2013; Revised February 4, 2014; Accepted February 17, 2014)

Original Article

DOI: 10.5582/bst.8.24

Purification and refolding of anti-T-antigen single chain antibodies (scFvs) expressed in *Escherichia coli* as inclusion bodies

Noriyuki Yuasa, Tsubasa Koyama, Yoko Fujita-Yamaguchi*

Department of Applied Biochemistry, Tokai University School of Engineering, Hiratsuka, Kanagawa, Japan.

Summary **T-antigen (Galβ1-3GalNAcα-1-Ser/Thr) is an oncofetal antigen that is commonly expressed as a carbohydrate determinant in many adenocarcinomas. Since it is associated with tumor progression and metastasis, production of recombinant antibodies specific for T-antigen could lead to the development of cancer diagnostics and therapeutics. Previously, we isolated and characterized 11 anti-T-antigen phage clones from a phage library displaying human single-chain antibodies (scFvs) and purified one scFv protein, 1G11. More recently, we purified and characterized 1E8 scFv protein using a *Drosophila* S2 expression system. In the current study, four anti-T-antigen scFv genes belonging to Groups 1-4 were purified from inclusion bodies expressed in *Escherichia coli* cells. Inclusion bodies isolated from *E. coli* cells were denatured in 3.5 M Gdn-HCl. Solubilized His-tagged scFv proteins were purified using Ni^{2+}-Sepharose column chromatography in the presence of 3.5 M Gdn-HCl. Purified scFv proteins were refolded according to a previously published method of step-wise dialysis. Two anti-T-antigen scFv proteins, 1E6 and 1E8 that belong to Groups 1 and 2, respectively, were produced in sufficient amounts, thus allowing further characterization of their binding activity with T-antigen. Specificity and affinity constants determined using enzyme-linked immunosorbent assay (ELISA) and surface plasmon resonance (SPR), respectively, provided evidence that both 1E8 and 1E6 scFv proteins are T-antigen specific and suggested that 1E8 scFv protein has a higher affinity for T-antigen than 1E6 scFv protein.**

Keywords: T-antigen, ScFv, phage display, anti-carbohydrate antibodies, inclusion bodies

1. Introduction

Antibodies are a modular defense system that identifies and neutralizes foreign objects such as bacteria and viruses. Each antibody recognizes a specific, unique target antigen that binds at the antibody's antigen-binding site. This binding mechanism allows an antibody to tag a microbe and an infected cell to be attacked by other parts of the immune system as well as to directly neutralize its target. Antibodies contain variable domains characterized by structurally hypervariable regions, also known as complementarity determining regions (CDRs). The variable-region fragment (Fv fragment) is the smallest unit of an immunoglobulin molecule with functional antigen-binding activity. A single-chain variable fragment (scFv) consists of variable regions in the form of a heavy chain (VH) and a light chain (VL) that are joined by a flexible peptide linker and that are readily expressed in *E. coli* (*1*).

Alterations in cell surface carbohydrates are commonly found in cancerous tissues (*2*). T-antigen (Galβ1-3GalNAcα-1-Ser/Thr), also known as Thomsen-Friedenreich antigen (TF antigen), is an oncofetal antigen. It is commonly expressed as carbohydrate determinants of many adenocarcinomas and is also associated with tumor progression and metastasis (*3-5*). The availability of human antibodies against T-antigen would thus greatly facilitate the development of cancer diagnostics as well as cancer therapeutics.

In the authors' laboratory, phage display technology has been used to obtain scFv genes with specificities for carbohydrate moieties since many carbohydrates are self-antigens that seldom induce an immune response in animals (*6,7*). Genes encoding anti-Man3, anti-Lewis X,

**Address correspondence to:*
Dr. Yoko Fujita-Yamaguchi, Department of Applied Biochemistry, Tokai University School of Engineering, 4-1-1 Kitakaname, Hiratsuka, Kanagawa 259-1292, Japan.
E-mail: yokoyamaguchi@tokai-u.jp

anti-Tn-antigen, and anti-T-antigen scFv proteins have been isolated from a phage library displaying human scFvs that had been characterized after purification of scFv proteins expressed in different expression systems (*8-12*).

Escherichia coli expression systems are the most prevalent systems for production of recombinant proteins (*13,14*). Efficient microbial production systems have allowed the production of heterologous proteins in sufficient amounts for diagnostic and therapeutic purposes as well as for structural studies (*15-18*). When heterologous proteins were highly expressed in *E. coli*, however, the proteins tended to form inclusion bodies in the cytoplasm. Purification of recombinant proteins from inclusion bodies requires refolding processes that are rather tedious, although the current authors recently reported purification and characterization of scFv proteins (*19,20*).

Previously, 11 anti-T-antigen phage clones were isolated from a phage library and categorized into four groups using a gycolipid, Galβ1-3GalNAcα-hexaethylene glycol-3,5-bis-8-dodecyloxy benzamide (T-antigen E6-BDB) (*11*). Of those, Group 4 scFv protein (1G11) was expressed in *E. coli* from its phagemid and purified to near homogeneity (*11*). However, the level of expression of the 1G11 scFv protein in *E. coli* was not sufficient for further characterization. More recently, a Group 1 1E8 scFv protein was successfully expressed and purified in a *Drosophila* S2 expression system (*21*). To compare scFv proteins belonging to Groups 1-4, the current study expressed and purified four different types of anti-T-antigen scFv genes using an *E. coli* expression system. Of four scFv proteins purified, levels of expression of 1E6 and 1E8 scFv proteins were high enough for characterization of their binding specificity and affinity for T-antigen. Enzyme-linked immunosorbent assay (ELISA) and surface plasmon resonance (SPR) analyses confirmed the binding activity of both scFv proteins to various T-antigen-presenting conjugates. Affinity constants determined using SPR suggested that 1E8 scFv protein bound to T-antigen with one-order higher affinity than 1E6 scFv protein. These results may provide a basis for the future development of cancer diagnostics and therapeutics.

2. Materials and Methods

2.1. *Materials*

E. coli strain BL21(DE3), Benzonase® Nuclease, and the pET22b(+) expression vector were obtained from Novagen (Germany). The vector was modified to encode the *pel*B leader and His-tag at the C-termini. *E. coli* strain JM109 was obtained from TaKaRa BIO (Shiga, Japan). Bovine serum albumin (BSA), human immunoglobulin G (hIgG), Trizma base, guanidine hydrochloride (Gdn-HCl), tween 20, oxidized L-glutathione (GSSG), reduced L-glutathione (GSH), lysozyme, and 4-(2-hydroxyethyl)-1-piperazineethanesulfonic acid (HEPES) were purchased from Sigma-Aldrich (St Louis, MO, USA). The synthesis of neoglycolipids including T-antigen E6-BDB was previously described (11). Human serum albumin (HSA)-conjugated T-antigen was purchased from Glyco Tech (Gaithersburg, MD, USA). Ni^{2+}-Sepharose 6 Fast Flow, and SA sensor chips, and an amine coupling kit were obtained from GE Healthcare (Uppsala, Sweden). ABTS reagent was obtained from Roche Diagnostics K.K. (Basel, Switzerland). B-PER® reagent and His Probe-HRP were obtained from Thermo Fisher Scientific Inc. (Waltham, MA, USA). Anti His-tag mouse monoclonal antibody was purchased from Abcam (Cambridge, MA, USA). Dithiothreitol (DTT), L(+) arginine, carbenicillin, isopropyl-β-D-thiogalactopyranoside (IPTG), and other chemicals were obtained from Wako Pure Chemical Industries (Osaka, Japan).

2.2. *Anti T-antigen scFv-genes*

Anti-T-antigen scFv clones were obtained using a neoglycolipid, Galβ1-3GalNAcα-hexaethylene glycol-3,5-bis-8-dodecyloxy benzamide (T-antigen E6-BDB), as a probe from a phage library by panning and screening as previously described (*11*). Eleven phage clones were isolated and characterized using DNA sequencing and ELISA, which revealed four groups of clones with T-antigen binding activity. In this study, 1E8, 1E6, 1E10, and 1G11 scFv genes were selected as respective representatives of Groups 1, 2, 3, and 4 (*11*).

2.3. *Construction of scFv expression vectors for E. coli*

Four anti-T-antigen scFv genes, 1E8, 1E6, 1E10, and 1G11, were amplified by PCR from phagemids encoding respective scFv genes (*11*) as templates using corresponding sets of Fw and Rv primers as listed in Table 1. 1E8, 1E6, 1E10, and 1G11 scFv genes were ligated into *Bam*HI-*Not*I-digested pET22b to construct pET22b/1E8, pET22b/1E6, pET22b/1E10, and pET22b/1G11 expression vectors, respectively. *E. coli* JM109 and BL21(DE3) were used as host cells for plasmid preparation and expression of scFv proteins, respectively. The scFv sequences of pET22b/1E8, pET22b/1E6, pET22b/1E10, and pET22b/1G11 were confirmed by DNA sequencing.

2.4. *Expression, purification, and refolding of scFv proteins in E. coli BL21(DE3)*

E. coli BL21(DE3) cells transformed with pET22b/1E8, pET22b/1E6, pET22b/1E10, and pET22b/1G11 expression vectors were seeded into 60 mL of LB medium containing 50 μg/mL carbenicillin. After cells were grown to OD600 of ~0.5 by incubation at 37˚C

Table 1. PCR primers used for scFv gene cloning and vector construction

Primers	Sequences[a]
pET-1E6 Fw	5'-GCATGC*GGATCC*GCAGGTGCAGCTGGTGGAG
pET-1E6Rv	5'-GCATGC*GCGGCCGC*TTTGATATCCACTTTGGTCCCAGG
pET-1E8 Fw	5'-GCATGC*GGATCC*GCAGGTGCAGCTGCAGCAG
pET-1E8 Rv	5'-GCATGC*GCGGCCGC*TAGGACGGTCAGCTTGGT
pET-1E10 Fw	5'-GCATGC*GAATTC*GCAGGTGCAGCTACAGCAG
pET-1E10 Rv	5'-GCATGC*GCGGCCGC*TTTGATTTCCACCTTGGTCCCTG
pET-1G11 Fw	5'-GCATGC*GAATTC*GCAGGTGCAGCTGCAGGAGT
pET-1G11 Rv	5'-GCATGC*GCGGCCGC*TTTAATCTCCAGTCGTGTCCCT

[a] Underlined italic sequences are restriction sites for enzymes.

with shaking, expression of scFv proteins was induced by the addition of 1 mM IPTG. Bacterial cells were incubated for 4 h and then harvested by centrifugation at 2,900× g for 30 min, after which they were stored at -30˚C for future experiments. Inclusion bodies were prepared from the bacterial cells by suspension in B-per Bacterial Protein Extraction Reagent according to the manufacturer's protocol. Briefly, 2.5 mL of the reagent containing 500 μg of lysozyme and 63 U of benzonase per 1 g of wet cells was added to bacterial cells. After the mixture was gently shaken for 10 min, pellets were collected by centrifugation at 14,500× g for 20 min and these were then resuspended in 15 mL of 10-fold diluted B-per reagent. After the mixture was gently shaken for 10 min, pellets were collected as inclusion bodies by centrifugation at 14,500 g for 20 min.

Inclusion bodies were solubilized in 20 mM sodium phosphate buffer, pH 7.4, containing 3.5 M Gdn-HCl and 0.2 M NaCl (3.5 M Gdn-HCl buffer), and centrifuged at 14,500× g for 30 min. Ni^{2+}-Sepharose slurry (0.5 mL) was added to test tubes containing the supernatant. After the tubes were inverted overnight at 25˚C, the Ni^{2}-Sepharose slurry was packed into columns. The columns were washed thoroughly with 3.5 M Gdn-HCl buffer containing 40 mM imidazole. ScFv proteins were then eluted with 3.5 M Gdn-HCl buffer containing 500 mM imidazole and 5 mM DTT. The eluted proteins were refolded as described below according to the method previously described (*16*) with some modifications. The scFv proteins purified in the presence of 3.5 M Gdn-HCl were refolded by stepwise dialyses as follows. The concentrations of the affinity-purified denatured scFv proteins were adjusted to 3.3 mM in 3.5 M Gdn-HCl buffer. The denatured scFv proteins in 20 mL were dialyzed against 300 mL of 50 mM Tris-HCl buffer, pH 8.0, containing 0.2 M NaCl and 1 mM EDTA (dialysis buffer) in the presence of 2 M Gdn-HCl, and then stepwise dialysis was done against (i) 80 mL of the dialysis buffer containing 1 M Gdn-HCl, 0.4 M L-arginine, 1 mM GSSG, and 2 mM GSH; (*ii*) 80 mL of the dialysis buffer containing 0.5 M Gdn-HCl, 0.4 M L-arginine, 1 mM GSSG, and 2 mM GSH; and (*iii*) 300 mL of PBS (10 mM sodium phosphate buffer, pH 7.4, containing 0.15 M NaCl). Protein concentrations were determined with a Bio-Rad protein assay reagent using human IgG (Sigma-Aldrich) as standard protein.

2.5. *SDS-PAGE and Western blotting*

The purified scFv proteins were analyzed with SDS-PAGE (5-20 % gradient polyacrylamide gel) under reducing or non-reducing conditions. Separated proteins were stained with Coomassie Brilliant Blue (CBB). For immunoblotting, the proteins on the SDS-PAGE gel were transferred onto a polyvinylidene difluoride (PVDF) membrane (Millipore, Billerica, MA, USA). The membrane was blocked with PBS containing 3% BSA for 2 h at room temperature. The membrane was washed with PBS and then incubated with HRP-conjugated anti-His-Tag antibody at room temperature for 1 h. The membrane was washed five times with PBS containing 0.2% Tween 20. Bound primary antibodies were detected with HRP-conjugated secondary antibodies and color development using Ez West blue (ATTO Co., Tokyo, Japan). Alternatively, blotted scFv proteins were detected with His Probe-HRP.

2.6. *CD spectra of the purified scFv proteins*

CD measurements were performed with a J-820 CD spectrophotometer (JASCO Corporation, Japan). Far-UV CD spectra were recorded at 25˚C using 400 μL of each sample in a cuvette with a path length of 2 mm. Spectra were obtained after 10 scans and subtracted from the spectra of the buffer obtained under the same conditions. CD spectra were obtained for 1E6 and 1E8 scFv proteins in PBS buffer, pH 7.4.

2.7. *ELISA of the purified and refolded scFv proteins from E. coli cells binding to neoglycolipids or human IgA (hIgA)*

Wells of a 96-well plate were coated with T-antigen-, Tn-antigen-, and Man3-E6-BDB pre-mixed with E6-

BDB at a ratio of 50 pmol:450 pmol per well. E6-BDB was used as a control. 1E6 and 1E8 scFv proteins were diluted with 20 mM Tris-HCl containing 1% BSA and 0.005% Tween 20 to a concentration of 1.67 μM and incubated at 37˚C for 1 h. Unbound scFvs were washed three times with 200 μL of 10 mM Tris-buffered saline, pH7.4 (TBS). Anti-His-tag mouse monoclonal antibody was used as a primary antibody for detection of scFv proteins. After HRP-conjugated second antibody treatment, 100 μL of ABTS solution was added for color development. The reaction was stopped by 100 μL of 1% oxalic acid. Absorbance at 415 nm was measured with a plate reader (Bio-Rad, Hercules, CA, USA).

Alternatively, human immunoglobulin A (hIgA) was used as a natural glycoprotein ligand since IgA contains six varieties of *O*-glycans, including T-antigen, in the hinge region (*22*). Wells of a 96-well plate were coated with human IgA class 1 (50 μg/mL) and then blocked with 3% BSA/TBS. ScFv proteins at concentrations of 85 nM and 420 nM were added to the hIgA-immobilized wells and incubated at 37˚C for 1h. HRP-conjugated RCA_{120} lectin (1 μg/mL), which recognizes galactose residues at the non-reducing termini, was used as a positive control. Detection of bound scFvs or RCA was carried out as described above.

2.8. *SPR analyses of purified scFv proteins against T-antigen*

Real-time measurements of the binding of 1E8 and 1E6 scFv proteins to T-antigen were performed with SPR at 25˚C on a Biacore 3000 biosensor (GE Healthcare, Uppsala, Sweden) using 10 mM HEPES, pH 7.4, containing 150 mM NaCl and 0.005% Tween 20 (running buffer) at a flow rate of at 20 μL/min. T-antigen pre-immobilized on the sensor chip (D301: Galβ1-3GalNAcα1-6Glc) was purchased from SuDx-Biotec Corp. (Kagoshima, Japan). Since this sensor chip does not contain a dextran matrix, non-specific binding is minimized in comparison to sensor chips such as the CM5 or CM3 that are normally used. 1E6 and 1E8 scFv proteins were injected to T-antigen for 2 min, and then dissociation phases were observed. Alternatively, 1E6 scFv protein was measured using T-antigen biotin-immobilized on the sensor chip SA with glucose-biotin as a negative control. To reduce non-specific binding to the sensor chip surface, NaCl was added to the analyte solutions to reach a final concentration of 0.3 M NaCl. Samples were injected to ligands for 4 min, and then dissociation phases were observed.

During SPR experiments, flow cells were regenerated by injection of the running buffer containing 3.5 M Gdn-HCl followed by thorough washing with the running buffer. Kinetics parameters were calculated using BIAevaluation software version 3.2. These sensorgrams were fitted to a 1:1 Langmuir binding model using a simultaneous non-linear program.

3. Results

3.1. *Expression, purification, and refolding of anti T-antigen 1E8, 1E6, 1E10, and 1G11 scFv proteins from E. coli cells*

Anti T-antigen 1E8, 1E6, 1E10, and 1G11 scFv proteins were purified from inclusion bodies, prepared from 40 mL of the culture medium, by solubilization with 3.5 M Gdn-HCl. These scFv proteins were subjected to Ni^{2+}-Sepharose chromatography in the presence of 3.5 M Gdn-HCl and they were then refolded by stepwise dialysis (*19,23*). Figures 1A and B show comparable results of SDS-PAGE followed by Coomassie Brilliant Blue (CBB) staining and Western blot analyses for the four scFv proteins purified and refolded from the respective inclusion bodies. Figure 1 shows the starting material for the purification of the scFv proteins in the inclusion bodies (lane 1) as well as the scFv proteins

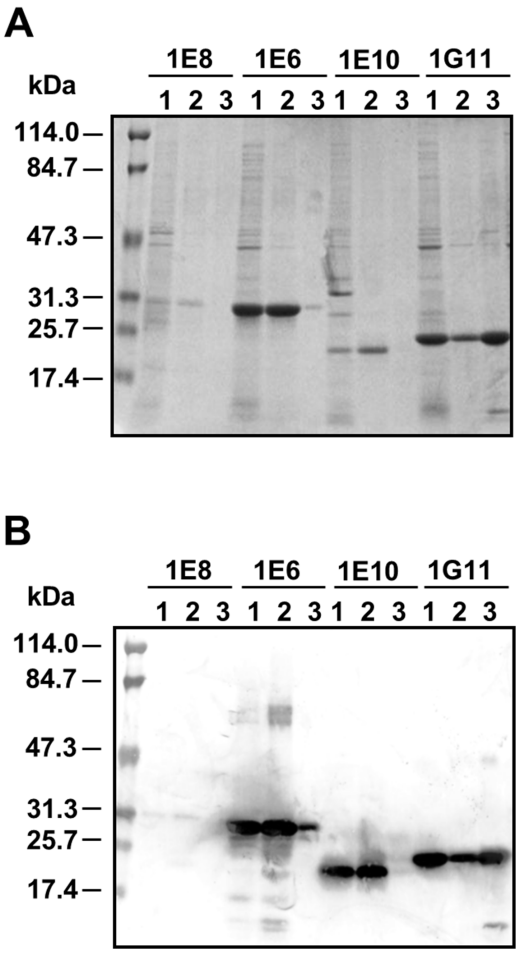

Figure 1. SDS-PAGE (A) and Western blot (B) analyses of 1E8, 1E6, 1E10, and 1G11 scFv proteins prepared from inclusion bodies by purification and refolding. Shown are results for inclusion bodies (lane 1) and soluble (lane 2) and insoluble (lane 3) fractions after purification and refolding. Proteins were visualized by CBB-staining **(A)**. Western blot analyses were carried out using an HRP-conjugated anti-His-tag mouse monoclonal antibody**(B)**.

Table 2. Summary of purification and refolding of scFv proteins expressed in *E. coli*

Items	scFv protein	1E8	1E6	1E10	1G11
Purification & refolding of scFvs from 60 mL culture	3.5 M Gdn-HCl soluble fractions (mg)	5.0	10.2	4.52	13.6
	Affinity-purified scFvs in 3.5 M Gdn-HCl (mg)	0.2	2.0	0.50	2.4
	Soluble fractions after refolding (mg) (% recovery from denatured scFvs)	0.2 (100)	1.9 (95)	0.53 (106)	0.31 (13)
Production yield of scFv protein (mg/L culture)		3.3	31.7	8.8	5.2

recovered from the soluble and insoluble fractions after refolding (lanes 2 and 3, respectively). A summary of purification and refolding of all four scFv proteins is presented in Table 2. 1E8, 1E6, and 1E10 scFv proteins were effectively recovered from the soluble fractions (Figure 1A, lane 2), indicating that most of the scFv proteins are folded. In contrast, 1G11 scFv protein was not readily recovered from the soluble fraction. While 1E8 expression was the lowest among the four scFv proteins, its efficient recovery from the soluble fraction allowed its further characterization. Each refolded scFv protein contained basically a single protein band (Figure 1), confirming it's near homogeneity. The molecular size of the 1E10 scFv protein was smaller than its theoretical molecular weight (Figure 1). 1E10 scFv protein moved faster than 1G11 scFv protein, which is an incomplete scFv lacking CDRs in its VL domain (*11*).

3.2. *Structural characterization of purified 1E6 and 1E8 scFv proteins*

CD spectroscopy was used to determine the secondary structures of the refolded scFv proteins (Figures 2A and 2B). Proteins with β-sheet structures are known to show a single negative peak with a minimum at 217 nm (*24*). The purified 1E6 and 1E8 scFv proteins showed a single negative peak with a minimum at approximately 217 nm. In the CD spectra, the molar ellipticity at 217 nm was −6,500 for the 1E6 scFv proteins and −2,500 for the 1E8 scFv proteins.

3.3. *Binding of the 1E6 and 1E8 scFv proteins to T-antigen according to ELISA and SPR*

ELISA was performed using two types of T-antigen ligands: synthetic and natural. First, the binding of scFv proteins to neoglycolipids was analyzed (Figure 3A). Both 1E6 and 1E8 scFv proteins bound to T-antigen E6-BDB but not to GalNAcα-E6-BDB (Tn-antigen-E6-BDB) or mannotoriose-E6 BDB (Man3-E6-BDB). Second, human IgA (hIgA)-containing galactose at the non-reducing termini was used to determine the T-antigen activity of the 1E8 and 1E6 scFv proteins (Figure 3B). A galactose-specific lectin, RCA_{120}, was used as the positive control. Results clearly demonstrated that the 1E6 scFv protein had binding activity to hIgA whereas

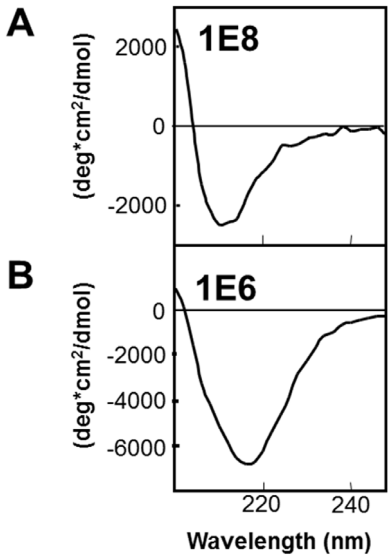

Figure 2. CD spectra of the purified and refolded scFv proteins. CD spectra of 1E8 and 1E6 scFv proteins were measured using 1E8 and 1E6 scFv proteins in PBS at 5.5 μM and 3.3 μM, respectively.

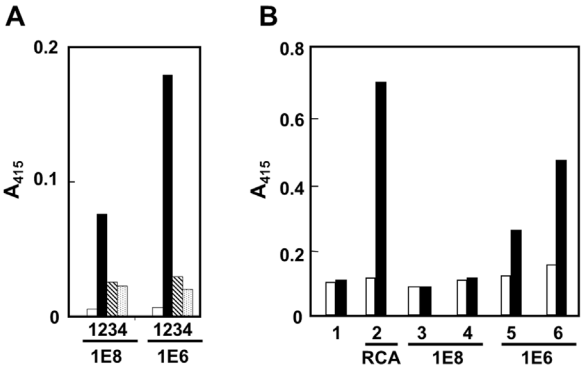

Figure 3. Binding of the purified and refolded scFv proteins to neoglycolipids (A) or human IgA (hIgA) (B) as analyzed with ELISA. In **(A)**, wells coated with E6-BDB (1; control; white bar), T-antigen-E6-BDB (2; black bar), Tn-antigen-E6-BDB (3; shaded bar), and Man3-E6-BDB (4; dotted bar) were incubated with 1E6 scFv or 1E8 scFv protein at a concentration of 1.67μM at 37˚C for 1 h. Anti-His-tag mouse monoclonal antibody was used as a primary antibody for detection of scFv proteins as described in the Methods. In **(B)**, hIgA containing six *O*-glycans in the hinge region was used as a glycoprotein anti-T-antigen substrate. 1E8 and 1E6 scFv proteins at 85 nM (3, 5) and 420 nM (4, 6) were analyzed. PBS and RCA_{120}-HRP (1μg/mL) were used as negative (1) and positive (2) control, respectively. White bars show binding to BSA (background control) whereas black bars show the binding of scFv proteins to hIgA.

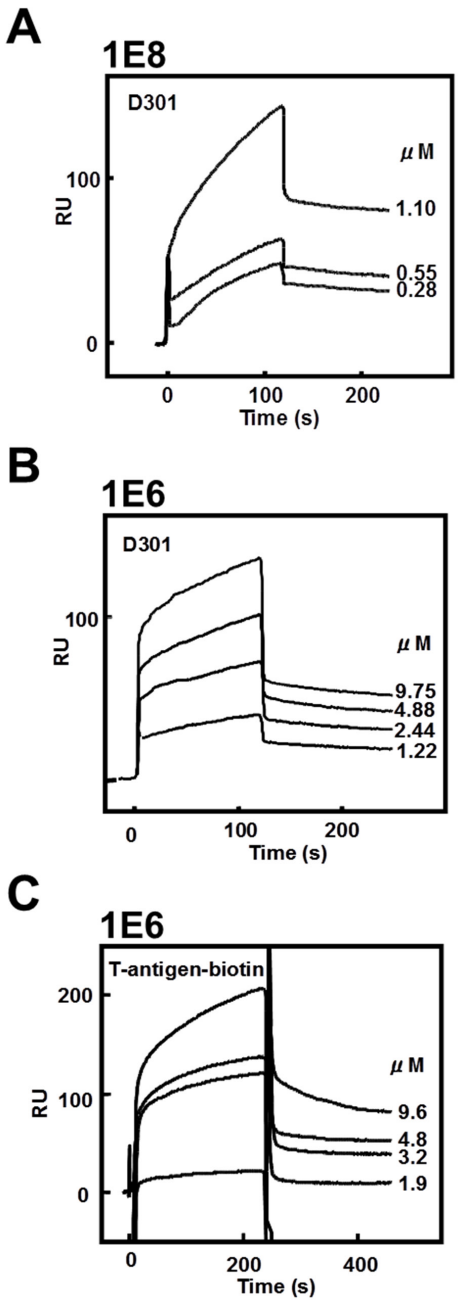

Figure 4. SPR analyses of purified and refolded 1E8 (A) and 1E6 scFv (B & C). Two different types of sensor chips were used: T-antigen immobilized sensor chip D301 **(A & B)** purchased from SuDx Biotec and T-antigen-biotin immobilized sensor chip SA. Binding of the purified and refolded 1E8 scFv **(A)** and 1E6 scFv **(B)** to D301 was measured at scFv protein concentrations of 0.28 μM, 0.55 μM, and 1.1 μM and 1.22 μM, 2.44 μM, 4.88 μM, and 9.75 μM, respectively. In **(C)**, the binding kinetics of 1E6 scFv protein were further analyzed using biotin-immobilized T-antigen on the SA sensor chip at concentrations of 1.9 μM, 3.2 μM, 4.8 μM, and 9.6 μM.

the 1E8 scFv protein did not.

SPR analyses were performed to further confirm the T-antigen binding activity of both the 1E6 and 1E8 scFv proteins (Figure 4). Kinetic parameters of 1E8 scFv and 1E6 scFv binding to T-antigen are summarized in Table 3. Both the 1E8 and 1E6 scFv proteins had good affinity for D301 (T-antigen-immobilized sensor chip) (Figures 4A and 4B, respectively), as indicated by respective *KD* values of 8.3×10^{-8} M and 1.3×10^{-6} M (Table 3). 1E6 scFv protein was analyzed using the biotinylated T-antigen sensor chip (Figure 4C) and was found to have $KD = 8.0 \times 10^{-7}$ M (Table 3).

4. Discussion

The current authors and their colleagues previously isolated genes encoding human scFv proteins with specificity against various carbohydrate moieties from a phage library displaying human scFv proteins (*8-12*). Eleven anti-T-antigen phage clones were isolated from a phage library and categorized into four groups (*11*). An anti-T-antigen 1G11 scFv protein from Group 4 was purified by DEAE-cellulose and Ni^{2+}-Sepharose affinity chromatography from the solubilized fraction of *E. coli* cells transfected with a phagemid bearing the 1G11 scFv gene (*11*). More recently, a Group 1 1E8 scFv protein was successfully expressed and purified in a *Drosophila* S2 expression system (*21*).

The current study used an *E.coli* expression system to purify and characterize four anti-T-antigen scFv proteins from Groups 1-4 (*11*). Two anti-T-antigen scFv proteins, 1E8 and 1E6 respectively belonging to Groups 1 and 2, were successfully purified for further characterization. *E. coli* strains, such as BL21(DE3), produce native bacterial proteins that exhibit a high affinity for divalent cations like nickel. Such native bacterial proteins may be co-purified with His-tagged recombinant proteins *via* Ni^{2+}-Sepharose chromatography (*25*). The use of inclusion bodies consisting of mostly recombinant proteins as the starting material could help avoid this problem of contamination. Inclusion bodies were denatured under mild conditions in 3.5 M Gdn-HCl and His-tagged scFv proteins were purified using Ni^{2+}-Sepharose column chromatography in the presence of 3.5 M Gdn-HCl. The purified scFv proteins were refolded by step-wise dialysis in the presence of arginine according to previously reported procedures (*23*). As shown in Table 2, 1E6 scFv protein was purified with the highest yield

Table 3. Kinetics parameters of 1E8 scFv and 1E6 scFv binding to T-antigen

scFv protein/Ligand	*ka* (1/Ms)	*kd* (1/s)	*KD* (M)	Sensorgrams
1E8/D301	8.8×10^{3}	7.3×10^{-4}	8.3×10^{-8}	Figure 4A
1E6/ D301	5.5×10^{2}	7.2×10^{-4}	1.3×10^{-6}	Figure 4B
1E6/ T-antigen biotin	1.1×10^{3}	9.2×10^{-4}	8.0×10^{-7}	Figure 4C

among the four scFv proteins. The level of production, 30 mg from a 1 L culture, was within the range expected from this procedure. Interestingly, when an alternative *Drosophila* S2 cells expression system was used to produce anti-T-antigen scFv proteins, we found that in contrast to this study, properly-folded 1E8 scFv protein was more efficiently expressed than 1E6 scFv protein (*21*).

The secondary structure formed by the refolded 1E8 and 1E6 scFv proteins was assessed using CD spectrometry. The far-UV CD spectra of the refolded scFv proteins revealed that both scFvs possess a β-sheet structure that is characteristic of such immunoglobulin fragments (*24,26*). The CD spectrum of 1E6 scFv indicates that it has a β-sheet structure with most of its proteins folded correctly. The CD spectrum of 1E8 scFv indicates the presence of a β-strand structure that is not as deep. This CD spectrum indicates that both correctly folded and unfolded proteins may be present in the refolded 1E8 scFv sample, suggesting that improvements on refolding procedures are required for purification of 1E8 scFv protein from inclusion bodies. The 1E8 scFv protein expressed in *Drosophila* S2 cells, however, was found to be qualitatively much better than *E. coli*-expressed and properly refolded as judged by CD and NMR (*21*).

1E10 scFv protein should have a molecular mass similar to those of 1E6 and 1E8, but the 1E10 scFv protein moved faster than both 1E6 and 1E8 scFv proteins according to SDS-PAGE (Figure 1). This indicates that the expressed 1E10 scFv protein may not be intact. There is no apparent explanation for the production of 1E10 scFv protein with a smaller molecular mass, so further study is needed.

Both 1E8 and 1E6 scFv proteins specifically bound to T-antigen-E6-BDB, which was the T-antigen probe used to screen phages displaying scFv proteins (Figure 3A). When phage antibodies representing 1E8, 1E6, 1E10, or 1G11 scFv proteins were originally analyzed for specificity, 1E8, 1E6, and 1E10 bound to T- and Tn-antigen equally whereas 1G11 bound specifically to T-antigen (*11*). The results of the current study confirm that both 1E8 and 1E6 scFv proteins exhibit T-antigen specificity. 1E6 scFv bound to hIgA, but binding of 1E8 scFv to hIgA was not detected (Figure 3B). The reason for the poor binding of 1E8 scFv protein to hIgA is not apparent. The binding activity of 1E8 scFv protein with T-antigen has been confirmed since it bound to T-antigen moieties conjugated to lipid (Figure 3A) and gold surfaces (Figure 4A).

Table 3 summarizes the kinetic parameters calculated from the sensorgrams shown in Figure 4. The results indicate that the 1E6 scFv protein bound similarly to T-antigen that was immobilized covalently on the gold surface (D301), or *via* biotin to SA, with a *KD* of approximately 1×10^{-6} M. 1E8 scFv bound to D301 with an affinity of approximately 1×10^{-7} M. These results demonstrate that both 1E6 and 1E8 scFv proteins have a definite affinity for T-antigen, with the former having a lower affinity (one order) than the latter. Since protein-carbohydrate interactions are generally weak, these human scFv proteins with rather high affinities for oncofetal T-antigen have high potential for future development of cancer therapeutics. For example, an anti-T-antigen monoclonal antibody JAA-F11 has been shown to block the adhesion of human and mouse tumor cells in metastatic models in *in vitro* and *in vivo* studies (*27*). Further characterization of 1E8 and 1E6 scFv proteins, their affinity improvement, and their effects on tumor growth and metastasis will be needed for future clinical application of these scFv proteins.

In conclusion, this study successfully purified and compared four anti-T-antigen scFv proteins from inclusion bodies expressed in *E. coli* cells. Although four anti-T-antigen scFv genes belonging to Groups 1-4 were expressed and produced in an *E. coli* expression system, 1E6 and 1E8 scFv proteins were produced at sufficient levels for further characterization of their T-antigen binding. Specificity and affinity constants determined using ELISA and SPR, respectively, provided evidence that Group 1 and 2 scFv proteins are T-antigen-specific and suggested that 1E8 scFv protein has a higher affinity for T-antigen than 1E6 scFv protein.

Acknowledgements

The authors wish to thank Dr. Ayano Matsumoto-Takasaki for her significant contribution to the first part of this project. The authors also wish to thank Dr. Hitoo Iwase, Kitasato University Medical School, and Drs. Hiroko Kawakami and Kazunori Toma, the Noguchi Institute, for providing IgA and neoglycolipids, respectively. Finally, the authors wish to thank Drs. Hiroshi Kamiguchi and Tadayuki Sato, Education and Research Support Center of Tokai University, for their valuable technical assistance. This work was supported by a grant 22570125 from the Japan Society of the Promotion of Science (JSPS).

References

1. Huston JS, Levinson D, Mudgett-Hunter M, Tai MS, Novotný J, Margolies MN, Ridge RJ, Bruccoleri RE, Haber E, Crea R, Oppermann H, Protein engineering of antibody binding sites: recovery of specific activity in an anti-digoxin single-chain Fv analogue produced in *Escherichia coli*. Proc Natl Acad Sci U S A. 1988; 85:5879-5883.
2. Heimburg-Molinaro J, Lum M, Vijay G, Jain M, Almogren A, Rittenhouse-Olson K. Cancer vaccines and carbohydrate epitopes. Vaccine. 2011; 29:8802-8826.
3. Yu LG. The oncofetal Thomsen-Friendenreich carbohydrate antigen in cancer progression. Glycoconj J.

2007; 24:411-420.
4. Glinsky VV, Glinsky GV, Rittenhouse-Olson K, Huflejt ME, Glinskii OV, Deutscher SL, Quinn TP. The role of Thomsen-Friedenreich antigen in adhesion of human breast and prostate cancer cells to the endothelium. Cancer Res. 2001; 61:4851-4857.
5. Yu LG, Andrews N, Zhao Q, McKean D, Williams JF, Connor LJ, Gerasimenko OV, Hilkens J, Hirabayashi J, Kasai K, Rhodes JM. Galectin-3 interaction with Thomsen-Friedenreich disaccharide on cancer-associated MUC1 causes increased cancer cell endothelial adhesion. J Biol Chem. 2007; 282:773-781.
6. Deng SJ, MacKenzie CR, Sadowska J, Michniewicz J, Young NM, Bundle DR, Narang SA. Selection of antibody single-chain variable fragments with improved carbohydrate binding by phage display. J Biol Chem. 1994; 269:9533-9538.
7. Ravn P, Danielczyk A, Jensen KB, Kristensen P, Christensen PA, Larsen M, Karsten U, Goletz S. Multivalent scFv display of phagemid repertoires for the selection of carbohydrate-specific antibodies and its application to the Thomsen-Friedenreich antigen. J Mol Biol. 2004; 343:985-996.
8. Sakai K, Shimizu Y, Chiba T, Matsumoto-Takasaki A, Kusada Y, Zhang W, Nakata M, Kojima N, Toma K, Takayanagi A, Shimizu N, Fujita-Yamaguchi Y. Isolation and characterization of phage-displayed single chain antibodies recognizing nonreducing terminal mannose residues. 1. A new strategy for generation of anti-carbohydrate antibodies. Biochemistry. 2007; 46:253-262.
9. Zhang W, Matsumoto-Takasaki A, Kusada Y, Sakaue H, Sakai K, Nakata M, Fujita-Yamaguchi Y. Isolation and characterization of phage-displayed single chain antibodies recognizing nonreducing terminal mannose residues. 2. Expression, purification, and characterization of recombinant single chain antibodies. Biochemistry. 2007; 46:263-270.
10. Yuasa N, Zhang W, Goto T, Sakaue H, Matsumoto-Takasaki A, Kimura M, Ohshima H, Tsuchida Y, Koizumi T, Sakai K, Kojima T, Yamamoto K, Nakata M, Fujita-Yamaguchi Y. Production of anti-carbohydrate antibodies by phage display technologies: potential impairment of cell growth as a result of endogenous expression. J Biol Chem. 2010; 285:30587-30597.
11. Matsumoto-Takasaki A, Horie J, Sakai K, Furui Y, Sato R, Kawakami H, Toma K, Takayanagi A, Shimizu N, Fujita-Yamaguchi Y. Isolation and characterization of anti-T-antigen single chain antibodies from a phage library. Biosci Trends. 2009; 3:87-95.
12. Sakai K, Yuasa N, Tsukamoto K, Takasaki-Matsumoto A, Yajima Y, Sato R, Kawakami H, Mizuno M, Takayanagi A, Shimizu N, Nakata M, Fujita-Yamaguchi Y. Isolation and characterization of antibodies against three consecutive Tn-antigen clusters from a phage library displaying human single-chain variable fragments. J Biochem. 2010; 147:809-817.
13. Baneyx F. Recombinant protein expression in *Escherichia coli*. Curr Opin Biotechnol. 1999; 10:411-421.
14. Chen R. Bacterial expression systems for recombinant protein production: E. coli and beyond. Biotechnol Adv. 2012; 30:1102-1107.
15. Colcher D, Pavlinkova G, Beresford G, Booth BJM, Choudhury A, Batra SK. Pharmacokinetics and biodistribution of genetically-engineered antibodies. Q J Nucl Med. 1998; 42:225-241.
16. Huston JS, George AJ, Adams GP, Stafford WF, Jamar F, Tai MS, McCartney JE, Oppermann H, Heelan BT, Peters AM, Houston LL, Bookman MA, Wolf EJ, Weiner LM. Single-chain Fv radioimmunotargeting. Q J Nucl Med. 1996; 40:320-333.
17. Dana Jones S, Marasco WA. Antibodies for targeted gene therapy: extracellular gene targeting and intracellular expression. Adv Drug Deliv Rev. 1998; 31:153-170.
18. Subedi GP, Satoh T, Hanashima S, Ikeda A, Nakada H, Sato R, Mizuno M, Yuasa N, Fujita-Yamaguchi Y, Yamaguchi Y. Overproduction of anti-Tn antibody MLS128 single-chain Fv fragment in *Escherichia coli* cytoplasm using a novel pCold-PDI vector. Protein Expr Purif. 2012; 82:197-204.
19. Matsumoto-Takasaki A, Yuasa N, Katagiri D, Koyama T, Sakai K, Zamri N, Phung S, Chen S, Nakada H, Nakata M, Fujita-Yamaguchi Y. Characterization of three different single chain antibodies recognizing non-reducing terminal mannose residues expressed in Escherichia coli by an inducible T7 expression system. J Biochem. 2011; 150:439-450.
20. Yuasa N, Ogawa H, Koizumi T, Tsukamoto K, Matsumoto-Takasaki A, Asanuma H, Nakada H, Fujita-Yamaguchi Y. Construction and expression of anti-Tn-antigen-specific single-chain antibody genes from hybridoma producing MLS128 monoclonal antibody. J Biochem. 2012; 151:371-381.
21. Yuasa N, Koyama T, Subedi GP, Yamaguchi Y, Matsushita M, Fujita-Yamaguchi Y. Expression and structural characterization of anti-T-antigen single chain antibodies (scFvs) and analysis of their binding to T-antigen by surface plasmon resonance and NMR spectroscopy. J Biochem. 2013; 154:521-529.
22. Takahashi K, Hiki Y, Odani H, Shimozato S, Iwase H, Sugiyama S, Usuda N. Structural analyses of *O*-glycan sugar chains on IgA1 hinge region using SELDI-TOFMS with various lectins. Biochem Biophys Res Commun. 2006; 350:580-587.
23. Umetsu M, Tsumoto K, Hara M, Ashish K, Goda S, Adschiri T, Kumagai I. How additives influence the refolding of immunoglobulin-folded proteins in a stepwise dialysis system. Spectroscopic evidence for highly efficient refolding of a single-chain Fv fragment. J Biol Chem. 2003; 278:8979-8987.
24. Venyaminov SY, Yang JT. Determination of protein secondary structure. In: Fasman GD (ed) Circular dichroism and the conformational analysis of biomolecules. Plenum, New York, USA, 1996; pp. 69-107.
25. Bolanos-Garcia VM, Davies OR. Structural analysis and classification of native proteins from *E. coli* commonly co-purified by immobilized metal affinity chromatography. Biochim Biophys Acta. 2006; 1760:1304-1313.
26. Ben Naya R, Matti K, Guellier A, Matagne A, Boquet D, Thomas D, Friboulet A, Avalle B, Padiolleau-Lefèvre S. Efficient refolding of a recombinant abzyme: Structural and catalytic characterizations. Appl Microbiol Biotechnol. 2013; 97:7721-7731.
27. Heimburg J, Yan J, Morey S, Glinskii OV, Huxley VH, Wild L, Klick R, Roy R, Glinsky VV, Rittenhouse-Olson K. Inhibition of Spontaneous Breast Cancer Metastasis by Anti-Thomsen-Friedenreich Antigen Monoclonal Antibody JAA-F111. Neoplasia. 2006; 8:939-948.

(Received October 13, 2013; Revised January 17, 2014; Accepted February 3, 2014)

Original Article

DOI: 10.5582/bst.8.32

Cytokines as potential biomarkers of liver toxicity induced by *Dioscorea bulbifera* L.

Yuchen Sheng[2], Yibo Ma[1], Zhongping Deng[2], Zhengtao Wang[1], Lili Ji[1,*]

[1] *The MOE Key Laboratory for Standardization of Chinese Medicines and Shanghai Key Laboratory of Complex Prescription, Institute of Chinese Materia Medica, Shanghai University of Traditional Chinese Medicine, Shanghai, China;*
[2] *Center for Drug Safety Evaluation and Research, Shanghai University of Traditional Chinese Medicine, Shanghai, China.*

Summary **The present study is designed to search for the serum cytokine biomarker for liver injury induced by *Dioscorea bulbifera* L., which is a traditionally used herbal medicine in China. Mice were orally given various doses of ethyl acetate extract (EF) isolated from *D. bulbifera* for 12 days. The activity of serum alanine/aspartate transaminases (ALT/AST) was increased in EF (400 mg/kg)-treated mice. Histological assessment further confirmed EF (400 mg/kg)-induced liver injury. Results of a cytokine-antibody array demonstrated that there were 10 cytokines up-regulated and 1 cytokine down-regulated in EF (400 mg/kg)-treated mice. Enzyme-linked immunosorbent assay (ELISA) further confirmed the increased level of CD30 ligand (CD30L) and decreased level of interlukin-3 (IL-3) in EF-treated mice. In conclusion, our results demonstrate that the altered expression of CD30L and IL-3 may be potential biomarkers for hepatotoxicity induced by *D. bulbifera.***

Keywords: *Dioscorea bulbifera* L., hepatotoxicity, cytokines, CD30L, IL-3

1. Introduction

Dioscorea bulbifera L. is a native plant in Africa and Asia, and it is also an invasive species in many tropical areas, including Florida in the United States. *D. bulbifera* is generally used to treat thyroid disease (especially goiter) and cancer in clinics in China (*1*). However, during clinical practice *D. bulbifera* has been found to have hepatotoxicity, which has caused a great obstacle for its application in the clinic (*2*). Recently, study of the hepatotoxicity of *D. bulbifera* has attracted great interest. Our previous studies have already showed that an ethyl acetate extract (EF) isolated from *D. bulbifera* could induce oxidative stress liver injury (*3,4*). Meanwhile, our studies and other reports found that diterpenoids were the main hepatotoxic compounds in *D. bulbifera*, such as diosbulbin B and diosbulbin D (*3,5*).

**Address correspondence to:*
Dr. Lili Ji, The MOE Key Laboratory for Standardization of Chinese Medicines and Shanghai Key Laboratory of Complex Prescription, Institute of Chinese Materia Medica, Shanghai University of Traditional Chinese Medicine, 1200 Cailun Road, Shanghai 201203, China.
E-mail: lichenyue1307@126.com

Drug-induced liver injury (DILI) has been a public health issue for many years, and it is the major cause for withdrawal of approved drugs from the market and leads to blockage of development of potential drugs. Generally, herbal medicines are regarded as having no toxicity or side-effects, and they are increasingly used worldwide as dietary supplements (*6,7*). However, there are increased reports about the hepatotoxicity induced by herbal medicines. For example, herbal medicines as dietary supplements caused about 9% of cases of DILI, while in Asia the percentage was about 20-55% cases of DILI (*8,9*). Thus, liver injury induced by herbal medicines needs to be paid more attention.

Currently, conventional widely used biochemical markers for evaluating liver injury are serum alanine aminotransferase (ALT), aspartate aminotransferase (AST), and cholestatic markers such as alkaline phosphatase (ALP), and γ-glutamyltransferase (γGT) (*10,11*). However, all of these biomarkers sometimes can not accurately reflect liver injury (*11*). Serum ALT activity has also been associated with toxicity of other organs and thus it leads to false positives due to other sources of serum ALT activity because it has specificity beyond the liver (*12*). Meanwhile, there is a report that serum ALT activity is variable in people, which will also lead to possible false positive or negative results

(*13*). Thus, searching for more simple and sensitive biomarkers as a supplementary index for DILI is an urgent problem that needs to be solved.

Cytokines are a diverse group of soluble proteins, peptides or glycoproteins, which have various biological functions. Recently, innate and acquired immunity mediated by cytokines has been reported to play a critical role in DILI, and thus cytokines have the potential value as biomarkers for DILI (*14,15*). In the present study, we employed a cytokine-antibody array to search for potential cytokine biomarkers for liver injury induced by *D. bulbifera*.

2. Materials and Methods

2.1. *Chemicals and reagents*

The rhizomes of *D. bulbifera* were collected in Qingyang, Anhui Province and authenticated by Prof. Shou-Jin Liu (Anhui College of Traditional Chinese Medicine, Anhui, China). The specimens were deposited in the herbarium of the Institute of Chinese Materia Medica, Shanghai University of Traditional Chinese Medicine. The preparation of ethyl acetate extracts (EF) isolated from *D. bulbifera* was previously reported in our published papers, and the content of diosbulbin B is 13.72% (*16*). The kits for determining ALT/AST activity were obtained from Jiancheng Bioengineering Institute (Nanjing, Jiangsu, China). RayBio™ Mouse Cytokine Antibody Array III was purchased from RayBiotech, Inc. (Norcross, GA, USA). ELISA kits were purchased from RapidBio (West Hills, CA, USA). Other reagents unless indicated were purchased from Sigma Chemical Co. (St. Louis, MO, USA).

2.2. *Experimental animals*

Specific pathogen free male ICR mice (18-22 g body weight) were purchased from the Chinese Academy of Sciences (Shanghai, China). The mice were fed a standard laboratory diet and given free access to tap water, kept in a controlled room temperature (22 ± 1°C), humidity (65 ± 5%), and a 12:12-h light/dark cycle. All mice received humane care in compliance with the institutional animal care guidelines approved by the Experimental Animal Ethical Committee of Shanghai University of Traditional Chinese Medicine.

2.3. *Treatments of animals*

Mice were orally administered EF (100, 200, and 400 mg/kg, suspended in 0.5% CMC-Na, $n = 7$) for 12 days, and 0.5% CMC-Na was used as a vehicle control ($n = 8$). Animals were killed 24 h after the last administration. Blood was collected from the eyeball for measurement of ALT, AST, and cytokine analysis. Livers were collected for histological assessment.

2.4. *Serum ALT/AST analysis*

Blood samples obtained from mice of all groups were allowed to coagulate for 2 h on ice. Serum was then isolated following centrifugation at 840 × g for 15 min. Serum ALT, and AST activity were measured with kits according to the manufacturer's instructions.

2.5. *Histological examination*

Portions of the liver were fixed in 10% formalin and embedded in paraffin. Samples were subsequently sectioned (5 μm) and stained with hematoxylin-eosin (HE) for further histological analysis.

2.6. *Cytokine antibody array*

Serum cytokines were assayed by Raybio Mouse Cytokine Antibody Array III according to the manufacturer's instructions. This array is capable of simultaneously detecting 62 different cytokines with high specificity. Chemiluminescence signals were visualized by exposure to light sensitive films. Films were digitized, and densitometric quantifications were analyzed with ScanAlyze software, and then the ratio of EF/Control was calculated. Differentially expressed cytokines were defined as over 2 fold alteration between the control and EF-treated groups.

2.7. *ELISA analysis*

Serum was used for ELISA analysis according to the manufacturer's instructions.

2.8. *Statistical analysis*

The results were expressed as Means ± SEM. SPSS 18.0 was used for statistical analysis. Significance difference between various groups was determined by One-Way ANOVA, and between two groups was evaluated by an independent-sample *t*-test. $p < 0.05$ was considered as indicating statistically significant differences.

3. Results

3.1. *EF induced liver injury*

As shown in Figure 1A, EF (400 mg/kg) increased serum ALT and AST activity ($p < 0.001$). Further, histological assessment showed normal liver shape and structure in control mice (Figure 1B). EF (400mg/kg)-treated mice exhibited severe liver damage indicated by intrahepatic hemorrhage, lymphocyte infiltration and the destruction of liver structure (Figure 1B).

3.2. *Distinct serum cytokine expression in normal and EF-treated mice*

To identify the cytokine biomarker for *D. bulbifera*-induced liver injury, we analyzed the content of 62 cytokines in serum by a cytokine antibody array in control and EF (400 mg/kg)-treated mice. Table 1 is the layout of the cytokine antibody array, and Figure 2 is the results of the array. After analyzing, as shown in Table 2, ten cytokines were up-regulated and one cytokine was down-regulated over 2-fold in EF (400 mg/kg)-treated mice as compared to control. The up-regulated cytokines are CD30L, fractaline, interferon inducible monokine (CRG2), granulocyte macrophage colony-stimulating factor (GM-CSF), thymus-expressed chemokine (TECK), monocyte chemoattactant protein 5 (MCP-5), IL-4, IL-

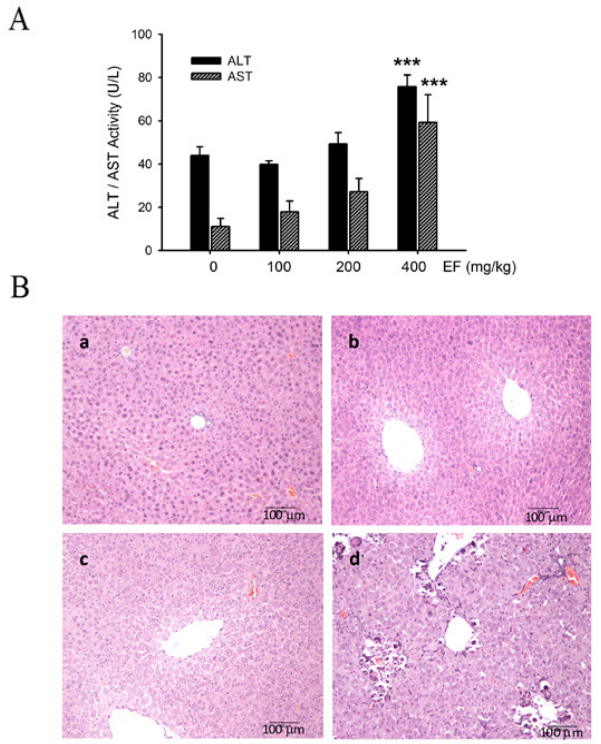

Figure 1. EF induced liver injury. (A) ALT and AST activity. Data are expressed as means ± SEM (n = 8 for control and n = 7 for experimental group). *** $p < 0.001$ compared with control. **(B)** Histological observation of EF-induced liver injury. **a**. Control; **b**. EF (100 mg/kg); **c**. EF (200 mg/kg); **d**. EF (400 mg/kg). Typical images were chosen from each experimental group. (original magnification: ×100).

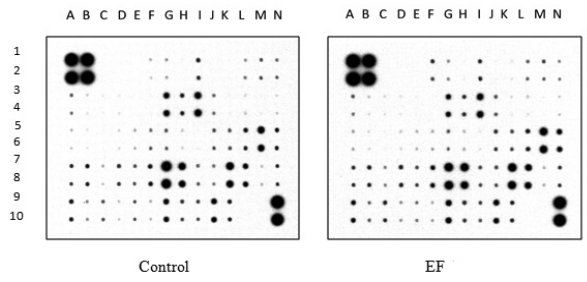

Figure 2. Results of cytokine antibody array. The images of control and EF (400 mg/kg)-treated mice in the cytokine antibody array. n = 8 for control and n = 7 for experimental group.

Table 1. The layout of cytokine antibody array

	A	B	C	D	E	F	G	H	I	J	K	L	M	N
1	POS	POS	NEG	NEG	Blank	Axl	BLC	CD30L	CD30T	CD40	CRG-2	CTACK	CXCL16	Eotaxin
2	POS	POS	NEG	NEG	Blank	Axl	BLC	CD30L	CD30T	CD40	CRG-2	CTACK	CXCL16	Eotaxin
3	Eotaxin -2	Fas ligand	Fractalkine	G-CSF	GM-CSF	IFNγ	IGFBP-3	IGFBP-5	IGFBP-6	IL-1α	IL-1β	IL-2	IL-3	IL-3Rb
4	Eotaxin-2	Fas ligand	Fractalkine	G-CSF	GM-CSF	IFNγ	IGFBP-3	IGFBP-5	IGFBP-6	IL-1α	IL-1β	IL-2	IL-3	IL-3Rb
5	IL-4	IL-5	IL-6	IL-9	IL-10	IL-12 p40/70	IL-12 p70	IL-13	IL-17	KC	Leptin R	Leptin	LIX	L Selectin
6	IL-4	IL-5	IL-6	IL-9	IL-10	IL-12 p40/70	IL-12 p70	IL-13	IL-17	KC	Leptin R	Leptin	LIX	L Selectin
7	Ln/XCL-1	MCP1	MCP-5	M-CSF	MIG	MIP-1α	MIP-1γ	MIP-2	MIP-3β	MIP-3α	PF-4	P Selectin	RANTES	SCF
8	Ln/XCL-1	MCP1	MCP-5	M-CSF	MIG	MIP-1α	MIP-1γ	MIP-2	MIP-3β	MIP-3α	PF-4	P Selectin	RANTES	SCF
9	SDF-1α	TARC	TCA-3	TECK	TIMP-1	TNFα	sTNFRI	sTNFRII	TPO	VCAM-1	VEGF	Blank	Blank	POS
10	SDF-1α	TARC	TCA-3	TECK	TIMP-1	TNFα	sTNFRI	sTNFRII	TPO	VCAM-1	VEGF	Blank	Blank	POS

Table 2. List of differentially changed cytokines between control and EF group

Row	Column	Cytokine symbol (Used on array)	Full name	The ratio (EF/Cont)
1,2	F	Axl	Axl receptor tyosine kinase	3.96
1,2	H	CD30L	CD30 ligand	2.22
1,2	K	CRG-2	Interferon inducible monokine	2.17
3,4	C	Fractalkine	-	2.20
3,4	E	GM-CSF	Granulocyte macrophage colony-stimulating factor	3.42
3,4	M	IL-3	Interleukin-3	0.26
5,6	A	IL-4	Interleukin-4	2.39
5,6	B	IL-5	Interleukin-5	2.02
5,6	C	IL-6	Interleukin-6	5.63
7,8	C	MCP-5	Monocyte chemoattactant protein 5	2.05
9,10	D	TECK	Thymus-expressed chemokine	2.11

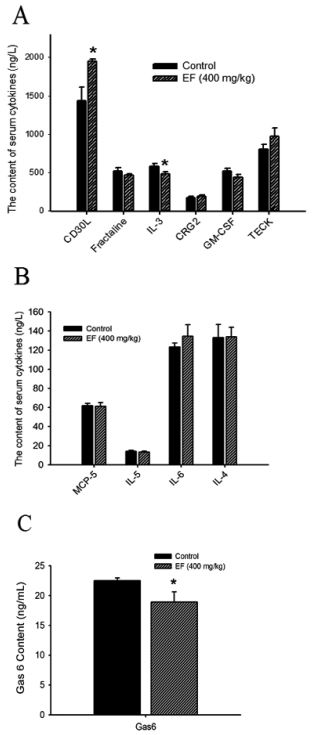

Figure 3. ELISA results. (A) The contents of serum CD30L, fractaline, IL-3, CRG-2, GM-CSF, TECK. **(B)** The contents of serum MCP-5, IL-5, IL-6, IL-4. **(C)** The content of serum Gas6. Data are expressed as means ± SEM (n = 8 for control and n = 7 for experimental group). * $p < 0.05$ compared with control.

5, IL-6, and axl receptor tyosine kinase (Axl), while the down-regulated cytokine is IL-3.

3.3. *ELISA assay of changed cytokine*

Next, ELISA assays were used to validate the change of those cytokines in the cytokine antibody array. Figure 3A showed that CD30L was increased and IL-3 was decreased in EF (400 mg/kg)-treated mice ($p < 0.05$), which is consistent with the results of the cytokine antibody array. There were no obvious changes of other cytokines such as fractaline, CRG2, GM-CSF, TECK, MCP-5, IL-5, IL-6, or IL-4 (Figures 3A and 3B), which is inconsistent with the results of the cytokine antibody array. Growth arrest-specific 6 (Gas 6), the ligand for axl receptor tyosine kinase (Axl), was decreased in EF (400 mg/kg)-treated mice ($p < 0.05$) in the ELISA assay (Figure 3C).

4. Discussion

In China, *D. bulbifera* is traditionally used to treat thyroid disease. Recently, *D. bulbifera* has been found to have a good therapeutic effect for some solid cancers, and now is commonly used in cancer therapy in the clinic. However, with the increased application of *D. bulbifera* in the clinic, its induced hepatotoxicity has widely attracted attention. The present study shows that after treatment with EF isolated from *D. bulbifera* for 12 days, serum ALT and AST activities were increased. Further, histological assessment demonstrated liver destruction in EF-treated mice. All of these results indicate the potential hepatotoxicity of *D. bulbifera*, when used for a stage treatment in cancer therapy.

Inflammation is reported to contribute to progressive liver damage induced by exogenous chemical hepatotoxins including drugs like acetaminophen, cycloheximide **etc**. (*17-20*). Cytokines are a family of secreted proteins that promote inflammation and participate in both innate and adaptive immune responses which play important roles in DILI (*15,21,22*). To our knowledge the present study is the first study using a cytokine antibody array to identify potential serum biomarkers for DILI. In the study, the primary screen using cytokine antibody array demonstrated 11 cytokines differentially altered after treatment with EF. Further, ELISA results confirmed that 2 cytokines were significantly changed after treatment with EF, which are CD30L and IL-3. The other 9 cytokines were not changed when measured by ELISA, which may be due to the limitations of the cytokine antibody array. There is already a report demonstrating that a linear response between the chemiluminescent signal and quantity may not always exist, which may lead to the false results shown in the cytokine antibody array (*23*), so further verification experiments such as ELISA are necessary.

CD30L is the ligand for CD30, which represents the newest member of the tumor necrosis factor receptor (TNF-R) family (*24*). Up-regulation of CD30/CD30L is associated with several hematological malignancies such as Hodgkin's disease (HD), anaplastic large cell lymphoma (ALCL) and subsets of Non-Hodgkin's lymphomas (NHL's) (*25*). Recently, the interaction of CD30/CD30L was reported to play some role in the crosstalk between natural killer and dendritic cells, and is critical for humoral immunity (*26,27*). Meanwhile, some studies demonstrate that CD30L/CD30 might be useful as a novel biological therapy for allergic rhinitis, inflammatory bowel disease, autoimmune diabetes, and chronic inflammatory skin diseases like psoriasis or atopic dermatitis (*28-31*). However, there is no report about whether there is some role of CD30L in liver injury. The present study found that serum CD30L was increased in EF-treated mice, which suggests potential involvement of CD30L in *D. bulbifera*-induced liver injury. This result is the first report about the potential role of CD30L in liver injury, and the concrete mechanism needs further investigation.

IL-3 is a key cytokine which promotes survival, proliferation, differentiation and maturity of bone marrow-derived hematopoietic stem cells, and thus it is widely studied to treat different states of bone marrow failure or hematologic malignancies (*32,33*). In addition, recent studies demonstrate that IL-3 participates in the response of the organism to various types of stress (*34*). Although there are already reports about the change of IL-3 in hemorrhage or alcohol-induced liver injury, the role of IL-3 in liver injury is still not clear (*35,36*). Our results demonstrate the down-regulation of serum IL-3 in EF-treated mice, which suggest potential involvement of IL-3 in *D. bulbifera*-induced liver injury.

In conclusion, the present study demonstrates that serum CD30L and IL-3 levels were up-regulated and down-regulated respectively in EF-treated mice, which demonstrates that inflammation may contribute to the liver injury induced by *D. bulbifera*, and the concrete mechanism needs further investigation.

Acknowledgements

This work was financially supported by the Program of Shanghai Municipal Education Commission (2012JW26); the Program for New Century Excellent Talents in University (NCET-11-1054); and State major science and technology special projects during the 12th five year plan (2012ZX09505001-002).

References

1. Jiangsu New Medical College. Chinese Dictionary (Second Volume). Shanghai Science and Technology Press, Shanghai, China, 1977; pp. 2059-2061.
2. Liu JR. Two cases of toxic hepatitis caused by *Dioscorea bulbifera L.* Adverse Drug Reactions J. 2002; 2:129-130.
3. Wang JM, Liang QN, Ji LL, Liu H, Wang CH, Wang ZT. Gender-related difference in liver injury induced by *Dioscorea bulbifera L*. rhizome in mice. Hum Exp Toxicol. 2011; 30:1333-1341.
4. Wang JM, Liu H, Ji LL, Wang ZT. Study of the hepatotoxicity induced by *Dioscorea bulbifera L*. rhizome in mice. BioSci Trends. 2010; 4:79-85.
5. Ma M, Jiang Z, Ruan J, Tan X, Liu J, Wang C, Zha XM, Zhang L. The furano norclerodane diterpenoid disobulbin-D induces apoptosis in normal human liver L-02 cells. Exp Toxicol Pathol. 2012; 64:611-618.
6. Su D, Li L. Trends in the use of complementary and alternative medicine in the United States: 2002-2007. J Health Care Poor Underserved. 2011; 22:296-310.
7. Nin Chau T, Cheung WI, Ngan T, Lin J, Lee KW, Tat Poon W, Leung VK, Mak T, Tse ML. Causality assessment of herb-induced liver injury using multidisciplinary approach and Roussel Uclaf Causality Assessment Method (RUCAM). Clin Toxicol (Phila). 2011; 49:34-39.
8. Chalasani N, Fontana RJ, Bonkovsky HL, Watkins PB, Davern T, Serrano J, Yang H, Rochon J. Causes, clinical features, and outcomes from a prospective study of drug-induced liver injury in the United States. Gastroenterology. 2008; 135:1924-1934.
9. Wai CT, Tan BH, Chan CL, Sutedja DS, Lee YM, Khor C, Lim SG. Drug-induced liver injury at an Asian center: A prospective study. Liver Int. 2007; 27:465-474.
10. Kim WR, Flamm SL, Di Bisceglie AM, Bodenheimer HC. Serum activity of alanine aminotransferase (ALT) as an indicator of health and disease. Hepatology. 2008; 47:1363-1370.
11. Cummings J, Ward TH, Greystoke A, Ranson M, Dive C. Biomarker method validation in anticancer drug development. Br J Pharmacol. 2008; 153:646-656.
12. Ozer J, Ratner M, Shaw M, Bailey W, Schomaker S. The current state of serum biomarkers of hepatotoxicity. Toxicology. 2008; 245:194-205.
13. Ruhl CE, Everhart JE. Diurnal variation in serum alanine aminotransferase activity in the US population. J Clin Gastroenterol. 2013; 47:165-173.
14. Chalasani N, Bjornsson E. Risk factors for idiosyncratic drug-induced liver injury. Gastroenterology. 2010; 138:2246-2259.
15. Laverty HG, Antoine DJ, Benson C. The potential of cytokines as safety biomarkers for drug-induced liver injury. Eur J Clin Pharmacol. 2010; 66:961-976.
16. Wang JM, Ji LL, Branford-White C, Wang ZY, Shen KK, Liu H, Wang ZT. Antitumor activity of *Dioscorea bulbifera L*. rhizome *in vivo*. Fitoterapia. 2012; 83:388-394.
17. Szabo G, Mandrekar P, Dolganiuc A. Innate immune response and hepatic inflammation. Semin Liver Dis. 2007; 27:339-350.
18. Prandota J. Important role of proinflammatory cytokines/other endogenous substances in drug-induced hepatotoxicity: Depression of drug metabolism during infections/inflammation states, and genetic polymorphisms of drug-metabolizing enzymes/cytokines may markedly contribute to pathology. Am J Ther. 2005; 12:254-261.
19. Jaeschke H, Williams CD, Ramachandran A, Bajt ML. Acetaminophen hepatotoxicity and repair: The role of sterile inflammation and innate immunity. Liver Int.

2012; 32:8-20.
20. Kumagai K, Kiyosawa, N, Ito K, Yamoto T, Teranishi M, Nakayama H, Manabe S. Influence of kupffer cell inactivation on cycloheximide-induced hepatic injury. Toxicology. 2007; 241:106-118.
21. Holt MP, Ju C. Mecahnsims of drug-induced liver injury. AAPS J. 2006; 8:E48-54.
22. Ju C, Reilly T. Role of immune reactions in drug-induced liver injury (DILI). Drug Metab Rev. 2012; 44:107-115.
23. Budowle B, Hudlow WR, Lee SB, Klevan L. Using a CCD camera imaging system as a recording device to quantify human DNA by slot hybridization. Biotechniques. 2001; 30:680-685.
24. Horie R, Watanabe T. CD30: Expression and function in health and disease. Semin Immunol. 1998; 10:457-470.
25. Oflazoglu E, Grewal IS, Gerber H. Targeting CD30/CD30L in oncology and autoimmune and infammatory diseases. Adv Exp Med Biol. 2009; 647:174-185.
26. Kennedy MK, Willis CR, Armitage RJ. Deciphering CD30 ligand biology and its role in humoral immunity. Immunology. 2006; 118:143-152.
27. Simhadri VL, Hansen HP, Simhadri VR, Reiners KS, Bessler M, Engert A, von Strandmann EP. A novel role for reciprocal CD30-CD30L signaling in the cross-talk between natural killer and dendritic cells. Biol Chem. 2012; 393:101-106.
28. Fuchiwaki T, Sun X, Fujimura K, Yamada H, Shibata K, Muta H, Podack ER, Kawauchi H, Yoshikai Y. The central role of CD30L/CD30 interactions in allergic rhinitis pathogenesis in mice. Eur J Immunol. 2011; 41:2947-2954.
29. Somada S, Muta H, Nakamura K, Sun X, Honda K, Ihara E, Akiho H, Takayanagi R, Yoshikai Y, Podack ER, Tani K. CD30 ligand/CD30 interaction is involved in pathogenesis of inflammtory bowel disease. Dig Dis Sci. 2012; 57:2031-2037.
30. Chakrabarty S, Nagata M, Yasuda H, Wen L, Nakayama M, Chowdhury SA, Yamada K, Jin Z, Kotani R, Moriyama H, Shimozato O, Yagita H, Yokono K. Critical roles of CD30/CD30L interactions in murine autoimmune diabetes. Clin Exp Immunol. 2003; 133:318-325.
31. Fischer M, Harvima IT, Carvalho RFS, Moller C, Naukkarinen A, Enblad G, Nilsson G. Mast cell CD30 ligand is upregualted in cutaneous inflammation and mediates degranulation-independent chemokine secretion. J Clin Invest. 2006; 116:2748-2756.
32. Eder M, Geissler G, Ganser A. IL-3 in the clinic. Stem cells. 1997; 15:327-333.
33. Johnson DE. Regulation of survival pathways by IL-3 and induction of apoptosis following IL-3 withdrawal. Front Biosci. 1998; 3:d313-324.
34. Bessler H, Bergman M, Salman H. Interleukin-3 and stress. Biomed Pharmacother. 2000; 54:299-304.
35. Anaya-Prado R, Toledo-Pereyra LH, Guo RF, Reuben J, Ward PA, Walsh J. The attentuation of hemorrhage-induced liver injury by exogenous nitric oxide, L-arginine, and inhibition of inducible nitric oxide synthase. J Invest Surg. 2003; 16:247-261.
36. Zhang XG, Xu P, Liu Q, Yu CH, Zhang Y, Chen SH, Li YM. Effect of tea polyphenol on cytokine gene expression in rats with alcoholic liver disease. Hepatobiliary Pancreat Dis Int. 2006; 5:268-272.

(Received December 5, 2013; Revised January 22, 2014; Accepted February 6, 2014)

Original Article

DOI: 10.5582/bst.8.38

The supercritical CO_2 extract from the skin of *Bufo bufo gargarizans* Cantor blocks hepatitis B virus antigen secretion in HepG2.2.15 cells

Xiaoyan Cui[1,2], Yoshinori Inagaki[2], Dongliang Wang[2], Jianjun Gao[2], Fanghua Qi[2], Bo Gao[3], Norihiro Kokudo[2], Dingzhi Fang[4], Wei Tang[2,4,*]

[1] *Translational Center for Stem Cell Research, Tongji Hospital, Department of Regenerative Medicine, Tongji University School of Medicine, Shanghai, China;*
[2] *Hepato-Biliary-Pancreatic Surgery Division, Department of Surgery, Graduate School of Medicine, The University of Tokyo, Bunkyo-ku, Tokyo, Japan;*
[3] *Anhui China Resources Jinchan Pharmaceutical Co., Ltd., Huaibei, Anhui, China;*
[4] *Department of Biochemistry and Molecular Biology, West China School of Preclinical and Forensic Medicine, Sichuan University, Chengdu, Sichuan, China.*

Summary **The skin of *Bufo bufo gargarizans* Cantor has long been used for the treatment of hepatitis B in China and supercritical carbon dioxide extraction (SC-CO_2) is widely used in extracting active ingredients from natural products. The aim of present study was to assess the anti-hepatitis B virus (HBV) effect of the supercritical CO_2 extract from the skin of *Bufo bufo gargarizans* Cantor (SCE-BC). Cytotoxicity of SCE-BC was analyzed using an MTT [3-(4,5-dimethylthiazol-2yl)-2,5-diphenyltetrazolium bromide] assay in HepG2.2.15 cells. The hepatitis B surface antigen (HBsAg), hepatitis B e antigen (HBeAg), and hepatitis B core-related antigen (HBcrAg) concentrations in cell culture medium were determined by chemiluminescent enzyme immunoassay. HBV mRNA in cells was determined using real-time polymerase chain reaction. SCE-BC concentrations below 10^{-2} μg/mL had no significant toxicity to HepG2.2.15 cells. SCE-BC at 10^{-4} μg/mL effectively inhibited the secretion of HBeAg by 23.36% on day 6. It was more potent than the positive control lamivudine (100 μg/mL) in terms of the inhibition of HBeAg and HBcrAg secretion on day 6. Consistent with the HBV antigen reduction, HBV mRNA expression was markedly inhibited in comparison to the control when HepG2.2.15 cells were treated with SCE-BC. Moreover, SCE-BC had greater inhibitory activity with respect to HBeAg than to HBsAg. Since HBeAg promotes immune tolerance and persistent infection during HBV infection, the present results suggest that immune tolerance induced by HBeAg might be overcome by SCE-BC. Therefore, SCE-BC warrants further investigation.**

Keywords: Hepatitis B virus, traditional Chinese medicine, *Bufo bufo gargarizans* Cantor, HepG2.2.15 cells

1. Introduction

Hepatitis B virus (HBV), a member of the hepadnavirus (hepatotropic DNA viruses) family, infects approximate 400 million people, making it the most common chronic infectious disease worldwide (*1*). Chronic HBV infection can lead to cirrhosis, liver failure, and hepatocellular carcinoma, accounting for more than a million global deaths annually (*2,3*). Currently, only several antiviral drugs, including interferon-α and lamivudine (3TC), have been approved for the treatment of hepatitis B. However, the therapeutic effect of interferon-α and 3TC may be accompanied by adverse effects and drug resistance following prolonged administration (*4,5*). Therefore, there remains an urgent need for alternative drugs against HBV. Traditional Chinese medicines (TCMs), widely used to treat

**Address correspondence to:*
Dr. Wei Tang, Hepato-Biliary-Pancreatic Surgery Division, Department of Surgery, Graduate School of Medicine, The University of Tokyo; 7-3-1 Hongo, Bunkyo-ku, Tokyo 113-8655, Japan.
E-mail: TANG-SUR@h.u-tokyo.ac.jp

hepatitis B in China and many parts of the world (*6*), could provide a great opportunity for screening safe and more effective anti-HBV agents.

The venom and skin of toad *Bufo bufo gargarizans* Cantor has long been used in TCM (*7,8*). Chansu, a preparation of toad venom, has been used for the treatment of canker sores, toothache, sinusitis, and local inflammations in China for many years (*7*). Cinobufacini (Huachansu), the aqueous extract of the *Bufo bufo gargarizans* Cantor skin, is a Chinese medicine and has been extensively used in clinics to treat a number of diseases, such as malignant tumors, chronic hepatitis B, and systemic and local infection (*9-12*). It is reported the negative conversion rates of HBsAg and HBeAg increased significantly in patients treated with cinobufacini compared to the control group (patients untreated with cinobufacini) (*13*). Moreover, abnormal serum hepatic enzyme levels significantly decreased after treatment. In our previous study, cinobufacini at 1 μg/mL effectively inhibited the secretion of HBsAg and HBeAg by 29.58 and 32.87% in HepG2.2.15 cells on day 6. It was more potent than lamivudine (100 μg/mL), which served as a positive control (*14*).

In recent years, some new techniques, including ultrasonic extraction and supercritical carbon dioxide extraction (SC-CO_2), are widely used in extracting active ingredients from traditional Chinese medicine. SC-CO_2 is a separation technique based on the enhanced solvating power of CO_2 above its critical point (*15*). This technology has advantage over traditional technology because of the non-toxic, non-flammable characteristics of CO_2 and its availability in high purity with low cost. Moreover, CO_2 has low critical temperature (31.1°C) and low critical pressure (73.8 bar). Therefore CO_2 can be treated as an ideal solvent for extraction of natural products (*16*). Our previous study indicates the aqueous extract of the *Bufo bufo gargarizans* Cantor skin cinobufacini possess significant activity against HBV (*15*). However, it is still unclear whether the supercritical CO_2 extract from the skin of *Bufo bufo gargarizans* Cantor (SCE-BC) possess the activity against HBV. In the present study, in order to search and develop more effective anti-HBV drug, SCE-BC was investigated for the inhibition of HBV replication and secretion of HBV antigen in HBV-infected hepatocytes.

2. Materials and Methods

2.1. *Drugs*

SCE-BC, which was prepared by extracting 10 g of the toad skin with dynamic extraction using 200 mL CO_2 at 40°C and 20 MPa followed by concentration to 1 mL, was obtained from Anhui China Resources Jinchan Pharmaceutical Co., Ltd. (Anhui, China). It was dissolved in dimethylsulfoxide (DMSO) as a 100 mg/mL stock solution and kept at 4°C. 3TC was from Moravek Biochemicals (Brea, CA, USA) and served as the positive control. Dilutions of the drugs were performed on the day of medium change. The final concentration of DMSO in the samples was less than 0.001% (v/v).

2.2. *Cell culture and treatment*

The human HBV-transfected cell line HepG2.2.15 (*17*) was maintained in RPMI 1640 medium supplemented with 10% fetal calf serum (both from Gibco-Invitrogen, Carlsbad, CA, USA), 100 units/mL penicillin, 100 μg/mL streptomycin, and 200 μg/mL G418 (all from Sigma, St Louis, MO, USA) at 37°C in a humidified incubator with 5% CO_2. Cells were maintained for 24 h before treatment to reach confluence. The confluent HepG2.2.15 cells were treated with SCE-BC or 3TC at various concentrations in serum-free medium for 3 days or 6 days. The culture medium was replaced with a fresh one on day 3, with or without (negative control conditions) different concentrations of SCE-BC or 3TC during the 6-day experiment.

2.3. *Cytotoxicity assay*

HepG2.2.15 cells were seeded in 96-well plates at a density of 1.5×10^4 per well and treated with different concentrations (10^{-4}, 10^{-3}, 10^{-2}, 10^{-1}, 1, or 10 μg/mL) of SCE-BC for 3 or 6 days. The cytotoxicity of SCE-BC was analyzed with an MTT [3-(4,5-dimethylthiazol-2yl)-2,5-diphenyltetrazolium bromide] assay using the Cell Proliferation Kit I (Roche, Mannheim, Germany) following the manufacturer's instructions. Each experiment was performed in triplicate. The cell viability was expressed as a percentage of the control.

2.4. *Measurement of HBV antigens*

HepG2.2.15 cells were seeded in 6-well plates at a density of 4.5×10^5 per well for measurement of HBV antigens. After incubation with various concentrations of SCE-BC or 3TC for 3 or 6 days, the culture medium was collected, cell debris was removed, and the result was stored at -70°C until analysis. Hepatitis B surface antigen (HBsAg), hepatitis B e antigen (HBeAg), and hepatitis B core-related antigen (HBcrAg) in culture supernatants of HepG2.2.15 cells were respectively measured with a Lumipulse® II or I kit or HBcrAg kit (Fuji Rebio, Tokyo, Japan). These kits use a method of chemiluminescent enzyme immunoassay (CLEIA) based on the chemiluminescent capture of specific antigen–antibody reactions.

2.5. *Quantification of HBV DNA in the culture medium*

The HBV viral load in culture supernatants of HepG2.2.15 cells was quantified with a HBV DNA

quantitative kit (SRL, Tokyo, Japan). This kit is based on transcription-mediated amplification and hybridization protection assay (*18*). Briefly, a mixture of 10 μL of cell culture supernatants or amplification standards, Sample Diluent I, Sample Diluent II, and Primer Reagent and 50 μL of oil were placed in a reaction tube. The tube was heated at 95°C for 10 min and then incubated at 37°C for 5 min. Neutralization reagent and reconstituted amplification reagent solution were added and the reaction mixture was incubated at 37°C for 3 h. RNA amplicons were detected with a hybridization protection assay. The measurement range was 3.7-8.7 log genome equivalent/mL (LGE/mL).

2.6. *Determination of HBV RNA*

Total RNA was isolated from HepG2.2.15 cells using Trizol reagent (Invitrogen) in accordance with the manufacturer's instructions. The mRNA was then reverse-transcribed to make cDNA using a QuantiTect Rev. Transcription Kit (Qiagen GmbH, Hilden, Germany) and oligo dT primer following the manufacturer's instructions. The cDNA was quantified using the Thermal Cycler Dice™ Real Time System (Takara, Shiga, Japan). The polymerase chain reaction (PCR) was performed using primers (synthesized by Invitrogen): HBV surface region F 5`-GCCAAAATTCGCAGTCC-3` and R 5`-ACGGGCAACATACCTT-3`; HBV core region F 5`-AGACCACCAAATGCCCCTAT-3` and R 5`-GATCTTCTGCGACGCGGCGA-3`; glyceraldehyde-3-phosphate dehydrogenase (GAPDH) (internal control) F (h) 5`-AGGGGTCATTgATGGCAACAATATCCA-3` and R (h) 5`-TTTACCAGAGTTAAAAGCAGCCCT GGTG-3`. Controls included water blanks and RNA extracts that were not subjected to reverse transcription. A series of dilutions of Topo-HBV plasmid containing HBV genes and Topo-GAPDH plasmid containing GAPDH cDNA were used to create standard curves for quantifying HBV and GAPDH mRNA levels, respectively. These plasmid concentrations were as follows (copy/μl): 10^2, 10^3, 10^4, 10^5, 10^6, 10^7, and 10^8. Taq readymix with SYBR green (Sigma, St Louis, MO, USA) was used to amplify and detect DNA during the reaction. Thermal cycling parameters for the HBV core region and GAPDH consisted of a hot start for 2 min at 94°C followed by 40 cycles of 9 °C for 15 s, 60°C for 30 s, and then 72°C for 40 s. Thermal cycling parameters for the HBV surface region consisted of a hot start for 2 min at 94°C followed by 45 cycles of 94°C for 15 s, 58°C for 30 s, and then 72°C for 30 s. Specificity of the polymerase chain reaction products was verified by melting curve analysis and agarose gel electrophoresis.

2.7. *Measurement of active components resibufogenin and cinobufagin using HPLC*

To compare active components resibufogenin and cinobufagin in cinobufacini and SCE-BC, we performed HPLC. HPLC conditions: reversed-phase COSMOSIL Cholester C-18 column (Waters, 4.6 mm × 150 mm, 5 μm); mobile phase, 45% acetonitrile; flow rate, 1 mL/min; detection wavelength, 200-400 nm.

2.8. *Statistical analysis*

All the items determined in this study were repeated at least three times, and the results were expressed as mean ± S.D. Statistical significance was determined using analysis of variance (ANOVA) or a rank sum test and an independent-samples *t* test. A value of $p < 0.05$ was considered statistically significant.

3. Results

3.1. *Cytotoxic effect of SCE-BC on HepG2.2.15 cell viability*

The viabilities of the HepG2.2.15 cells in the presence of different concentrations of SCE-BC were examined with a MTT assay. The results showed that SCE-BC concentrations below 10^{-2} μg/mL had no significant toxicity to HepG2.2.15 cells (Figure 1). SCE-BC significantly inhibited the growth of HepG2.2.15 cells at concentrations above 10^{-2} μg/mL. The cytotoxicity of SCE-BC was examined to determine the treatment concentrations in the following HepG2 2.2.15 cell culture experiments.

3.2. *Effects of SCE-BC on HBV antigens and DNA*

In this anti-HBV assay, HepG2.2.15 cells were treated with different concentrations of SCE-BC for 3 or 6 days. On day 3, SCE-BC at concentrations of 10^{-4} and 10^{-2} μg/mL had no action on HBsAg secretion in the culture medium (Table 1). On day 6, SCE-BC at concentrations of 10^{-4} μg/mL decreased HBsAg secretion by 8.08%

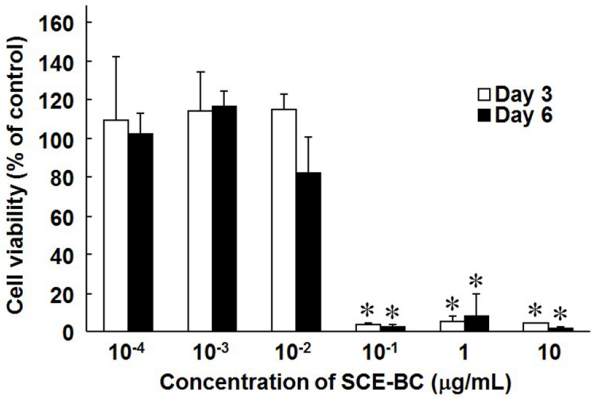

Figure 1. MTT cytotoxicity assay results of SCE-BC. The cell viability was expressed as a percentage of the control. Data shown represent the mean values (± S.D.) based on three independent experiments. Symbols represent statistical significance. * $p < 0.05$ *vs*. control using a rank sum test.

and the positive control 3TC (100 μg/mL) decreased HBsAg secretion by 21.88%. SCE-BC at concentrations of 10^{-4} and 10^{-2} μg/mL inhibited HBeAg secretion on day 3 and 6 (Table 2). Moreover, on day 6 SCE-BC at a concentration of 10^{-4} exhibited more potent activity than the positive control 3TC (100 μg/mL) in terms of the inhibition of HBeAg secretion. SCE-BC at a concentration of 10^{-4} decreased HBeAg secretion by 23.36% while 3TC at 100 μg/mL reduced the secretion of this antigen by 20.81%. Based on this analysis, SCE-BC has greater inhibitory activity with respect to HBeAg than to HBsAg. SCE-BC at concentrations of 10^{-4} and 10^{-2} μg/mL had no action on HBcrAg secretion in the culture medium on day 3 (Table 3). However, on day 6 SCE-BC exhibited more potent activity than the positive control 3TC (100 μg/mL) in terms of the inhibition of HBcrAg secretion. There were no significant differences between SCE-BC treatment and the control in terms of the HBV DNA levels in the culture medium (Table 4).

3.3. *Effect of SCE-BC on HBV mRNA expression*

To determine if the effects of SCE-BC on HBV antigen expression were induced by decreases in HBV RNA

Table 1. Inhibitory effect of SCE-BC on HBsAg secretion in HepG2.2.15 cells

Group	Dose (μg/mL)	Day 3		Day 6	
		(COI) × 10^2	Inhibition (%)	(COI) × 10^2	Inhibition (%)
Control	0	7.09 ± 0.09	–	12.86 ± 0.22	–
3TC	100	6.49 ± 0.18*	8.34	10.05 ± 0.22*	21.88
SCE-BC	10^{-2}	7.16 ± 0.18	–	13.31 ± 0.11	–
	10^{-4}	7.46 ± 0.16	–	11.82 ± 0.10*	8.08

COI: cut-off index. Data shown represent the mean values (± S.D.) based on three independent experiments. Symbols represent statistical significance. * $p < 0.05$ *vs*. control.

Table 2. Inhibitory effect of SCE-BC on HBeAg secretion in HepG2.2.15 cells

Group	Dose (μg/mL)	Day 3		Day 6	
		(COI) × 10^2	Inhibition (%)	(COI) × 10^2	Inhibition (%)
Control	0	1.06 ± 0.25	–	1.73 ± 0.32	–
3TC	100	0.98 ± 0.29	7.71	1.37 ± 0.17*	20.81
SCE-BC	10^{-2}	0.89 ± 0.06	16.18	1.49 ± 0.08	13.91
	10^{-4}	0.99 ± 0.09	6.02	1.32 ± 0.05*	23.36

COI: cut-off index. Data shown represent the mean values (± S.D.) based on three independent experiments. Symbols represent statistical significance. * $p < 0.05$ *vs*. control.

Table 3. Inhibitory effect of SCE-BC on HBcrAg secretion in HepG2.2.15 cells

Group	Dose (μg/mL)	Day 3		Day 6	
		(kU/mL) × 10^2	Inhibition (%)	(kU/mL) × 10^2	Inhibition (%)
Control	0	18.46 ± 0.24	–	58.46 ± 0.60	–
3TC	100	20.22 ± 0.05	–	48.30 ± 0.40*	17.38
SCE-BC	10^{-2}	19.34 ± 0.05	–	45.89 ± 0.10*,#	21.51
	10^{-4}	19.33 ± 0.15	–	40.37 ± 0.12*,#	30.94

Data shown represent the mean values (± S.D.) based on three independent experiments. Symbols represent statistical significance. * $p < 0.05$ *vs*. control. # $p < 0.05$ *vs*. 3TC (100 μg/mL).

Table 4. Inhibitory effect of SCE-BC on HBV DNA release in HepG2.2.15 cells

Group	Dose (μg/mL)	Day 3		Day 6	
		LGE × 10^2	Inhibition (%)	LGE × 10^2	Inhibition (%)
Control	0	5.4	–	5.9	–
3TC	100	5.2	36.90	5.1	84.15
SCE-BC	10^{-2}	5.4	–	6.0	–
	10^{-4}	5.5	–	5.9	–

LGE/mL: log genome equivalent/mL.

levels, real-time PCR analysis was performed using total RNA isolated from HepG2.2.15 cells. When treated with SCE-BC at a concentration of 10^{-4} μg/mL for 6 days, inhibition of HBV mRNA was observed with a 33.64% reduction in the HBV surface/GAPDH mRNA ratio and 61.06% reduction in the HBV core/GAPDH mRNA ratio in comparison to controls (Figure 2). These results showed that the HBV mRNA expression was markedly inhibited in comparison to the control when HepG2.2.15 cells were treated with SCE-BC at a lower concentration. This finding revealed that the inhibitory effects of SCE-BC on HBV antigens would be induced by the specific inhibition of HBV mRNA expression.

3.4. *Content of active components resibufogenin and cinobufagin*

The levels of resibufogenin and cinobufagin were measured using HPLC (Figure 3). The concentrations of resibufogenin and cinobufagin in cinobufacini were respectively 3.20 and 1.56 μg/g of the toad skin, while the concentrations of resibufogenin and cinobufagin in SCE-BC were respectively 121.17 and 33.43 μg/g of the toad skin. The levels of these two active components in SCE-BC were obviously higher than those in cinobufacini.

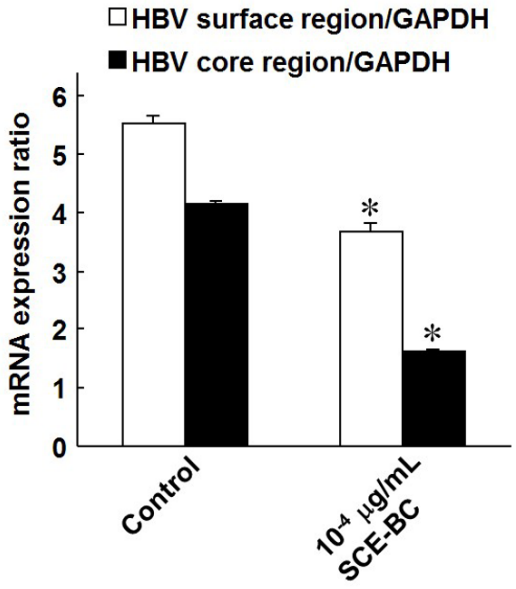

Figure 2. Effect of SCE-BC at a concentration of 10^{-4} μg/mL on the mRNA levels of HBV from the surface and core regions in HepG2.2.15 cells on day 6. Data shown represent the mean values (± S.D.) based on three independent experiments. Symbols represent statistical significance. * $p < 0.05$ *vs*. control using an independent-samples *t* test.

4. Discussion

The skin of toad *Bufo bufo gargarizans* Cantor (Bufonidae) has long been used in Chinese medicine for the treatment of hepatitis B in China (*11,13,19*) and its extract has also been considered to have the efficacy in the management of HBV infection (*20*). Our previous study indicates the aqueous extract of the *Bufo bufo gargarizans* Cantor skin, cinobufacini possess significant activity against HBV (*14*). In the present study, the anti-HBV activity of the supercritical CO_2 extract from the toad skin was evaluated in the HepG2.2.15 cell line. SCE-BC at a concentration of 10^{-4} μg/mL exhibited more potent activity than the positive control 3TC (100 μg/mL) in terms of the inhibition of HBeAg and HBcrAg secretion after treatment of HepG2.2.15 cells for 6 days. This effect of 3TC was consistent with that noted in a previous report (*21*). Moreover, no cytotoxicity was observed with SCE-BC at 10^{-4} μg/mL. These results clearly revealed that SCE-BC had anti-HBV properties and that its inhibitory activity was not induced by cytotoxicity. Although SCE-BC at 10^{-4} μg/mL exhibited lower activity than cinobufacini at 1 μg/mL in terms of the inhibition of HBsAg and HBeAg secretion (*14*), the concentration of SCE-BC was much lower than the concentration of cinobufacini used to treat HepG2.2.15 cells. Moreover, the levels of two active components resibufogenin and cinobufagin in SCE-BC were obviously higher than those in cinobufacini. The supercritical CO_2 extract from the toad skin produced 37-fold and 20-fold increase of the levels of resibufogenin and cinobufagin than the aqueous extract. Therefore, SCE-BC may have better anti-HBV effects than cinobufacini.

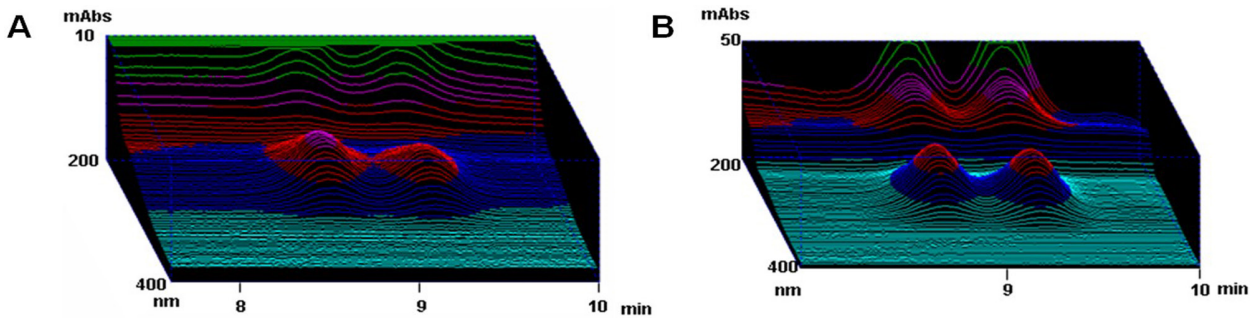

Figure 3. HPLC 3D chromatographic graph of cinobufacini and SCE-BC. (A) The concentrations of resibufogenin and cinobufagin in cinobufacini were respectively 3.20 and 1.56 μg/g of the toad skin. **(B)** The concentrations of resibufogenin and cinobufagin in SCE-BC were respectively 121.17 and 33.43 μg/g of the toad skin.

The effects of SCE-BC at a lower concentration (10^{-4} μg/mL) were more potent than those of this drug at a higher concentration (10^{-2} μg/mL) in terms of inhibiting HBV antigen secretion on day 6. This result could be explained by 18.30% of toxic effect induced by SCE-BC at 10^{-2} μg/mL on day 6. The impairment of cells might affect the release of HBV particles, which were increased.

In the present study, SCE-BC inhibited HBV antigen secretion. This role may take place at the transcription level (*22*). HBV enhancers, the transcriptional regulatory DNA fragments, may mediate the transcriptional suppression by binding several transcription factors. Alternatively, host's general transcription regulatory proteins, such as histone modification enzymes, epigenetic readers and transcription co-activators, are targeted to alter the transcription of a broad spectrum of host and viral genes (*23*). Therefore, the HBV mRNA level was determined in HepG2.2.15 cells in this study. Data demonstrated that in comparison to the control HBV mRNA levels were significantly decreased by SCE-BC. These results revealed that HBV antigen inhibition by SCE-BC was attributed to the specific inhibition of HBV mRNA expression. More work is needed to determine the mechanism of the transcriptional suppression.

In conclusion, the present study demonstrated that SCE-BC blocked HBV antigen secretion *in vitro*. This role of SCE-BC might take place at the transcription level. Moreover, SCE-BC had greater inhibitory activity with respect to HBeAg than to HBsAg. Since HBeAg promotes immune tolerance and persistent infection during HBV infection (*24*), the present results suggest that immune tolerance induced by HBeAg might be overcome by SCE-BC. Therefore, SCE-BC warrants further investigation.

Acknowledgements

The authors wish to thank Dr. Nobuyoshi Akimitsu (The University of Tokyo) for providing the Thermal Cycler Dice™ Real Time System for this study.

References

1. Bader T, Korba B. Simvastatin potentiates the anti-hepatitis B virus activity of FDA-approved nucleoside analogue inhibitors *in vitro*. Antiviral Res. 2010; 86:241-245.
2. Zhang CY, Zhong YS, Guo LP. Strategies to prevent hepatitis B virus infection in China: Immunization, screening, and standard medical practices. Biosci Trends. 2013; 7:7-12.
3. Song PP, Feng XB, Zhang KM, Song TQ, Ma KS, Kokudo N, Dong JH, Yao LN, Tang W. Screening for and surveillance of high-risk patients with HBV-related chronic liver disease: Promoting the early detection of hepatocellular carcinoma in China. Biosci Trends. 2013; 7:1-6.
4. Feld J, Locarnini S. Antiviral therapy for hepatitis B virus infections: new targets and technical challenges. J Clin Virol. 2002; 25:267-283.
5. Perrillo RP. Current treatment of chronic hepatitis B: benefits and limitations. Semin Liver Dis. 2005; 25 (Suppl.):20-28.
6. Zhang L, Wang G, Hou W, Li P, Dulin A, Bonkovsky HL. Contemporary clinical research of traditional Chinese medicines for chronic hepatitis B in China: An analytical review. Hepatology. 2010; 51:690-698.
7. Chen KK, Kovaríková A. Pharmacology and toxicology of toad venom. J Pharm Sci. 1967; 56:1535-1541.
8. Zhang J, Sun Y, Liu JH, Yu BY, Xu Q. Microbial transformation of three bufadienolides by *Nocardia sp*. and some insight for the cytotoxic structure–activity relationship (SAR). Bioorg Med Chem Lett. 2007; 17:6062-6065.
9. Qi FH, Li AY, Lv H, Zhao L, Li JJ, Gao B, Tang W. Apoptosis-inducing effect of cinobufacini, *Bufo bufo gargarizans* Cantor skin extract, on human hepatoma cell line BEL-7402. Drug Discov Ther. 2008; 2:339-343.
10. Dai LP, Gao HM, Wang ZM, Wang WH. Isolation and structure identification of chemical constituents from the skin of *Bufo bufo gargarizans*. Yao Xue Xue Bao. 2007; 42:858-861.
11. Lan YN. Long-term efficacy of cinobufacini for treatment of chronic hepatitis B. Chin J Clin Hepatol. 2002; 18:374-375.
12. Cui XY, Wang YL, Kokudo N, Fang DZ, Tang W. Traditional Chinese medicine and related active compounds against hepatitis B virus infection. Biosci Trends. 2010; 4:39-47.
13. Wang WM, Li RH. Clinical observation of cinobufacini injection on 118 patients with chronic hepatitis B. Mod J Integr Tradit Chin West Med. 2001; 10:1632-1633.
14. Cui XY, Inagaki Y, Xu HL, Wang DL, Qi FH, Kokudo N, Fang DZ, Tang W. Anti-hepatitis B virus activities of cinobufacini and its active components bufalin and cinobufagin in HepG2.2.15 cells. Biol Pharm Bull. 2010; 33:1728-1732.
15. Lenucci MS, Caccioppola A, Durante M, Serrone L, Leonardo R, Piroa G, Dalessandro G. Optimisation of biological and physical parameters for lycopene supercritical CO2 extraction from ordinary and high-pigment tomato cultivars. J Sci Food Agric. 2010; 90:1709-1718.
16. Marongiua B, Pirasa A, Porceddaa S, Falconierib D, Gonçalves MJ, Salgueiroc L, Maxiad A, Lai R. Extraction, separation and isolation of volatiles from Vitex agnus-castus L. (Verbenaceae) wild species of Sardinia, Italy, by supercritical CO2. Nat Prod Res. 2010; 24:569–579.
17. Sells MA, Chen ML, Acs G. Production of hepatitis B virus particles in Hep G2 cells transfected with cloned hepatitis B virus DNA. Proc Natl Acad Sci USA. 1987; 84:1005-1009.
18. Kamisango K, Kamogawa C, Sumi M, Goto S, Hirao A, Gonzales F, Yasuda K, Iino S. Quantitative detection of hepatitis B virus by transcription-mediated amplification and hybridization protection assay. J Clin Microbiol. 1999; 37:310-314.
19. Ji GS. Effect of lamivudine alone or in combination with cinobufacini on serum markers in patients with hepatitis B. Chin J Integrated Trad and Western Med on Liver

Diseases. 2005; 15:53-54.
20. Wang DL, Qi FH, Tang W, Wang FS. Chemical constituents and bioactivities of the skin of *Bufo bufo gargarizans* Cantor. Chem Biodivers. 2011; 8:559-567.
21. Wang S, Li J, Huang H, Gao W, Zhuang C, Li B, Zhou P, Kong D. Anti-hepatitis B virus activities of astragaloside IV isolated from radix Astragali. Biol Pharm Bull. 2009; 32:132-135.
22. Zhou Z, Zhang Y, Ding XR, Chen SH, Yang J, Wang XJ, Jia GL, Chen HS, Bo XC, Wang SQ. Protocatechuic aldehyde inhibits hepatitis B virus replication both *in vitro* and *in vivo*. Antiviral Res. 2007; 74:59-64.
23. Rowe HM, Kapopoulou A, Corsinotti A, Fasching L, Macfarlan TS, Tarabay Y, Viville S, Jakobsson J, Pfaff SL, Trono D. TRIM28 repression of retrotransposon-based enhancers is necessary to preserve transcriptional dynamics in embryonic stem cells. Genome Res. 2013; 23:452-461.
24. Ito K, Kim KH, Lok AS, Tong S. Characterization of genotype-specific carboxyl-terminal cleavage sites of hepatitis B virus e antigen precursor and identification of furin as the candidate enzyme. J Virol. 2009; 83:3507-3517.

(Received November 11, 2013; Revised February 1, 2014; Accepted February 16, 2014)

Original Article

DOI: 10.5582/bst.8.45

Shufeng Jiedu Capsule protect against acute lung injury by suppressing the MAPK/NF-κB pathway

Zhengang Tao[1], Jingyan Gao[2], Guoliang Zhang[3], Mingming Xue[1], Weiqiang Yang[4], Caoyang Tong[1], Ying Yuan[5,*]

[1] *Emergency Department, Zhongshan Hospital, Fudan University, Shanghai, China;*
[2] *Department of Human Anatomy and Histo-embryology, Fudan University, Shanghai, China;*
[3] *Department of Infectious Diseases, Anhui Province Hospital of Traditional Chinese Medicine, Anhui University of Chinese Medicine, Anhui Province, China;*
[4] *Emergency Department, Renji Hospital, Shanghai Jiaotong University, Shanghai, China;*
[5] *Geriatrics Department, Zhongshan Hospital, Fudan University, Shanghai, China.*

Summary **This study sought to investigate the protective effect of an alternative medicine, Shufeng Jiedu Capsule, in acute lung injury and inflammation signaling pathways related to that action. Hematoxylin and eosin (HE) staining was used to observe pathological changes in rat lung tissue, arterial blood was subjected to blood gas analysis and lactic acid levels were determined, immunofluorescent staining for interleukin-1β (IL-1β) was performed, enzyme linked immunosorbent assay (ELISA) was used to detect biomarkers of the nuclear factor-κB (NF-κB) inflammation pathway including IL-1β and tumor necrosis factor α (TNF-α), biomarkers of the mitogen-activated protein kinase (MAPK) signal pathway including P-selectin, transforming growth factor β (TGF-β), keratinocyte-derived chemokine (KC), and C-Jun/AP-1 were measured, and real-time PCR was used to detect NF-κB mRNA. Results in rats with lipopolysaccharide-induced acute lung injury suggested that Shufeng Jiedu Capsule may increase the partial pressure of oxygen in lung tissue, decrease lactic acid levels, inhibit inflammatory factors such as IL-1β and TNF-α, and suppress the levels of P-selectin, TGF-β, KC, C-Jun/AP-1, and NF-κB mRNA. Thus, Shufeng Jiedu Capsule is a traditional medicine that may alleviate acute lung injury by suppressing the MAPK/NF-κB signaling pathway.**

Keywords: Acute lung injury, Shufeng Jiedu Capsule, dexamethasone, rat model, MAPK/NF-κB signaling pathway

1. Introduction

H7N9 avian influenza, a disease caused by the H7N9 avian influenza virus, can lead to acute lung injury. In March 2013, H7N9 avian influenza was found in Shanghai and Anhui Province in China and recurred in eastern and southern China in early 2014. Human infection with the virus has resulted in a high mortality rate of about 20-30% according to recent data (*1*). Human infection with H7N9 avian influenza has received a great deal of attention from China's Ministry of Health and the World Health Organization. In the early stages of H7N9 influenza, patients have flu-like symptoms such as a fever, coughing, and headaches. Some patients have more severe symptoms, such as a high fever that remains above 39°C, expiratory dyspnea, hemoptysis, and acute lung injury; patients usually die of acute respiratory distress syndrome caused by respiratory failure (*2*).

Acute lung injury (ALI) is characterized by acute hypoxemic respiratory failure with several potential causes, including trauma, shock, viruses, and bacterial endotoxins (*3*). ALI can lead to injury of alveolar epithelial cells and capillary endothelial cells and diffuse pulmonary interstitial and alveolar edema. When lung tissue is affected by a virus or bacterial endotoxin, G protein-coupled receptors (membrane proteins) in lung cells are activated. Cells are increasingly exposed to intracellular oxidative stress and the downstream

*Address correspondence to:
Dr. Ying Yuan, Geriatrics Department, Zhongshan Hospital, Fudan University, 180 Fenglin Road, Shanghai 200032, China.
E-mail: yuan.ying@zs-hospital.sh.cn

inflammatory pathway is triggered, leading to ALI (*4,5*).

Dexamethasone (DXMS) is a type of synthetic glucocorticoid and is a routine medication to control the inflammatory response (*6*). DXMS alleviates hypernomic inflammation and injury by inhibiting NF-κB activity. However, there is disagreement as to the clinical value of DXMS since it cannot improve prognosis in the early stages (*7*). Thus, only a small dose of DXMS is recommended to treat advanced cases of fibrosis. DXMS causes several adverse reactions such as decreased immune function, blood pressure and blood glucose fluctuations, hemorrhaging of the digestive tract, and femoral neck necrosis (*8,9*). Thus, there is an urgent need for an alternative in clinical settings.

Shufeng Jiedu Capsule (SFJDC) is a traditional Chinese medicine that is mainly used to treat upper respiratory tract infections such as the flu, swelling and pain in the throat, mumps, and strep throat (*10*). A previous study has suggested that SFJDC can inhibit viruses such as Adv-7, RSV, HSV-1, and the flu virus and bacteria such as *Staphylococcus aureus*, *Staphylococcus epidermidis*, and *Pseudomonas aeruginosa* (*11*). In China, SFJDC has been listed as drug to combat avian influenza. Studies have reported that active constituents of SFJDC such as resveratrol and quercetin may alleviate inflammation by suppressing the mitogen-activated protein kinase (MAPK)/nuclear factor-κB (NF-κB) signaling pathway (*12-14*). However, few studies have examined the effect of SFJDC on cellular signaling pathways. Thus, the current study sought to explore the effect of treatment with DMXS and SFJDC in rats with lipopolysaccharide (LPS)-induced ALI.

2. Materials and Methods

2.1. *Materials*

Endotoxin was purchased from Sigma Aldrich (St. Louis, MO, USA). SFJDC were purchased from Jiren Pharmaceutical (Anhui, China). A real-time PCR kit and enzyme linked immunosorbent assay (ELISA) kit for interleukin-1β (IL-1β) were purchased from Univ-Bio (Shanghai, China). ELISA kits for P-selectin, transforming growth factor β (TGF-β), tumor necrosis factor α (TNF-α), C-Jun/AP-1, and keratinocyte-derived chemokine (KC) were purchased from Shanghai United Cell Biotechnology Corporation (Shanghai, China).

2.2. *Animals*

Eighty specific-pathogen-free male Sprague-Dawley rats weighing 250 ± 20 g were purchased from Fudan University's Animal Research Center (Shanghai, China). ALI model rats were induced by intraperitoneal injection of 10 mg/kg LPS. Rats were randomly divided into four groups: a saline control group, rats with LPS-induced ALI, rats with LPS-induced ALI that were treated with dexamethasone (DXMS), and rats with LPS-induced ALI that were treated with SFJDC. There were 20 rats in each group.

The saline control group and rats with untreated ALI were administered 2 mL/kg saline. Rats treated with DXMS were intraperitoneally injected with dexamethasone 5 mg/kg, and rats treated with SFJDC were intragastrically administered SFJDC 100 mg/kg. The above treatments were given once daily and continued for 7 days. On day 1, day 3, day 5, and day 7, rats were anesthetized with ether and sacrificed. Tissue specimens were taken from 5 random rats in each of the 4 groups. Arterial blood was collected and the lungs were removed. Tissue of the right lower lung was preserved in liquid nitrogen. The left lung was fixed in 40% paraformaldehyde and then sliced into paraffin sections. These paraffin sections were used in hematoxylin and eosin (HE) staining and confocal laser scanning microscopy (Leica TCS SP8, Solms, Germany) of IL-1β fluorescence.

2.3. *ELISA assay for IL-1β, P-selectin, TGF-β, TNF-α, KC, and C-Jun/AP-1*

The right lower lung was removed from liquid nitrogen, washed with cold saline, and dried with filter paper. One hundred mg of lung tissue was made into a homogenate with cold saline. ELISA was used to detect levels of IL-1β, P-selectin, TGF-β, TNF-α, KC, and C-Jun/AP-1 expression in this homogenate.

2.4. *Real-time PCR detection of NF-κB mRNA*

Total RNA was collected using Trizol (Gibco-BRL, Gaithersburg, USA). cDNA was prepared using a 1-step PCR kit (Promega, USA) and PTC-200 PCR device (MJ Research, USA). The primer sequence was as follows: rGAPD (5'-AGTGCCAGCCTCGTCTCATAG-3' and 5'-CGTTGAACTTGCCGTGGGTAG-3'). The primer had a melting temperature (Tm) of 59°C. Glyceraldehyde 3-phosphate dehydrogenase (GAPDH) served as an internal reference. PCR products were analyzed using Quantity One software (Bio-Rad, Hercules, USA).

2.5. *Confocal laser scanning imaging*

Tissue slices were washed 3 times with PBS, fixed in methanol for 30 min, washed 3 times with PBS, denatured with HCl for 40 min, washed 3 times with PBS, blocked with sheep serum for 30 min, washed 3 times with PBS, and incubated with IL-1β monoclonal body overnight. Slices were washed 3 times with PBS and incubated with the secondary antibody. Confocal laser scanning microscopy (Leica TCS SP8, Solms, Germany) was used to observe fluorescence.

2.6. *Statistical analysis*

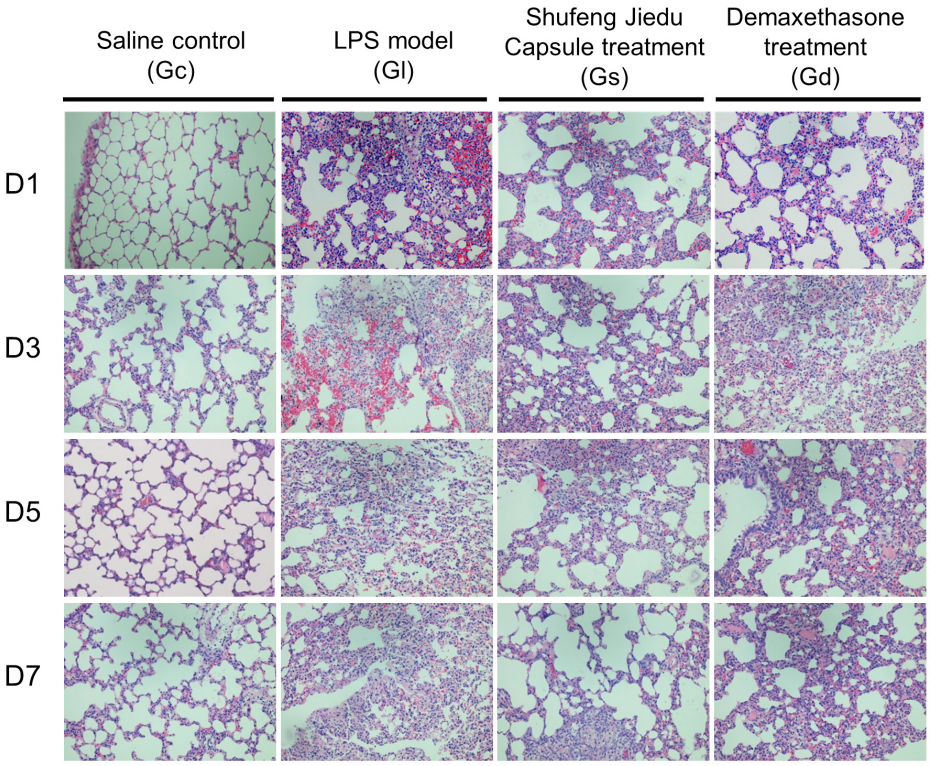

Figure 1. HE staining of rat lung tissue. D1: day 1; D3: day 3; D5: day 5; D7: day 7.

Data were analyzed using SPSS 18.0 software and are presented as the mean ± standard deviation (S.D.). A homogeneity of variance and a normal distribution were verified. Once data were found to have a homogeneity of variance and a normal distribution, one-way ANOVA was performed. If results were statistically significant, a pair-wise comparison was done using the least significant difference test. A $p < 0.05$ was considered statistically significant.

3. Results

3.1. *Morphological changes in lung tissue*

As shown in Figure 1, lung tissue from rats with untreated ALI had severe alveolar exudation, hemorrhaging, edema, small airway collapse, and necrosis of airway epithelial cells on day 1. Exudation and hemorrhaging were not noted in tissue from rats treated with DXMS and rats treated with SFJDC. Lung tissue retained its basic structure, and the inflammatory response was milder in rats treated with DXMS or SFJDC than in rats with untreated ALI. On day 3, more severe inflammation was noted in lung tissue from rats with untreated ALI with obvious exudation and destruction of alveolar structures. Rats treated with DXMS and rats treated with SFJDC also had inflammation but alveolar structures remained and inflammation was mild. Rats treated with SFJDC had milder inflammation than rats treated with DXMS. On day 5 and day 7, inflammation had subsided in all of the rats. The inflammatory response was much milder in rats treated with SFJDC.

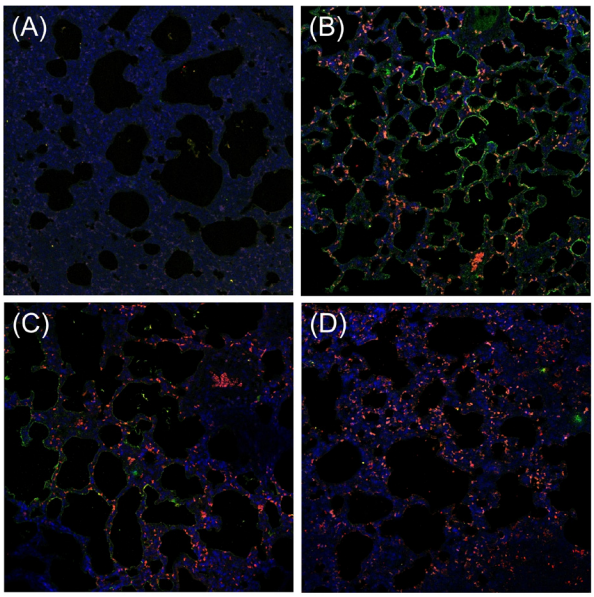

Figure 2. Confocal laser scanning microscopy image of rat lung tissue. Rat lung tissue sections were labeled with IL-1β (Green) and were then observed using confocal laser scanning microscopy. **(A)**: saline control group; **(B)**: rats with untreated ALI; **(C)**: rats treated with Shufeng Jiedu Capsule; **(D)**: rats treated with dexamethasone.

3.2. *Immunofluorescent staining for IL-1β*

As shown in Figure 2, the saline control group had no obvious green fluorescence for IL-1β, indicating

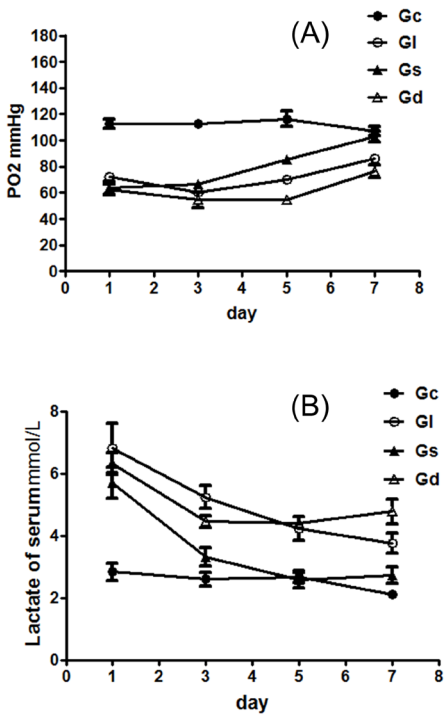

Figure 3. Partial pressure of oxygen and lactic acid levels. The partial pressure of oxygen and lactic acid levels in arterial blood from rats were measured. **(A)**: measurement of the partial pressure of oxygen; **(B)**: determination of lactic acid levels. Gc: saline control group; Gl: rats with untreated ALI; Gs: rats treated with Shufeng Jiedu Capsule; Gd: rats treated with dexamethasone.

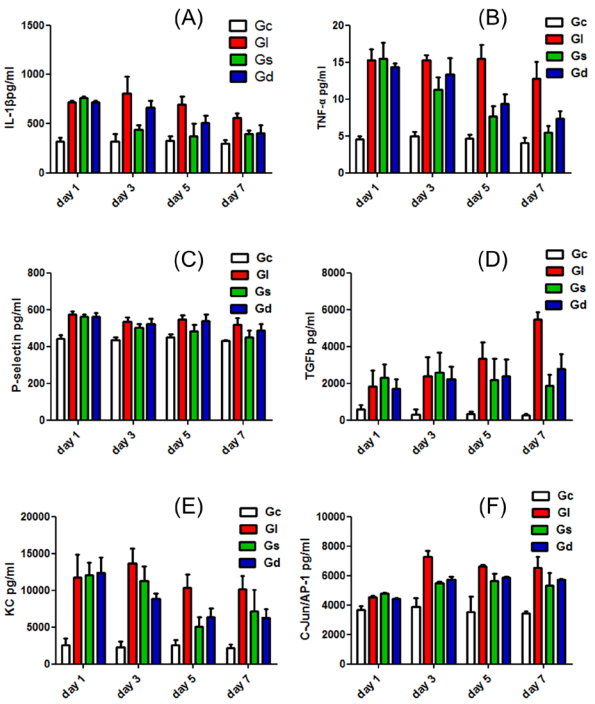

Figure 4. ELISA detection of IL-1β, TNF-α, P-selectin, TGF-β, KC, and C-Jun/AP-1 in rat lung tissue. Levels of IL-1β **(A)**, TNF-α **(B)**, P-selectin **(C)**, TGF-β **(D)**, KC **(E)**, and C-Jun/AP-1 **(F)** expression in rat lung tissue were detected using ELISA. Gc: saline control group; Gl: rats with untreated ALI; Gs: rats treated with Shufeng Jiedu Capsule; Gd: rats treated with dexamethasone.

a very low level of IL-1β. Rats with untreated ALI had significant green fluorescence. Compared to the saline control group, rats treated with SFJDC and rats treated with DXMS had green fluorescence, indicating an increased level of IL-1β. Green fluorescence was markedly less intense than that noted in rats with untreated ALI, indicating that SFJDC and DXMS had decreased the level of IL-1β.

3.3. *Blood gas analysis of arterial blood and determination of lactic acid levels*

As shown in Figure 3, the partial pressure of oxygen remained between 107-113 mmHg in the saline control group. On day 1, day 3, day 5, and day 7, the partial pressure of oxygen increased gradually from 60 mmHg to 86 mmHg in rats with untreated ALI. The partial pressure of oxygen generally increased from 64 mmHg to 103 mmHg in rats treated with SFJDC and it increased slightly from 54 mmHg to 76 mmHg in rats treated with DXMS. These results indicate that rats treated with SFJDC had a higher partial pressure of oxygen than did rats with untreated ALI on day 5 and day 7. However, rats treated with DXMS had a lower partial pressure of oxygen than rats did with untreated ALI at these two times. On day 1, day 3, day 5, and day 7, the lactic acid level in the saline control group remained between 2.6-2.8 mmol/L. The lactic acid level ranged from 6.8 mmol/L to 3.8 mmol/L in rats with untreated ALI, from 5.7 mmol/L to 2.7 mmol/L in rats treated with SFJDC, and from 6.3 mmol/L to 4.4 mmol/L in rats treated with DXMS. SFJDC markedly reduced the level of lactic acid on day 3, day 5, and day 7 ($p < 0.05$) in comparison to that in rats with untreated ALI. However, there was no evidence of a decrease in the level of lactic acid in rats treated with DXMS.

3.4. *Results of ELISA detection of IL-1β, TNF-α, P-selectin, TGF-β, KC, and C-Jun/AP-1*

As shown in Figure 4, ELISA was used to determine levels of IL-1β, TNF-α, P-selectin, TGF-β, KC, and C-Jun/AP-1 in each group at different times. The level of IL-1β remained between 300-325 pg/mL in the saline control group. The level of IL-1β ranged from 809 to 557 pg/mL in rats with untreated ALI, from 761 to 376 pg/mL in rats treated with SFJDC, and from 715 to 399 pg/mL in rats treated with DXMS. Compared to rats with untreated ALI, rats treated with SFJDC had an obvious decrease in the level of IL-1β on day 3, day 5, and day 7 ($p < 0.05$). There were no significant differences in the level of IL-1β for rats treated with SFJDC and rats treated with DXMS. The level of TNF-α remained between 4.0-4.9 pg/mL in the saline control group. The level of TNF-α ranged from 15.5 to 12.8 pg/mL in rats with untreated ALI, from

15.5 to 5.5 pg/mL in rats treated with SFJDC, and from 14.3 to 7.4 pg/mL in rats treated with DXMS. Compared to rats with untreated ALI, rats treated with SFJDC had an obvious decrease in the level of TNF-α on day 3, day 5, and day 7 ($p < 0.05$). There were no significant differences in the level of TNF-α for rats treated with SFJDC and rats treated with DXMS. The level of P-selectin remained between 442-451 pg/mL in the saline control group. The level of P-selectin ranged from 574 to 517 pg/mL in rats with untreated ALI, from 562 to 452 pg/mL in rats treated with SFJDC, and from 561 to 487 pg/mL in rats treated with DXMS. Compared to rats with untreated ALI, rats treated with SFJDC had an obvious decrease in the level of P-selectin on day 5 and day 7 ($p < 0.05$). The level of TGF-β remained between 253-585 pg/mL in the saline control group. The level of TGF-β ranged from 1,828 to 5,466 pg/mL in rats with untreated ALI, from 2,595 to 1,874 pg/mL in rats treated with SFJDC, and from 1,712 to 2,801 pg/mL in rats treated with DXMS. Compared to rats with untreated ALI, rats treated with SFJDC had an obvious decrease in the level of TGF-β on day 5 and day 7 ($p < 0.05$). There were no significant differences in the level of TGF-β for rats treated with SFJDC and rats treated with DXMS. The level of KC remained between 2,215-2,606 pg/mL in the saline control group. The level of KC ranged from 13,666 to 10,148 pg/mL in rats with untreated ALI, from 12,099 to 5,034 pg/mL in rats treated with SFJDC, and from 12,400 to 6,309 pg/mL in rats treated with DXMS. Compared to rats with untreated ALI, rats treated with SFJDC had an obvious decrease in the level of KC on day 3, day 5, and day 7 ($p < 0.05$). There were no significant differences in the level of KC for rats treated with SFJDC and rats treated with DXMS. The level of C-Jun/AP-1 remained between 3,426-3,676 pg/mL in the saline control group. The level of C-Jun/AP-1 ranged from 4,551 to 6,644 pg/mL in rats with untreated ALI, from 4,780 to 5,341 pg/mL in rats treated with SFJDC, and from 4,426 to 5,727 pg/mL in rats treated with DXMS. Compared to rats with untreated ALI, rats treated with SFJDC had an obvious decrease in the level of C-Jun/AP-1 on day 3, day 5, and day 7 ($p < 0.05$). There were no significant differences in the level of C-Jun/AP-1 for rats treated with SFJDC and rats treated with DXMS.

3.5. *Level of NF-κB mRNA expression*

As shown in Table 1, the level of NF-κB mRNA expression in rat lung tissue was determined using real-time PCR and was analyzed using the 2-ΔΔCt method. The mean value of nucleic acid fluorescent intensity was first determined. The mean value for the control group was subtracted from the mean value for an experimental group, and the difference was squared. The resulting values reflected a relative change in mRNA expression. The level of expression remained at around 2.0 in the saline control group, it increased from 1.80 (day 1) to 5.99 (day 3) and then decreased to 3.14 (day 7) in rats with untreated ALI, it increased from 1.5 (day 1) to 2.19 (day 3) and then decreased to 1.37 (day 7) in rats treated with SFJDC, and it increased from 2.57 (day 1) to 2.95 (day 3) and then decreased to 1.83 (day 7) in rats treated with DXMS. Compared to rats with untreated ALI, rats treated with SFJDC had an obvious decrease in the level of NF-κB mRNA ($p < 0.05$).

4. Discussion

According to previous studies, DXMS may alleviate the inflammatory response by suppressing the MAPK/NF-κB signaling pathway. Numerous studies have indicated that the active constituents of SFJDC, such as resveratrol, quercetin, and other flavonoids, inhibit

Table 1. Level of NF-κB mRNA expression in rat lung tissue

Day	Saline control	Rats with untreated ALI	Rats treated with SFJDC	Rats treated with DXMS
1	2.18 ± 0.95	1.80 ± 0.58*	1.50 ± 0.36#	2.57 ± 0.65
3	1.80 ± 0.28	5.99 ± 1.37*	2.19 ± 0.62#	2.87 ± 1.06
5	2.14 ± 0.69	4.22 ± 1.08*	1.84 ± 0.29#	2.95 ± 0.92
7	2.15 ± 0.70	3.14 ± 0.70*	1.37 ± 0.13#	1.83 ± 1.09

*$p < 0.05$; rats with untreated ALI *vs*. saline control; #$p < 0.05$ rats treated with SFJDC *vs*. rats with untreated ALI.

Table 2. Active constituents of Shufeng Jiedu Capsule and responding signaling pathways

Herb	Constituent type	Constituent	Anti-inflammation pathway	*Ref.*
Polygonum cuspidatum	stilbene	resveratrol	NF-κB pathway and PI3K pathway	(*12*)
	anthraquinone	emodin	MAPK and NF-κB pathway	(*15*)
		rhein	MAPK and NF-κB pathway	(*19*)
	flavonoid	quercetin	MAPK and NF-κB pathway	(*13*)
Forsythia suspensa	flavonoid	rutin	NF-κB pathway	(*20*)
Bupleurum chinense DC.	flavonoid	kaempferol and quercetin	MAPK and NF-κB pathway	(*16,13*)
Glycyrrhiza uralensis	flavonoid	liquiritigenin and liquiritin	NF-κB pathway	(*17*)

the MAPK/NF-κB signaling pathway in several cell lines (Table 2) (*15-21*). The current study sought to investigate whether SFJDC could provide protection from ALI by inhibiting inflammatory signaling pathways.

NF-κB is a key factor in the inflammatory response and is involved in the development of ALI (*22,23*). When patients are affected by trauma, shock, a virus, or a bacterial endotoxin, the NF-κB signaling pathway is activated. Inflammatory cells such as neutrophil granulocytes and macrophages are subsequently triggered, inflammatory mediators such as IL-1β and TNF-α are released, and oxidative stress is promoted (*24,25*). IL-1β and TNF-α may serve as biomarkers of the NF-κB inflammatory pathway. A previous study using DXMS as a positive control determined levels of IL-1β and TNF-α to assess the protective effect of SFJDC in a rat model of LPS-induced ALI (*26*). Confocal laser scanning imaging revealed an obvious decrease in the levels of IL-1β in both rats treated with SFJDC and rats treated with DXMS compared to rats with untreated ALI. This finding suggests that SFJDC may alleviate inflammation by inhibiting IL-1β in the NF-κB signaling pathway. Real-time PCR indicated that expression of NF-κB mRNA was effectively suppressed in rats treated with SFJDC in comparison to that in rats with untreated ALI ($p < 0.01$). Thus, SFJDC may alleviate ALI by inhibiting the NF-κB-dependent inflammatory response.

MAPKs (also known as MAP kinases) are serine/threonine/tyrosine-specific protein kinases belonging to the CMGC (CDK/MAPK/GSK3/CLK) kinase group, and the P38δ MAPK receptor is expressed at high levels in lung tissue (*27*). MAPK phosphorylation is associated with activation with NF-κB in the inflammatory response (*28*). MAPKs function in stress, inflammation, tumor, cell growth, differentiation, apoptosis, and fibrosis. P-selectin, TGF-β, KC, and C-Jun/AP-1 are involved in the MAPK signaling pathway, and they may serve as biomarkers of the MAPK pathway (*29-32*). An ELISA assay revealed that rats treated with SFJDC had a more obvious decrease in the level of P-selectin, TGF-β, KC, and C-Jun/AP-1 in lung tissue in comparison to rats with untreated ALI ($p < 0.01$). This indicates that SFJDC may alleviate LPS-induced stress injury, decrease lung cell apoptosis, and protect lung tissue by inhibiting the MAPK signaling pathway.

The pathology of rat lung tissue was observed using HE staining. Like rats treated with DXMS, rats treated with SFJDC had a much milder inflammatory response than rats with untreated ALI. Blood gas analysis of arterial blood and determination of lactic acid levels indicated that rats treated with SFJDC had an obvious increase in the partial pressure of oxygen and a lower lactic acid level than rats with untreated ALI. Thus, SFJDC effectively decreased the hypoxia-induced inflammatory response and protected lung tissue. In conclusion, this study revealed that SFJDC alleviates LPS-induced inflammation in a rat model by suppressing the MAPK/NF-κB signaling pathway. Thus, SFJDC might serve as an alternative medication to inhibit inflammation in different organs and SFJDC has great potential for wide clinical use.

References

1. National Health and Family Planning Commission of the People's Republic of China. Survey of human infection with avian influenza. *http://www.moh.gov.cn/yjb/s2907/list.shtml* (in Chinese) (accessed February 10, 2014).
2. Sun S, Zhao G, Liu C, Wu X, Guo Y, Yu H, Song H, Du L, Jiang S, Guo R, Tomlinson S, Zhou Y. Inhibition of complement activation alleviates acute lung injury induced by highly pathogenic avian influenza H5N1 virus infection. Am J Respir Cell Mol Biol. 2013; 49:221-230.
3. Vlaar AP, Juffermans NP. Transfusion-related acute lung injury: A clinical review. Lancet. 2013; 382:984-994.
4. Ellison MA, Ambruso DR, Silliman CC. Therapeutic options for transfusion related acute lung injury: The potential of the G2A receptor. Curr Pharm Des. 2012; 18:3255-3259.
5. Ward PA. Oxidative stress: Acute and progressive lung injury. Ann N Y Acad Sci. 2010; 1203:53-59.
6. Giuliano C, Smalligan RD, Mitchon G, Chua M. Role of dexamethasone in the prevention of migraine recurrence in the acute care setting: A review. Postgraduate Medicine. 2012; 124:110-115.
7. Gawarammana IB, Buckley NA. Medical management of paraquat ingestion. Br J Clin Pharmacol. 2011; 72:745-757.
8. Waldron NH, Jones CA, Gan TJ, Allen TK, Habib AS. Impact of perioperative dexamethasone on postoperative analgesia and side-effects: Systematic review and meta-analysis. Br J Anaesth. 2013; 110:191-200.
9. Schwartz JR. Dexamethasone premedication for prophylaxis of taxane toxicities: Can the doses be reduced when paclitaxel or docetaxel are given weekly? J Oncol Pharm Pract. 2012; 18:250-256.
10. Tao Z, Yang Y, Shi W, Xue M, Yang W, Song Z, Yao C, Yin J, Shi D, Zhang Y, Cai Y, Tong C, Yuan Y. Complementary and alternative medicine is expected to make greater contribution in controlling the prevalence of influenza. Biosci Trends. 2013; 7:253-256.
11. Song J, Zhang F, Tang S, Liu X, Gao Y, Lu P, Wang Y, Yang H. A module analysis approach to investigate molecular mechanism of TCM formula: A trial on Shu-feng-jie-du formula. Evid Based Complement Alternat Med. 2013; 2013:731370.
12. Busch F, Mobasheri A, Shayan P, Lueders C, Stahlmann R, Shakibaei M. Resveratrol modulates interleukin-1beta-induced phosphatidylinositol 3-kinase and nuclear factor kappaB signaling pathways in human tenocytes. J Biol Chem. 2012; 287:38050-38063.
13. Song Y, Liu J, Zhang F, Zhang J, Shi T, Zeng Z. Antioxidant effect of quercetin against acute spinal cord injury in rats and its correlation with the p38MAPK/iNOS signaling pathway. Life Sci. 2013; 92:1215-1221.
14. Gao J, Inagaki Y, Li X, Kokudo N, Tang W. Research progress on natural products from traditional Chinese medicine in treatment of Alzheimer's disease. Drug Discov Ther. 2013; 7:46-57.

15. Meng G, Liu Y, Lou C, Yang H. Emodin suppresses lipopolysaccharide-induced pro-inflammatory responses and NF-kappaB activation by disrupting lipid rafts in CD14-negative endothelial cells. Br J Pharmacol. 2010; 161:1628-1644.
16. Nepal M, Li L, Cho HK, Park JK, Soh Y. Kaempferol induces chondrogenesis in ATDC5 cells through activation of ERK/BMP-2 signaling pathway. Food Chem Toxicol. 2013; 62:238-245.
17. Chien YC, Sheu MJ, Wu CH, Lin WH, Chen YY, Cheng PL, Cheng HC. A Chinese herbal formula "Gan-Lu-Yin" suppresses vascular smooth muscle cell migration by inhibiting matrix metalloproteinase-2/9 through the PI3K/AKT and ERK signaling pathways. BMC Complement Altern Med. 2012; 12:137.
18. Kim A, Yim NH, Im M, Jung YP, Liang C, Cho WK, Ma JY. Ssanghwa-tang, an oriental herbal cocktail, exerts anti-melanogenic activity by suppression of the p38 MAPK and PKA signaling pathways in B16F10 cells. BMC Complement Altern Med. 2013; 13:214.
19. Wu JS, Shi R, Zhong J, Lu X, Ma BL, Wang TM, Zan B, Ma YM, Cheng NN, Qiu FR. Renal protective role of Xiexin Decoction with multiple active ingredients involves inhibition of inflammation through downregulation of the nuclear factor-kappaB pathway in diabetic rats. Evid Based Complement Alternat Med. 2013; 2013:715671.
20. Yoo H, Ku SK, Baek YD, Bae JS. Anti-inflammatory effects of rutin on HMGB1-induced inflammatory responses *in vitro* and *in vivo*. Inflamm Res. 2014; 63:197-206.
21. Xia JF, Gao JJ, Inagaki Y, Kokudo N, Nakata M, Tang W. Flavonoids as potential anti-hepatocellular carcinoma agents: recent approaches using HepG2 cell line. Drug Discov Ther. 2013; 7:1-8.
22. Chi G, Wei M, Xie X, Soromou LW, Liu F, Zhao S. Suppression of MAPK and NF-kappaB pathways by limonene contributes to attenuation of lipopolysaccharide-induced inflammatory responses in acute lung injury. Inflammation. 2013; 36:501-511.
23. Zhu T, Wang DX, Zhang W, Liao XQ, Guan X, Bo H, Sun JY, Huang NW, He J, Zhang YK, Tong J, Li CY. Andrographolide protects against LPS-induced acute lung injury by inactivation of NF-kappaB. PLoS One. 2013; 8:e56407.
24. Scholz CC, Cavadas MA, Tambuwala MM, Hams E, Rodriguez J, Kriegsheim A, Cotter P, Bruning U, Fallon PG, Cheong A, Cummins EP, Taylor CT. Regulation of IL-1beta-induced NF-kappaB by hydroxylases links key hypoxic and inflammatory signaling pathways. Proc Natl Acad Sci U S A. 2013; 110:18490-18495.
25. Tahir M, Rehman MU, Lateef A, Khan R, Khan AQ, Qamar W, Ali F, O'Hamiza O, Sultana S. Diosmin protects against ethanol-induced hepatic injury via alleviation of inflammation and regulation of TNF-alpha and NF-kappaB activation. Alcohol. 2013; 47:131-139.
26. Chuang KH, Peng YC, Chien HY, Lu ML, Du HI, Wu YL. Attenuation of LPS-induced lung inflammation by glucosamine in rats. Am J Respir Cell Mol Biol. 2013; 49:1110-1119.
27. Zhong J, Lardinois D, Szilard J, Tamm M, Roth M. Rat mesothelioma cell proliferation requires p38delta mitogen activated protein kinase and C/EBP-alpha. Lung Cancer. 2011; 73:166-170.
28. Sakai N, Wada T, Furuichi K, Iwata Y, Yoshimoto K, Kitagawa K, Kokubo S, Kobayashi M, Takeda S, Kida H, Kobayashi K, Mukaida N, Matsushima K, Yokoyama H. p38 MAPK phosphorylation and NF-kappa B activation in human crescentic glomerulonephritis. Nephrol Dial Transplant. 2002; 17:998-1004.
29. Santen S, Mihaescu A, Laschke MW, Menger MD, Wang Y, Jeppsson B, Thorlacius H. p38 MAPK regulates ischemia-reperfusion-induced recruitment of leukocytes in the colon. Surgery. 2009; 145:303-312.
30. Asano K, Shikama Y, Shoji N, Hirano K, Suzaki H, Nakajima H. Tiotropium bromide inhibits TGF-beta-induced MMP production from lung fibroblasts by interfering with Smad and MAPK pathways *in vitro*. Int J Chron Obstruct Pulmon Dis. 2010; 5:277-286.
31. Khajah M, Andonegui G, Chan R, Craig AW, Greer PA, McCafferty DM. Fer kinase limits neutrophil chemotaxis toward end target chemoattractants. J Immunol. 2013; 190:2208-2216.
32. Catalan U, Fernandez-Castillejo S, Angles N, Morello JR, Yebras M, Sola R. Inhibition of the transcription factor c-Jun by the MAPK family, and not the NF-kappaB pathway, suggests that peanut extract has anti-inflammatory properties. Mol Immunol. 2012; 52:125-132.

(Received December 6, 2013; Revised January 24, 2014; Re-revised February 13, 2014; Accepted February 15, 2014)

Original Article

DOI: 10.5582/bst.8.52

Clinical epidemiology of HIV/AIDS in China from 2004−2011

Min Li[1,*], Yinzhong Shen[1,*], Xiaofei Jiang[2], Qi Li[3], Xiaoming Zhou[1], Hongzhou Lu[1,2,4,]**

[1] *Shanghai Public Health Clinical Center, Fudan University, Shanghai, China;*
[2] *Huashan Hospital affiliated with Fudan University, Shanghai, China;*
[3] *InterSystems Corporation, Cambridge Massachusetts, USA;*
[4] *Shanghai Medical College, Fudan University, Shanghai, China.*

Summary **This study retrospectively analyzed Chinese publicly reported data on Human Immunodeficiency Virus/Acquired Immune Deficiency Syndrome (HIV/AIDS). The HIV/AIDS morbidity (1/100,000) and mortality (1/100,000) rates in China continually increased from 0.23 and 0.06 in 2004 to 1.53 and 0.69 in 2011, respectively. The AIDS case fatality rate decreased yearly from 53.57% in 2008 to 45.11% in 2011, and the fatality rate in rural areas (0.25-0.42%) was higher than that in cities (0.13-0.22%). The number of HIV/AIDS patients discharged from city-level hospitals increased from 329 in 2004 to 7,266 in 2011, and this number was higher than the number of similar patients discharged from county-level (rural) hospitals (the number of HIV/AIDS patients increased from 252 in 2004 to 5,957 in 2011). The factors contributing to these trends include: enhanced physician HIV/AIDS education regarding diagnosis, intervention, monitoring, testing, and treatment; improved safety of blood collection and use; and improved management of HIV/AIDS patients. Therefore, HIV/AIDS prevention and control in rural areas of China is the key to reducing HIV transmission and mortality in China.**

Keywords: HIV/AIDS, clinical epidemiology, China

1. Introduction

Among infectious diseases in China, Acquired Immune Deficiency Syndrome (AIDS) has recently become the leading cause of death, and the number of AIDS-related deaths is significantly higher than that due to any other infectious disease (*1*). Epidemiological reports of Human Immunodeficiency Virus (HIV)/AIDS from the United States, Brazil, and South Africa have been published (*2-6*). At present, there are several regional reports on the incidence of HIV/AIDS in China (*7-9*), but national reports of the clinical epidemiology of HIV/AIDS are rare. Therefore, HIV/AIDS prevention and control poses a challenge in China due to the lack of complete and accurate information on the epidemiology of HIV/AIDS. The current study retrospectively analyzed the HIV/AIDS morbidity, mortality, and case fatality rates, as well as hospital discharges in China from 2004 to 2011, to determine the distribution and characteristics of the HIV/AIDS population and provide further information on and guidance for HIV/AIDS prevention and control in China and the rest of the world.

2. Materials and Methods

2.1. *Data sources*

Most of the data in this study were obtained from the "China Public Health Statistics Yearbook (2005-2012)." The number of patients hospitalized each year and treatment outcomes were obtained from the "Statistical Annual Report of Medical Service in China." Data regarding morbidity, mortality, and fatality rates of infectious diseases were obtained from Annual Statistics on Infectious Diseases that Must be Reported by Law in the "Chinese Public Health Statistical Yearbook." These data were collected from a total of 31 regions in China and excluded Hong Kong and Macao.

*These authors contributed equally to this works.
***Address correspondence to:*
Dr. Hongzhou Lu, Department of Infectious Diseases, Shanghai Public Health Clinical Center, Fudan University, Caolang Road No. 2901, Jinshan District, Shanghai, China.
E-mail: luhongzhou@fudan.edu.cn

2.2. *Definitions*

Morbidity from infectious diseases that must be reported by law = number of cases of infectious diseases that must be reported by law/population × 100,000.

Mortality from infectious diseases that must be reported by law = number of deaths from infectious diseases that must be reported by law/population × 100,000.

Fatality rate from infectious diseases that must be reported by law = number of deaths from infectious diseases that must be reported by law/number of cases × 100%.

Age-specific mortality among males (females) = number of deaths among males (females) of a certain age group/average male (female) population of the same age group.

The number of discharged patients refers to the number of inpatients who were discharged from acute care hospitals.

Urban and rural area classification: urban areas include municipalities and prefecture-level cities while rural areas include counties and county-level cities, towns, and villages.

Urban and rural populations were calculated according to "Regulations on Statistical Classification of Urban and Rural Areas (draft)" released by the National Bureau of Statistics in 1999.

Population refers to the total number of living individuals within a certain area at a certain time point.

2.3. *Statistical analysis*

Data were analyzed using the Statistical Package for the Social Sciences (SPSS) version 19.0. A chi-square (χ^2) test was performed, and the mean ± standard deviation (S.D.) was determined.

3. Results

3.1. *HIV/AIDS in China*

The HIV/AIDS morbidity, mortality, and fatality rates per year were first determined based on the the total population of China for that year, and then the p value was calculated using a Chi-square (χ^2) test. The HIV/AIDS morbidity rate (1/100,000) and mortality rate (1/100,000) continually increased in China from 2004 to 2011 ($p < 0.01$). The AIDS fatality rate (%) increased from 2004 to 2008 and then decreased yearly from 2009 to 2011 ($p < 0.01$; Figure 1).

Statistical analysis of data from 31 regions in China from 2004−2011 indicated the following: *i*) The regions with the highest HIV/AIDS morbidity rates were Henan Province from 2004 to 2006, Guangxi Province from 2005 to 2011, and Yunnan Province from 2006 to 2011.

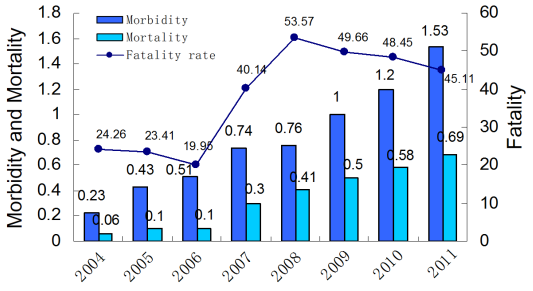

Figure 1. The HIV/AIDS morbidity (1/100,000), mortality (1/100,000), and fatality rates (%) in China from 2004−2011.

ii) The regions with the highest HIV/AIDS mortality rates were Henan Province from 2004 to 2009, Yunnan Province from 2007 to 2011, and Guangxi Province from 2009 to 2011. *iii*) The areas with the highest HIV/AIDS fatality rates included Gansu Province (90.91%) in 2004, Jiangxi Province (66.13%) in 2005, Gansu Province (80%), and the Ningxia Autonomous Region (100%) in 2006, Henan Province in 2008, the Inner Mongolia Autonomous Region (100%) in 2009, Henan and Hainan provinces (100%) in 2010, and Hainan Province (72.92%) in 2011. Regions with low HIV/AIDS fatality rates included Tibet (0%) in 2007 and Beijing (12.68%) in 2008. In addition, the regions with HIV/AIDS morbidity and mortality rates above the national averages were Xinjiang, Sichuan, and Chongqing from 2009 to 2011 (Table 1), while Shanghai had an HIV/AIDS morbidity rate above the national average from 2010 to 2011.

3.2. *HIV/AIDS mortality rate*

The HIV/AIDS mortality rate among Chinese residents from 2004 to 2011: The HIV/AIDS mortality rate in rural areas was higher than that in urban areas of China. In addition, the HIV/AIDS mortality rate among men was higher than that among women ($p < 0.01$; Figure 2).

3.3. *Hospitalization of HIV/AIDS patients in China*

Distribution by age groups. HIV/AIDS patients discharged from Chinese hospitals from 2004 to 2011 fell primarily into three age groups: 15-44 years, 45-59 years, and 60 years and older. The proportion of HIV/AIDS patients who were younger decreased from 72.7% in 2004 to 55.5% in 2011, the proportion of middle-aged patients increased from 18.3% to 27.1%, and the proportion of elderly patients increased from 6.6% to 15% (Figure 3). Men accounted for the majority of HIV/AIDS patients among individuals aged 60 years and older ($p < 0.01$).

Differences between rural and urban areas. From 2004 to 2011, the number of HIV/AIDS patients discharged from city-level hospitals was higher than that of HIV/AIDS patients discharged from county-level (rural) hospitals ($p > 0.05$) (Figure 4).

Table 1. Morbidity, mortality and fatality rates in China and six of it's regions from 2004-2011

Year	2004			2005			2006			2007			2008			2009			2010			2011		
Parameters	MBR	MTR	FR	MBR	MTR	FR	MBR	MTR	FR	MBR	MTR	FR	MBR	MTR	FR	MBR	MTR	FR	MBR	MTR	FR	MBR	MTR	FR
National averages	0.23	0.06	24.26	0.43	0.1	23.41	0.51	0.1	19.95	0.74	0.3	40.14	0.76	0.41	53.57	1	0.5	49.66	1.2	0.58	48.45	1.53	0.69	45.11
Guangxi	0.7	0.11	15.54	1.85	0.19	10.18	2.67	0.18	6.59	5.17	0.66	12.7	5	1.23	24.6	7.31	2.27	31.11	8.41	3.09	36.72	10.88	4.35	40.01
Yunnan	0.68	0.24	35.23	0.72	0.18	25.08	1.86	0.26	13.75	3.26	1.19	36.53	3.77	1.69	44.86	4.49	2.1	46.91	4.81	2.37	49.32	5.92	2.74	46.38
Xinjiang	0.1	0.03	27.78	0.53	0.03	5.77	1.33	0.06	4.48	1.23	0.19	15.42	1.04	0.72	69.27	1.91	1.2	62.81	2.5	1.65	66.05	3.18	2.05	64.65
Sichuan	0.11	0.04	35.29	0.11	0.04	33.33	0.16	0.06	39.55	0.5	0.26	51.34	0.67	0.39	58.75	1.06	0.53	49.6	1.94	0.97	50.19	2.68	1.26	46.94
Chongqing	0.06	0.03	39.29	0.15	0.05	32.61	0.16	0.06	35.56	0.34	0.12	34.74	0.65	0.34	52.75	1.06	0.55	52.16	1.49	0.67	44.94	2.54	1	39.24
Henan	1.35	0.2	14.9	2.35	0.59	25.2	2.28	0.53	23.2	2.44	1.81	74.18	1.91	1.96	102.86	1.96	1.84	93.84	1.58	1.54	97.6	1.86	1.44	77.4

Note: The data were obtained from the "China Public Health Statistics Yearbook" (2010-2012); MBR = Morbidity rate(1/100,000); MTR = Mortality rate(1/100,000); FR = Fatality rate (%).

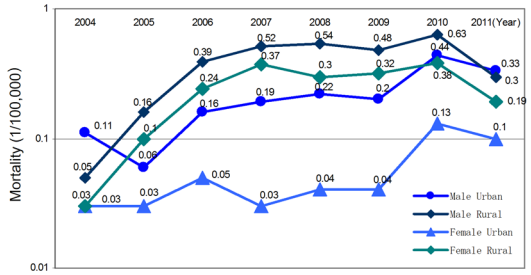

Figure 2. Gender-specific HIV/AIDS mortality rates (1/100,000) in rural and urban areas of China from 2004–2011.

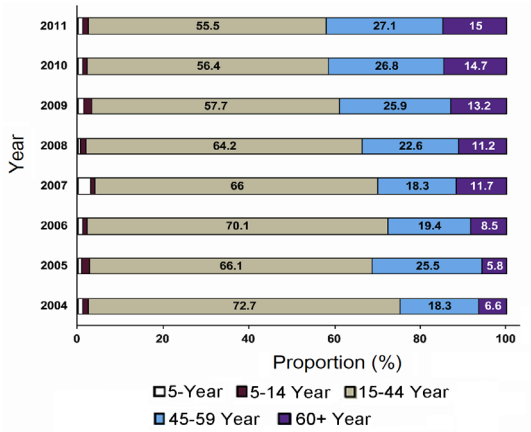

Figure 3. Age-specific proportions (%) of HIV/AIDS patients discharged from Chinese hospitals from 2004-2011.

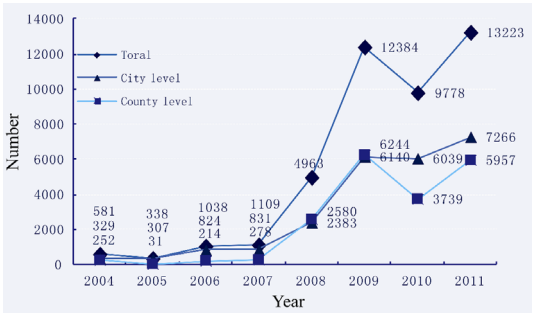

Figure 4. Number of HIV/AIDS patients discharged from Chinese hospitals from 2004-2011 (person) (total, city-level and county-level hospitals).

4. Discussion

4.1. *HIV/AIDS morbidity and mortality rates in China are continuing to increase*

The high HIV/AIDS morbidity rate in Henan Province was mainly due to the illegal selling of blood by poor donors (selling blood is illegal in China). This rate has decreased since 2007, as the government took great measures to crack down on the illegal blood trade (*10*). Guangxi and Yunnan are close to the Golden Triangle in Burma, where injectable drug use was once the main source of HIV transmission, but unprotected sex has recently become a major source of HIV transmission

(*10*). Studies in Guangxi found that most HIV/AIDS patients come from low-income families. HIV/AIDS patients in Yunnan Province primarily live in regions such as Honghe and Dehong (*11*). The HIV/AIDS morbidity rate continually increased in China from 2004 to 2011, primarily due to the high morbidity rates in these three provinces. In addition, the HIV/AIDS morbidity and mortality rates in Xinjiang, Sichuan, and Chongqing were higher than the national averages, with injectable drug use and sexual activity serving as the main modes of HIV transmission. These issues, as well as an increase in men having sex with men and HIV transmission between married couples, lack of services to prevent mother-to-child HIV transmission, and an increased resistance to anti-HIV drugs, are common in these regions.

The HIV/AIDS mortality rate in Henan Province decreased significantly when the morbidity rate was controlled, as high morbidity is always associated with high mortality (*1*). Yunnan Province is closer to Burma than Guangxi Province, and HIV transmission through transnational marriage is more common in Yunnan. The HIV/AIDS mortality rate continually increased in China from 2004 to 2011, primarily due to the high mortality rates in these three provinces.

4.2. *The HIV/AIDS fatality rate in China has continually decreased since 2009*

Despite the continuous increase in HIV/AIDS morbidity and mortality rates and the limited availability of anti-HIV drugs in China, the HIV/AIDS fatality rate has been effectively controlled, as many local governments have made great efforts to prevent and control HIV/AIDS. The "Four Frees and One Care" policy (free screening test, free treatment of poor AIDS patients, free schooling for orphans of AIDS patients, free counseling and antiretroviral therapy for pregnant women with HIV, and social assistance for affected households) is one such measure. However, some regions continue to suffer from a shortage of health care services, an increase in anti-HIV drug resistance, and inadequate attention to HIV/AIDS prevention and control, resulting in higher than national average fatality rates. These regions include Gansu, Ningxia, Inner Mongolia, and Jiangxi, where the economic conditions are relatively poor. The HIV/AIDS fatality rate increased in these provinces due to multiple factors, including a poor economy, a lack of health care services, individuals not wishing to be tested, patients not wishing to disclose their status, lack of early treatment, and opportunistic infections (*12,13*). Data from Hainan showed that high HIV/AIDS fatality rates increased for two years running. Therefore, the rate of HIV detection must increase and early treatment must be provided to HIV/AIDS patients in this province. According to current statistics, the HIV/AIDS fatality rates in Guangxi and Yunnan will probably increase in the near future. The low HIV/AIDS fatality rate in Tibet might be due to the low rate of HIV detection due to factors including its remote geographic location, health care conditions, and religion. Beijing is the political and cultural center of the country, with a booming economy and the country's best health care services. Therefore, the residents of Beijing are more aware of the importance of HIV prevention (*10*). Accordingly, Beijing had a low HIV/AIDS fatality rate in 2008.

4.3. *Differences between HIV/AIDS patients in rural and urban areas*

Rural areas of China are relatively poor, with high rates of drug use and unprotected sex. Low awareness of HIV/AIDS prevention and a lack of heath care service are more common in rural areas than in urban areas. HIV/AIDS typically remains undetected until the late stage of the disease. Therefore, the HIV/AIDS fatality rate in rural areas is higher than that in urban areas. This also means that the HIV/AIDS fatality rate is higher among HIV/AIDS patients who live in the poor regions of China.

Although the number of hospitalized HIV/AIDS patients in China increased from 581 in 2004 to 13,223 in 2011, this only accounted for a small proportion of the HIV/AIDS patients in China, as the number of new cases in China in 2011 totaled 20,450 (*1*). Rural areas had fewer hospitalized HIV/AIDS patients than did cities.

4.4. *Availability of HIV/AIDS specialists in China*

The proportion of Chinese physicians specializing infectious diseases dropped from 2.4% in 2005 to 0.9% in 2011. A three-tier medical treatment system has been established in China where general hospitals are the principal care provider, specialized hospitals provide backup, and basic medical and health facilities are auxiliaries. In 2011, 39.04% of Chinese medical and health facilities were general hospitals and these facilities outnumber specialized hospitals by 6.75 to 1. In addition, 44.63% of practitioners worked in general hospitals. The proportion of medical practitioners caring for urban and rural populations in China differed, with 2.78 physicians per 1,000 individuals in urban areas and 0.96 physicians per 1,000 individuals in rural areas in 2011. There are 164 infectious disease hospitals and 9,307 practicing physicians in China in 2011, and 135 hospitals were located in cities while only 29 were located in rural areas. There were 10,219,397 visits for outpatient services compared to 662,258 hospitalizations. The number of urban HIV patients exceeded that of rural patients by 1.22-fold (*1*). Overall, the outlook for general hospitals is more hopeful than that for specialized hospitals in China.

A huge workload and low income are the main causes of the high rate of turnover for doctors working in infectious disease hospitals. Based on these data, China is clearly experiencing a severe shortage of physicians, particularly in rural areas where there is a higher demand for HIV/AIDS health care professionals.

4.5. *Economic burden of HIV/AIDS care*

The estimated number of HIV/AIDS patients in China was approximately 780,000 until the end of 2011; of these, only 154,000 were AIDS patients and 48,000 were newly discovered cases (*14*). That means that approximately 578,000 cases were undetected. The average annual income per person in 2011 was 23,979.2 RMB in urban areas of China and 9,833.1 RMB in rural areas. The hospitalization cost was 7,108.2 RMB per discharged HIV/AIDS patient in China in 2011 (*1*). The total hospitalization cost could be as high as 93,990,000 RMB when calculated on the basis of 13,223 hospitalized patients. If the total hospitalization cost is calculated on the basis of 154,000 HIV/AIDS patients, then it would be a sizable economic burden for China. The financial cost of HIV/AIDS treatment is also a major financial burden for individual patients, particularly for those from poor regions, as not all care is covered by the government.

Hospitalized HIV/AIDS patients in China are primarily in the age range of 15-44 years. These young patients tend to work far from home, being part of the migrant population in cities (*10,15*). They may also transmit HIV to their sexual partners, many of whom might become pregnant. Not only are the life expectancy and quality of life of individuals with HIV affected, but many of their children become orphaned and represent a major societal burden (*6,16-18*).

The number of HIV/AIDS patients aged 60 years and older has increased. One reason is because many HIV/AIDS patients who were infected with HIV at a younger age have become older and fallen into this age group. In addition, male patients account for the majority of patients in this age group. Men over 60 still desire sex, regardless of whether they are from cities or rural areas. However, many of these individuals lack awareness of HIV prevention and rarely use condoms, thus increasing the rate of HIV infection (*10-12*).

4.6. *Measures taken by the Chinese Government to improve HIV/AIDS care*

The number of hospitalized HIV/AIDS patients is rather low in China and most of these patients receive treatment at city-level hospitals. This includes some rural patients who cannot receive appropriate treatment at local hospitals due to the lack of medical resources and poor economic conditions. Since the majority of HIV/AIDS patients live in poor rural areas of China, controlling HIV/AIDS morbidity and mortality rates in rural areas is difficult since county-level hospitals cannot provide appropriate diagnostic and treatment services. Therefore, the overall HIV/AIDS epidemic in China will be a challenge to control, and rural areas should be key targets for HIV/AIDS prevention and control in China. Public education of HIV prevention should be provided to increase awareness. The government's "Four Free and One Care" policy (free screening test, free treatment for poor AIDS patients, free schooling for orphans of AIDS patients, free counseling and antiretroviral therapy for HIV-infected pregnant women, and care and economic assistance to affected households) needs to be implemented in these areas. Long-distance medical services and knowledge sharing (*19,20*) are also keys to HIV/AIDS control in China, particularly in the poor regions.

The Chinese Government has directed great attention to the prevention and control of HIV/AIDS. Although problems such as the availability of many commercial and free anti-HIV medications remain because China is a developing country, the Government has taken important measures to prevent and control HIV/AIDS in China. These efforts include establishing the Classification and Diagnostic Criteria of HIV/AIDS for Adolescents and Adults and publishing materials such as the "National Manual for Free Antiretroviral Treatment of HIV/AIDS" and the "Guidelines on Diagnosis and Treatment of HIV/AIDS." In January 2012, the first 58 clinical pathways for diagnosis and treatment of HIV/AIDS and related diseases in China were recommended by the Clinical Pathway Pilot Project of the Ministry of Health of the People's Republic of China (*21*). At present, there are a total of 32 approved anti-HIV drugs from six major classes available in China. The recommended standard protocols include: highly active antiretroviral therapy (HAART): two nucleotide reverse transcriptase inhibitors (NRTIs) plus one NNRTI; or two NRTIs plus a boosted protease inhibitor (PI) (with ritonavir); and if necessary, combinations of three NRTIs. Since the availability of anti-HIV drugs in China is limited, the first-line regimen for patients who have not received any prior anti-virus medications is zidovudine (AZT) or stavudine (d4T) plus lamivudine (3TC) plus nevirapine (NVP) or efavirenz (EFV). For patients who fail to respond to the first-line regimen, the second-line regimen is tenofovir disoproxil fumarate (TDF) (abacavir [ABC] for children) plus 3TC + r (*22*). In January 2012, the "Notice regarding Publication of China's 12-Year Action Plan to Contain and Control HIV/AIDS" was issued by the General Office of the State Council of the People's Republic of China. This official document stated that the number of new HIV/AIDS cases should decrease by 25% and the fatality rate should decrease by 30% at the end of 2015 compared to 2010, and the total number of HIV/AIDS

patients should be less than 1,200,000 (*23*). Local governments at various levels are required to expand HIV/AIDS education and intervention, increase the safety of blood collection and use to prevent iatrogenic transmission, expand HIV/AIDS monitoring, testing, and treatment, improve services for and management of HIV/AIDS patients, and provide classification guidelines. Therefore, the Chinese Government is clearly determined to prevent and control HIV/AIDS.

In conclusion, information regarding the epidemiologic features of HIV/AIDS in China and early outcomes of government policies is the key to controlling the HIV/AIDS pandemic in China. This information can help with HIV/AIDS prevention and control around the world. Effective measures to control the HIV/AIDS pandemic in China include taking additional measures to surveil and monitor HIV infection among the migrant worker population in cities, among men over age 60, and in poor regions with high HIV/AIDS morbidity rates (*10,12,24-25*).

Acknowledgements

The authors wish to thank Victor L Yu, MD, Professor of Medicine, University of Pittsburgh, and Yusen Eason Lin, PhD, MBA, Professor, Graduate Institute of Human Resources and Knowledge Management, for reviewing and editing this manuscript.

This study was supported by the 12th Five-Year Infectious Disease Research Project: The Use and Optimization of the Standard Regimen for Diagnosis and Treatment of Tuberculosis in HIV/AIDS Patients in China (No. 2012ZX10001-003), the 12th Five-Year Major Science and Technology Project on Discovery of Major New Drugs: Construction of a Technology Platform for Clinical Evaluation of Anti-HIV Drugs (No. 2012ZX09303013), and the Three Year Action Plan to Enhance Development of the Public Health System in Shanghai: Construction of Dedicated Medical Facilities for AIDS Treatment in Shanghai (No. GW III-13).

References

1. Ministry of Health of the People's Republic of China. China Public Health Statistics Yearbook 2012. 1st ed., Peking Union Medical College Press, Beijing, China.
2. Metcalfe JZ, Porco TC, Westenhouse J, Damesyn M, Facer M, Hill J, Xia Q, Watt JP, Hopewell PC, Flood J. Tuberculosis and HIV co-infection, California, USA, 1993-2008. Emerg Infect Dis. 2012; 19:400-406.
3. De Souza SM, Teles SA, Rezza G, Pezzotti P, Gir E. Epidemiology of HIV infection in central Brazil: Data from voluntary counseling and testing centers. J Assoc Nurses AIDS Care. 2013; 2:1-9.
4. Saba HF, Kouyoumjian SP, Mumtaz GR, Abu-Raddad LJ. Characterising the progress in HIV/AIDS research in the Middle East and North Africa. Sex Transm Infect. 2013; 89 (Suppl 3):iii5-9.
5. Gow J. The HIV/AIDS epidemic in Africa: Implications for U.S. Policy. Health Affairs. 2002; 21:57-69.
6. J Madise N, Ziraba AK, Inungu J, Khamadi SA, Ezeh A, Zulu EM, Kebaso J, Okoth V, Mwau M. Are slum dwellers at heightened risk of HIV infection than other urban residents? Evidence from population-based HIV prevalence surveys in Kenya. Health Place. 2012; 18:1144-1152.
7. Lu L, Jia M, Zhang X, Luo H, Ma Y, Fu L, Lu J. Analysis for epidemic trend of Acquired Immunodeficiency Syndrome in Yunnan Province of China. Chin J Prev Med. 2004; 38:309-312. (in Chinese)
8. Zhu Q, Liu W, Chen J, Li R, Liang F, Zhuo Y, Guo N. Analysis of the prevalence of AIDS in Guangxi Province, China from 1989-2003. Journal of Applied Preventive Medicine 2009; 14:70-73. (in Chinese)
9. Sherer R, Gui X, Zhan F, Teter C, Ping DL, Wykoff RF. Rapid antiretroviral therapy scale-up in Hubei Province, China. Health Affairs. 2008; 27:1140-1147.
10. Zeng Y. AIDS prevention and control. Chinese Journal of Experimental and Clinical Virology. 2007; 21:1. (in Chinese)
11. Duan S, Ding Y, Yang Y, Lu L, Sun J, Wang N, Wang L, Xiang L, Jia M, Wu Z, He N. Prevalence and correlates of HIV discordance and concordance among Chinese-Burmese mixed couples in the Dehong prefecture of Yunnan province, China. Sex Health. 2012; 9:481-487.
12. Zeng Y, Wu Z. Containment of the AIDS epidemic in China. Bulletin of the Chinese Academy of Sciences. 2000; 2:115-119. (in Chinese)
13. Li L, Lin C, Wu Z, Lord L, Wu S. To tell or not to tell: HIV disclosure to family members in China. Dev World Bioeth. 2008; 8:235-241.
14. National Health and Family Planning Commission of the People's Republic of China. Brief Report on Disease Prevention & Control and Patriotic Health Work. The fifth Issue in 2011.
15. Imrie J, Hoddinott G, Fuller S, Oliver S, Newell ML. Why MSM in rural South African communities should be an HIV prevention research priority. AIDS Behav. 2013; 17:70-76.
16. Rochat TJ, Mkwanazi N, Bland R. Maternal HIV disclosure to HIV-uninfected children in rural South Africa. A pilot study of a family-based intervention. BMC Public Health. 2013; 13:147.
17. Gamell A, Letang E, Jullu B, Mwaigomole G, Nyamtema A, Hatz C, Battegay M, Tanner M. Uptake of guidelines on prevention of mother-to-child transmission of HIV in rural Tanzania: time for change. Swiss Med Wkly. 2013; 14:143-150.
18. Damonti J, Doykos P, Wanless RS, Kline M. HIV/AIDS in African children: The Bristol-Myers Squibb Foundation and Baylor response. Health Affairs. 2012; 31:1636-1642.
19. Tanser F, Bärnighausen T, Grapsa E, Zaidi J, Newell ML. High coverage of ART associated with decline in risk of HIV acquisition in rural KwaZulu-Natal, South Africa. Science. 2013; 339:966-971.
20. Campbell C, Nhamo M, Scott K, Madanhire C, Nyamukapa C, Skovdal M, Gregson S. The role of community conversations in facilitating local HIV competence: Case study from rural Zimbabwe. BMC Public Health. 2013; 13:354.
21. Lu H. Clinical Pathways for Treatment of HIV/AIDS and Related Diseases. 1st ed., Shanghai Science &

Technology Press, Shanghai, China, 2012.
22. Lu H. Diagnostic Protocol for HIV/AIDS and Related Diseases. 1st ed., Shanghai Science & Technology Press, Shanghai, China, 2009; pp. 2-14.
23. The Central People's Government of the People's Republic of China. Notice regarding Publication of China's 12-Year Action Plan to Contain and Control HIV/AIDS by the General Office of the State Council of the People's Republic of China. *http://www.gov.cn/zwgk/2012-02/29/content_2079097.htm* (accessed February 12, 2014).
24. Mayer KH, Bekker L, Stall R, Grulich AE, Colfax G, Lama JR. Comprehensive clinical care for men who have sex with men: An integrated approach. Lancet. 2012; 380:378-387.
25. Joska JA, Hoare J, Stein DJ, Flisher AJ. The neurobiology of HIV dementia: Implications for practice in South Africa. Afr J Psychiatry (Johannesbg). 2011; 14:17-22.

(Received October 4, 2013; Revised December 21, 2013; Accepted February 3, 2014)

Original Article

DOI: 10.5582/bst.8.59

Stroke volume variation fail to predict fluid responsiveness in patients undergoing pulmonary lobectomy with one-lung ventilation using thoracotomy

Qiang Fu*, Feng Zhao*, Weidong Mi, Hong Zhang**

Department of Anesthesiology, General Hospital of PLA, Beijing, China.

Summary **The purpose of this study was to investigate the ability of stroke volume variation (SVV) to predict fluid responsiveness in patients undergoing pulmonary lobectomy with one-lung ventilation (OLV). Thirty patients intubated with double-lumen tube were scheduled for a pulmonary lobectomy requiring OLV for at least 1 hour under general anesthesia. Hemodynamic variables including heart rate, mean arterial pressure, cardiac index (CI), stroke volume index (SVI), central venous pressure (CVP) and SVV were measured before and after volume expansion (VE) (8 mL/kg of 6% hydroxyethyl starch). Fluid responsiveness was defined as an increase in CI ≥ 10% after VE. Of the 30 patients, 16 (53%) were responders and 14 (47%) were nonresponders to intravascular VE. There were significant increases of CI, SVI in responders after VE ($p < 0.01$), but there were no significant changes in SVV in responders and nonresponders ($p > 0.05$). The baseline value of SVV, CVP, CI and SVI did not correlate significantly with ΔCI ($p > 0.05$). The area under the Receiver Operating Characteristic (ROC) curve were 0.507 for SVV (95% confidence interval, 0.294-0.720) and 0.556 for CVP (95% confidence interval, 0.339-0.773), neither was able to predict fluid responsiveness with sufficient statistical power. SVV measured by the Vigileo-FloTrac system was not able to predict fluid responsiveness in patients undergoing pulmonary lobectomy with OLV after thoractomy.**

Keywords: Stroke volume variation, open-chest condition, fluid responsiveness, thoracotomy

1. Introduction

Lung-isolation techniques are primarily designed to facilitate One-Lung Ventilation (OLV) in patients undergoing thoracic, cardiac, mediastinal or esophageal procedures involving the chest cavity. It is essential to maintain optimal organ perfusion by appropriate fluid infusion to achieve the balance between preventing fluid overload and optimizing organ perfusion (*1*). Preload assessment is crucial to guide fluid therapy during thoracic surgery procedures. However, determining left ventricular preload in the clinical routine is particularly difficult during surgery. Filling pressures like central venous pressure (CVP) and pulmonary capillary wedge pressure (PCWP) are normally used as parameters of right and left heart preload. But these static indicators have been shown to be poor predictors of fluid responsiveness (*2*).

A recent Vigileo/FloTrac system (Edwards Lifescience, LLC, Irvine, CA, USA) allows for continuous monitoring of the cardiac output (CO) based on pulse contour analysis and of the respiratory variations in stroke volume (SV) based on the analysis of the systemic arterial pressure wave. Stroke volume variation (SVV) is a parameter derived from changes in SV that is dependent on mechanical ventilation and has been found useful for predicting volume response in mechanically ventilated patients during perioperative phase (*3,4*). Only one study reported that SVV could predict fluid during OLV with PEEP in patients undergoing thoracoscopic lobectomy by using Vigileo system (*5*). However, all lobectomies in this study were performed under thoracoscopy in the same way. Since SVV during

*These authors contributed equally to this works.
***Address correspondence to:*
Dr. Weidong Mi, Department of Anesthesiology, General Hospital of PLA, Bei Jing, China, No.28 FuXing Road, Haidian District, Beijing 100853, China.
E-mail: dr_fuqiang@hotmail.com

OLV could be affected by the surgical procedure, it is still unknown whether SVV could predict fluid responsiveness during OLV with the chest open via a thoracotomy. The aim of this study was to examine the suitability of the established parameter of CVP and especially the new parameter of SVV to predict changes in cardiac index (CI) in patients undergoing pulmonary lobectomy with OLV after thoractomy.

2. Materials and Methods

2.1. *Patients characteristics*

This prospective study was approved by institutional review board of General Hospital of PLA. All patients gave informed consent. From October 2009 to July 2011, a total of 33 patients received a pulmonary lobectomy with OLV and intraoperative infusion with colloids under general anesthesia. All patients were diagnosed with lung cancer preoperatively by computerized tomography (CT) and/or magnetic resonance imaging (MRI). Exclusion criteria applied to patients younger than 18 yr, with fibrillation atrial or intracardiac shunt.

2.2. *Anesthesia and one-lung ventilation*

After the patient arrived in the operating room, routine monitoring including pulse oxymetry, three-lead electrocardiogram and non-invasive arterial pressure was applied. Anesthesia was induced with *i.v.* bolus administration of fentanil (3-5μg/kg), and propofol (1.5-2 mg/kg) 2 min later. Following loss of consciousness, orotracheal intubation was facilitated with rocuronium (0.6-0.9 mg/ kg). After anesthesia induction, a double-lumen endo-bronchial tube (Tyco Healthcare, Argyle, Mansfield, MA, USA) was inserted and the position was confirmed by fiberoptic bronchoscopy, the airway pressure was kept at 25-35 cm H_2O. With the proper position of securing the airway, a radial arterial catheter (REFRA-04220, Arrow international Inc., Reading, PA, USA) was inserted and a central venous catheter (ES-04301, Arrow international Inc., Reading, PA, USA) was placed through right internal jugular vein. All pressure transducers were zeroed at midaxillary line to ambient pressure and initial pressures were recorded with the patient in the supine position. After changing the patient's position to lateral decubitus, all pressure transducers were re-positioned at the same value of initially measured pressures in the supine position. Anaesthesia was maintained with target controlled infusion (TCI) of propofol (2-4 μg/mL) and continuous infusion of remifentanil (0.3-0.8 μg/kg/min) with bispectral index (BIS, Aspect 1000™, Aspect Medical Systems Inc., Natick, MA, USA) kept between 40 and 50. Following the initiation of OLV, patients were ventilated with a tidal volume of 8 mL/kg ideal body weight, a ventilation rate of 12 cycle/min, inspired oxygen fraction (FIO_2) was 1.0 and no PEEP was applied.

2.3. *Hemodynamic monitoring*

A dedicated transducer (FloTrac™, Edwards Lifesciences, LLC, Irvine, CA, USA) was connected to the radial arterial line on one side and to the Vigileo System (Vigileo™ Edwards Lifesciences, LLC, Irvine, CA, USA) on the other side. The system enables the continuous monitoring of SV, stroke volume index (SVI), CO, CI and SVV without calibration. The Vigileo (Software version 1.14) analyses the pressure waveform 100 times per second (100 Hz), and performs its calculations on the most recent 20 s data. CI obtained with this device was recorded and used to discriminate responder and non-responder patients after VE. SVV is calculated as the variation of beat-to-beat SV from the mean value during the most recent 20 s data and is displayed continuously. At each step of the study protocol, the following were recorded simultaneously: heart rate (HR), systolic arterial pressure, mean arterial pressure (MAP), diastolic arterial pressure and end-expiratory central venous pressure (CVP).

2.4. *Study protocol*

This study assessed the capability of SVV to predict fluid responsiveness during OLV. The study was started after finishing chest opening (thoracotomy) and collapsing one lung completely. During OLV, values of HR, MAP, CVP, SV/SVI, CO/CI and SVV were measured before (T_0) and 30 min (T_1) after fluid loading. Intraoperative infusion with 8 mL/kg of 6% hydroxyethyl starch was started when deemed necessary by the attending anesthesiologists, and completed in 30 min. Hemodynamic measurements were performed before, and within 30s after volume expansion (VE) without stimulation. All patients were studied at 30 min after starting OLV. During the VE, ventilator settings were kept consistent. If obvious hemorrhage (volume > 100 mL) or arrhythmias happened, the infusion protocol would be terminated and patient would be treated accordingly.

2.5. *Statistical analysis*

All data are presented as mean ± S.D. Distribution normality was assessed using Kolmogorov–Smirnov test. Changes in haemodynamic measures induced by VE were assessed using one-way analysis of variance (ANOVA). Patients were divided into two groups according to the percent increase in CI after intravascular VE. Responders were defined as patients demonstrating an increase in CI ≥ 10% after intravascular VE and non-responders as patients whose CI changed < 10%. Receiver operating characteristic

Table 2. Anti-HBV response of TCM and related active compounds in clinical trials

Items	Baseline	Volume expansion	*p1*	Baseline	*p2*	Volume expansion	*p3*
HR (beat/min)	71.2 ± 10.3	68.4 ± 11.9	0.760	71.9 ± 10.9	0.620	69.7 ± 9.5	0.120
MAP (mmHg)	72.8 ± 10.6	78.6 ± 8.2	0.661	77.7 ± 12.1	0.073	84.8 ± 11.9	0.514
CI (l/min/m^2)	2.9 ± 1.0	3.1 ± 1.1	0.649	2.7 ± 0.6	0.063	3.5 ± 0.7	0.001
CVP (mmHg)	6.89 ± 2.23	8.26 ± 3.02	0.065	6.95 ± 2.45	0.124	8.34 ± 3.14	0.087
SVI (mL/m^2)	41.3 ± 13.6	44.7 ± 16.7	0.705	39.9 ± 15.2	0.291	51.6 ± 15.8	0.003
SVV(%)	8.6 ± 2.8	7.1 ± 2.1	0.260	8.4 ± 3.1	0.095	6.9 ± 2.4	0.083

Values are mean ± S.D. HR, heart rate; MAP, mean arterial pressure; CI, cardiac output index; CVP, central venous pressure; SVI, stroke volume index; SVV, stroke volume variation. *p1*, volume expansion value *vs.* baseline value in non-responders; *p2*, baseline value in responders *vs.* baseline value in non-responders; *p3*, volume expansion value vs. baseline value in responders.

(ROC) curves were generated for SVV, SVI, CI, CVP and MAP. The areas under the ROC curves by varying the discriminating threshold for each parameter were calculated and compared according to the method described by Hanley and McNeil (*6*). Threshold value for each parameter was determined by considering values that yielded the greatest sensitivity and specificity. Pearson's test was used to test correlation. A *p*-value less than 0.05 was considered as statistically significant. All statistic analysis was performed using SPSS 15.0 software (SPSS Inc, Chicago, IL, USA).

3. Results

3.1. *Patients selection*

Thirty-three patients were initially included. Among them, three patients were excluded from analysis because of arrhythmia (two patients; one had ventricular premature contraction, one had atrial fibrillation) or obvious hemorrhage (one patient; bleeding > 100 mL during volume loads) during the protocol. Thirty patients in this study consisted of 21 males and 9 females from 47 to 58-year-old (mean age, 52.4 ± 4.7 year). There was no case requiring the administration of vasoactive agents during volume loading, BP and HR were kept in normal range.

3.2. *Changes in hemodynamic variables after volume expansion*

Hemodynamic measurements in the responders and nonresponders at baseline and after VE are given in Table 1. After VE, no significant changes were found in the nonresponders, while in the responders, there were significant changes of CI (from 2.7 ± 0.6 to 3.5 ± 0.7 l/min/m^2; $p = 0.001$), SVI (39.9 ± 15.2 to 51.6 ± 15.8 mL/m^2; $p = 0.008$). At the same time we observed no significant changes in both SVV and CVP in responders. Before VE, there was no difference in CI, SVI, CVP, MAP and SVV at baseline (Table 1).

3.3. *Fluid responsiveness to fluid therapy*

There were no significant correlations between baseline values of CVP, MAP, SVI, CI and the percent change in CI after fluid expansion ($r = -0.213$, $p = 0.114$; $r = 0.011$, $p = 0.954$; $r = -0.202$, $p = 0.294$; $r = -0.123$, $p = 0.517$, respectively). And the baseline value of SVV also did not correlate significantly with the change in CI induced by fluid expansion ($r = -0.171$, $p = 0.367$).

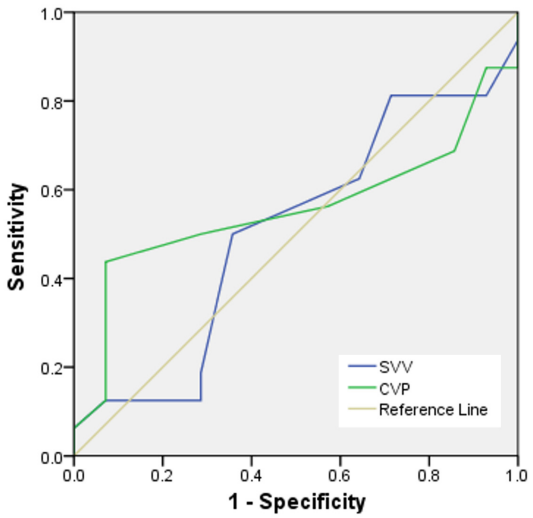

Figure. 1. ROC curve compared the SVV and CVP in the abilities to discriminate the responders and the non-responders. Patients were classified as the responders to fluid loading, when increases in cardiac index (CI) were at least 10%. ROC analysis showed that both SVV and CVP failed to predict fluid responsiveness in patients undergoing pulmonary lobectomy with OLV. Diagonal segments are produced by ties.

3.4. *Dynamic indices and static indices to predict fluid responsiveness*

The overall performance for SVV and CVP in predicting the responsiveness of the stroke volume to intravascular VE was evaluated by constructing ROC curves (Figure 1). The area under the ROC curve was 0.507 for SVV (95% confidence interval, 0.294-0.720), the area under the ROC curve was 0.556 for CVP (95% confidence interval, 0.339-0.773). The ROC analysis showed that both SVV and CVP failed to predict fluid responsiveness with sufficient statistical power in patients undergoing pulmonary lobectomy with OLV. There was no significant difference in the area under ROC curves between SVV and CVP.

4. Discussion

OLV is necessary in a variety of thoracic surgery to collapse one lung for surgical procedure. Several studies have demonstrated that SVV could predict fluid responsiveness in two-lung mechanically ventilated patients, and more efficiently than CI, CVP, MAP, which is in accordance with increasing evidence that static preload indicators are not suited for functional hemodynamic monitoring (*3,4,7*). Only one study evaluated the ability of SVV to predict fluid responsiveness in patients undergoing OLV, and they found that SVV measured by the Vigileo-FloTrac system was able to predict fluid responsiveness in patients undergoing surgery with OLV with acceptable levels of sensitivity and specificity. Of note, all surgeries were performed under thoracoscopy in the same way (*5*). With the chest opening via thoracotomy, whether SVV derived from Vigileo-FloTrac system could predict fluid responsiveness in patients with OLV is still unknown. In the present study, we found that SVV measured by the Vigileo-FloTrac system was not able to predict fluid responsiveness in patients undergoing pulmonary lobectomy with OLV after thoractomy.

Several studies have found that the dynamic volume responsive measurements like SVV and pulse pressure variation (PPV) obtained with PiCCO system may be more suitable for monitoring the volume status of patients particularly under open-heart conditions during cardiac surgery and especially after sternotomy (*8,9*). Conversely, the others found that SVV and PPV were unable to predict fluid responsiveness in open chest condition (*10,11*). It has been shown that opening the chest via a sternotomy may result in an increase in CI and a decrease in SVV (*9,10*) .The ventilated lung is actually not open to the atmosphere because its pleura are still intact and the mediastinum separates lungs from the atmosphere after sternotomy. But with the chest opening by thoracotomy, much of the pressure generated by the ventilator would not be transmitted to the pulmonary vessels but rather to the atmosphere (*5*). So SVV could not be predictive of fluid responsiveness in open-chest condition after thoractomy.

Positive intrathoracic pressure following mechanical ventilation induces a reduction in left ventricular preload. This is reflected by variations in the SV. These variations during a defined interval have proven to be useful parameters of cardiac preload (*12*). But the ventilatory issues, such as tidal volume (*13*), positive end-expiratory pressure (*14*), and chest and lung compliance (*15*) may also have effects on SVV. SVV could predict fluid responsiveness in patients undergoing thoracoscopic lobectomy during OLV only when tidal volume is at least 8 mL/ kg (*13*) and with PEEP (*14*). Another study showed that PPV could predict fluid responsiveness in patients who received protective OLV with tidal volume of 6 mL/ kg, FIO_2 of 0.5 and positive end-expiratory pressure (PEEP) of 5 cm H_2O for lung surgery using thoracotomy, but not in patients who received conventional OLV with tidal volume of 10 mL/ kg, FIO_2 of 1.0 and no PEEP ($_{16}$). In this study, OLV was started with a tidal volume of 8 mL/kg, FIO_2 of 1.0 and no PEEP was applied. But during OLV, if the same tidal volume is applied, the ventilated lung is exposed to double the tidal volume of two-lung ventilation. This could increase right ventricular afterload and exaggerate the cyclic variation in stroke volume (*17*). In addition, the venous return could be influenced by the mechanical ventilation under chest opening due to the decrease in chest compliance and airway pressure. Previous studies have showed that SVV could predict fluid responsiveness in patients undergoing OLV only when tidal volume is at least 8 mL/kg (*13*), so in this study tidal volume was set as 8mL/kg, which had been used previously in two-lung ventilation (*3,4*) or one-lung ventilation (*13*).

Mechanical ventilation method, hypoxic pulmonary vasoconstriction in the non-ventilated lung and significant pulmonary arteriovenous shunt amount through the non-ventilated lung can influence the predictive value of SVV for fluid responsiveness, regardless of the patient's preload state. Due to pulmonary vascular resistance increasement induced by hypoxic pulmonary vasoconstriction in non-ventilated lung, the blood flowed to the ventilated-side lung (*18*). During OLV, there is a 20-30% shunt through the non-ventilated lung even with optimal management. This shunt amount does not contribute to the generation of SVV because there is no cyclic change of intra-thoracic pressure in the non-ventilated lung (*19*). The results showed that SVV before the fluid challenge in both responders and nonresponders was fairly normal, we speculated that SVV was mainly associated with pulmonary flow distribution, did not correlate positively with tidal volume. The results of our study indicate that SVV failed to predict fluid responsiveness in patients undergoing pulmonary lobectomy with OLV after thoracotomy.

Some limitations of our study should be noted. Firstly, we measured CO with Vigileo-FloTrac system, but not a calibrated thermodilution CO monitor. Although thermodilution is considered as the clinical standard method to measure CO, but CO measured by Vigileo-FloTrac system correlated well with that measured by thermodilution. And due to the cost-effect, we did not prefer a calibrated thermodilution CO monitor or transesophagus echocardiograph. Secondly, we did not estimate shunt fraction, so could not draw a conclusion whether the less shunt fraction contributes to the bigger SVV that can predict fluid responsiveness. Thirdly, we could have compared two different ventilation strategies (*i.e.* lung-protective and conventional) to investigate SVV as a predictor of fluid

responsiveness during one-lung ventilation for lung surgery using thoracotomy, whether a clinically more relevant lung protective ventilation strategy would have yielded different results.

In conclusion, we evaluated the capability of SVV in predicting fluid responsiveness in patients receiving OLV. It was found that SVV measured by the Vigileo-FloTrac system was not able to predict fluid responsiveness in patients undergoing pulmonary lobectomy with OLV after thoracotomy.

Acknowledgements

Dr. Qiang Fu was supported by a Japan-China Sasagawa medical research fellowship. Thanks to Dr. Junko Kouhei and Prof. Makoto Ozaki (Tokyo Women's Medical University) for their kind guidance and help.

References

1. Rocca GD, Costa MG. Preload indexes in thoracic anesthesia. Curr Opin Anaesthesiol. 2003; 16:69-73.
2. Berkenstadt H, Margalit N, Hadani M, Friedman Z, Segal E, Villa Y, Perel A. Stroke volume variation as a predictor of fluid responsiveness in patients undergoing brain surgery. Anesth Analg. 200l; 92:984-989.
3. Cannesson M, Musard H, Desebbe O, Boucau C, Simon R, Hénaine R, Lehot JJ. The ability of stroke volume variations obtained with Vigileo/FloTrac system to monitor fluid responsiveness in mechanically ventilated patients. Anesth Analg. 2009; 108:513-517.
4. Qiang Fu, Weidong Mi, Hong Zhang. Stroke volume variation and pleth variability index to predict fluid responsiveness during resection of primary retroperitoneal tumors in Hans Chinese. Biosci Trends. 2012; 6:38-43.
5. Suehiro K, Okutani R.Stroke volume variation as a predictor of fluid responsiveness in patients undergoing one-lung ventilation.J Cardiothorac Vasc Anesth. 2010; 24:772-775.
6. Hanley JA, McNeil BJ. A method of comparing the areas under receiver operating characteristic curves derived from the same cases. Radiology. 1983; 148:839-843.
7. Osman D, Ridel C, Ray P, Monnet X, Anguel N, Richard C, Teboul JL. Cardiac filling pressures are not appropriate to predict hemodynamic response to volume challenge. Crit Care Med. 2007; 35:64-68.
8. Sander M, Spies CD, Berger K, Grubitzsch H, Foer A, Krämer M, Carl M, von Heymann C. Prediction of volume response under open-chest conditions during coronary artery bypass surgery. Crit Care. 2007; 11:R121-127.
9. Rex S, Brose S, Metzelder S, Hüneke R, Schälte G, Autschbach R, Rossaint R, Buhre W. Prediction of fluid responsiveness in patients during cardiac surgery. Br J Anaesth. 2004; 93:782-788.
10. de Waal EE, Rex S, Kruitwagen CL, Kalkman CJ, Buhre WF. Dynamic preload indicators fail to predict fluid responsiveness in open-chest conditions.Critical care med. 2009; 37:510-515.
11. Rex S, Schälte G, Schroth S, de Waal EE, Metzelder S, Overbeck Y, Rossaint R, Buhre W. Limitations of arterial pulse pressure variation and left ventricular stroke volume variation in estimating cardiac pre-load during open heart surgery. Acta Anaesthesiol Scand. 2007; 51:1258-1267.
12. Perel A. Assessing fluid responsiveness by the systolic pressure variation in mechanically ventilated patients. Systolic pressure variation as a guide to fluid therapy in patients with sepsis-induced hypotension. Anesthesiology. 1998; 89:1309-1310.
13. Suehiro K, Okutani R. Influence of tidal volume for stroke volume variation to predict fluid responsiveness in patients undergoing one-lung ventilation. J Anesth. 2011; 25:777-780.
14. Pizov R, Cohen M, Weiss Y, Segal E, Cotev S, Perel A. Positive end-expiratory pressure-induced hemodynamic changes are reflected in the arterial pressure wave form. Crit Care Med. 1996; 24:1381-1387.
15. Jardin F, Genevray B, Brun-Ney D, Bourdarias JP. Influence of lung and chest wall compliances on transmission of airway pressures to the pleural space in critically ill patients. Chest. 1985; 88:653-658.
16. Lee JH, Jeon Y, Bahk JH, Gil NS, Hong DM, Kim JH, Kim HJ. Pulse pressure variation as a predictor of fluid responsiveness during one-lung ventilation for lung surgery using thoracotomy: randomised controlled study. Eur J Anaesthesiol. 2011; 28:39-44.
17. Michard F, Teboul JL. Using heart-lung interactions to assess fluid responsiveness during mechanical ventilation. Crit Care. 2000; 4:282-289.
18. Trepte CJ, Haas SA, Nitzschke R, Salzwedel C, Goetz AE, Reuter DA. Prediction of volume-responsiveness during one-lung ventilation: A comparison of static, volumetric, and dynamic parameters of cardiac preload. J Cardiothorac Vasc Anesth. 2013; 27:1094-1100.
19. Slinger PD, Campos JH. Anesthesia for thoracic surgery. In: Miller's Anesthesia (Miller RD, ed.). 7th ed., Elsevier Churchill Livingstone, Philadelphia, USA, 2009; pp. 1819-1887.

(Received November 5, 2013; Revised January 19, 2014; Accepted February 6, 2014)

Case Report

DOI: 10.5582/bst.8.64

A case of psoriasis accompanied by arthritis after delivery

Hisashi Kanemaru, Masatoshi Jinnin*, Kae Asao, Asako Ichihara, Katsunari Makino, Ikko Kajihara, Akihiko Fujisawa, Satoshi Fukushima, Hironobu Ihn

Department of Dermatology and Plastic Surgery, Faculty of Life Sciences, Kumamoto University, Honjo, Kumamoto, Japan.

Summary **Psoriasis and psoriatic arthritis are chronic inflammatory diseases of the skin and joints, but the relationship between them has not been fully understood. Since the delay of treatment for psoriatic arthritis can result in the severe deformities, it is important to identify the pathological triggers of the arthritis. On the other hand, many reports suggest that the changes of immune balance during pre/postpartum period are associated with the state of autoimmune diseases. Here, we report a female case with psoriasis whose arthritis may be triggered by the delivery. Our report suggests that immune tolerance may diminish in the postpartum period, which may alter the susceptibility to arthritis. Female patients should be followed-up carefully during postpartum period against the development of arthritis.**

Keywords: Autoimmune diseases, immune tolerance, psoriatic arthritis

1. Introduction

Psoriasis is a chronic inflammatory dermatosis of the skin affecting as many as 1-2% of Caucasian and 0.02-0.1% of Japanese people (*1*). Among them, some cases are thought to be accompanied with arthritis. Psoriatic arthritis is different from rheumatoid arthritis (RA) in terms of its predilection for the distal interphalangeal joints and negative rheumatoid factors (RF), and therefore is included in seronegative spondyloarthropathy. The arthritis is associated with cutaneous psoriasis in more than 90% of cases, and is preceded by the cutaneous lesion in 75% cases (*2*). Though treatment with monoclonal antibodies against tumor necrosis factor (TNF) (*e.g.* infliximab and adalimumab) or soluble TNF receptor (etanercept) have been in clinical use recently, the delay of treatment may result in the reduced quality of life and the severe deformities resembling the joint changes seen in RA. Therefore, the early detection and treatment of arthritis is necessary in psoriasis patients, and it is important to identify the pathological triggers of the arthritis. Until today, genetic factors, mechanical stimulations, infections, drugs, and immunologic factors are reported as triggers of psoriatic arthritis (*2*). Here, we report a female case with psoriasis whose arthritis may be triggered by the delivery.

2. Case reports

A 37-year-old Japanese female visited our hospital, for the treatment of the eruption and arthritis. There was no record of similar conditions in her family history. She had been diagnosed as having psoriasis vulgaris more than 20 years ago, and treated with corticosteroid ointments. She had never had arthralgia. She got her first child 3 months before the first visit, without any problems related to the delivery. However, she started to complain of arthralgia after the delivery, and the arthritis as well as the eruption worsened gradually. On physical examination, the patients had the skin lesions in the trunk and extremities. The each lesion was well-demarcated, erythematous plaque covered by silver-white scales (Figure 1). Neither pustules nor nail changes were observed. She could not stand up by herself because of her joint swelling and pain, which was present in finger, wrist, elbow, knee, and ankle joints.

As laboratory findings, the white blood cell (WBC) count and C-reactive protein (CRP) levels was slightly increased at 9,000/uL and 2.07 mg/dL, respectively. Antinuclear antibody or anti-cyclic citrullinated

**Address correspondence to:*
Dr. Masatoshi Jinnin, Department of Dermatology and Plastic Surgery, Faculty of Life Sciences, Kumamoto University, 1-1-1 Honjo, Kumamoto, Japan.
E-mail: mjin@kumamoto-u.ac.jp

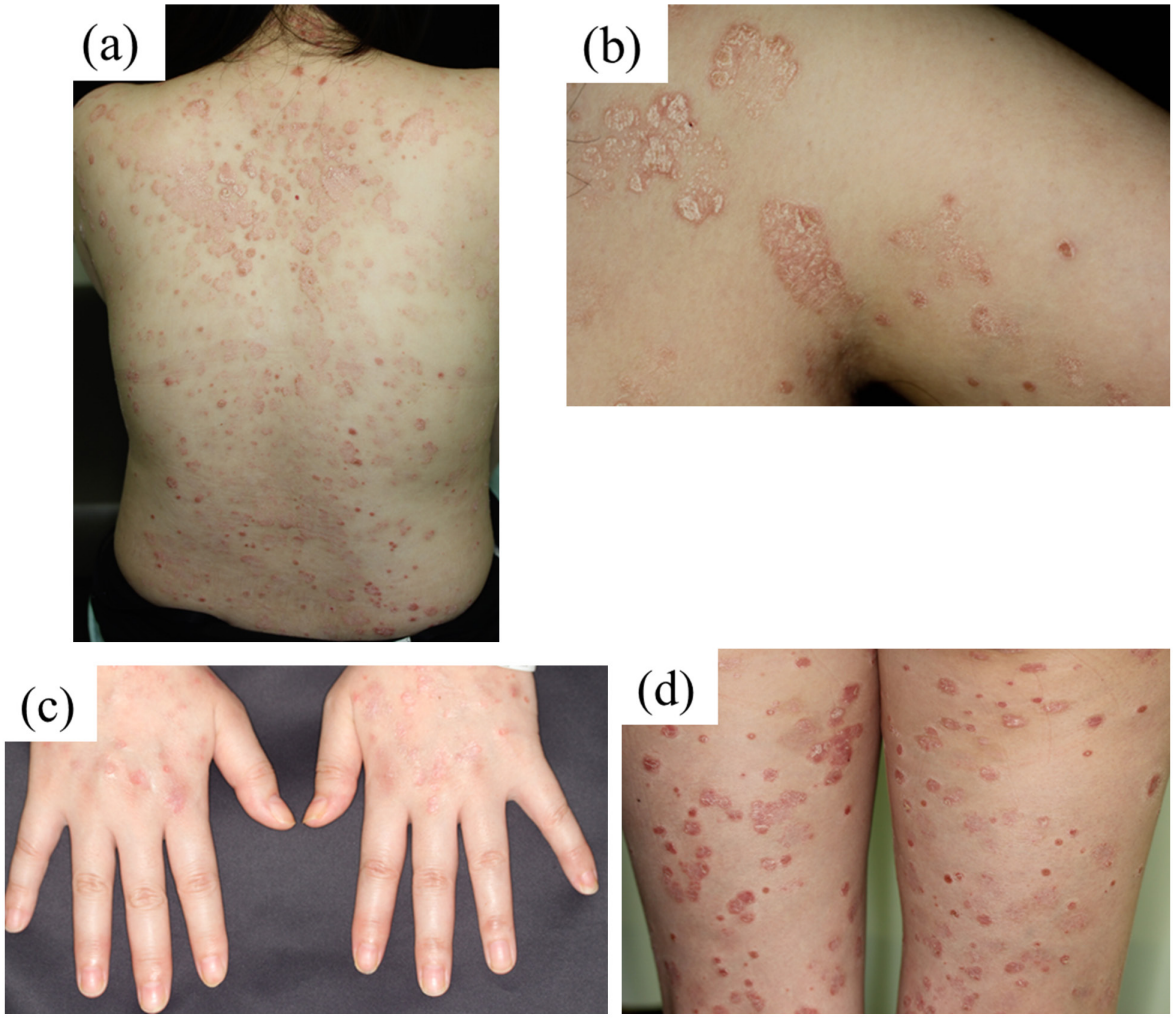

Figure 1. Well-demarcated, erythematous plaques covered by silver-white scales in the back (a), upper arm (b), hands (c), and thighs (d).

Figure 2. 99mTc-MDP bone scintigraphy showing the increased uptake in finger, wrist, elbow, knee, and ankle joints.

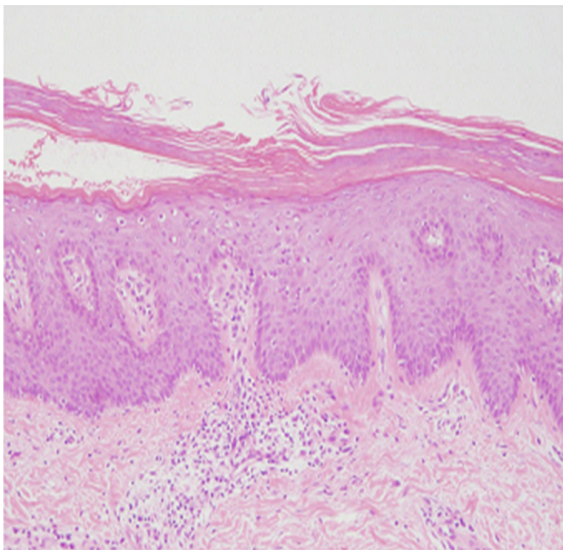

Figure 3. Haematoxylin and eosin (H&E) staining of biopsy specimen from cutaneous lesion.

peptide (CCP) antibody was not detected. RF was also negative (7 IU/mL, normally < 20 IU/mL), and the serum level of matrix metalloproteinase (MMP)-3 was not increased (32.1 ng/mL, normally < 59.7 ng/mL). Laboratory results of other blood cell counts, blood chemistry analysis (including serum albumin, p-glucose or HbA1c), urinalysis, and chest radiography were within normal limits. Bone scintigraphy showed increased uptake in multiple joints (Figure 2), which were identical to the swollen and painful joints.

A skin biopsy from the affected area revealed acanthosis, hypogranulosis and extensive overlying parakeratotic scale in the epidermis. Perivascular infiltration of neutrophils and lymphocytes in the dermis was also seen (Figure 3).

Based on the findings of blood examination, bone scintigram and skin biopsy, she was diagnosed as having psoriasis and postpartum development of arthritis. Her Psoriasis Area and Severity Index (PASI) of the cutaneous lesion, DAS28-CRP and visual analogue scale (VAS) of the arthritis was 22.6, 3.9, and 60, respectively.

The patient was treated with infliximab immediately. After three times of administration, her eruption and arthritis have disappeared completely (Figure 4). The PASI and VAS was also improved dramatically as shown in Figure 5.

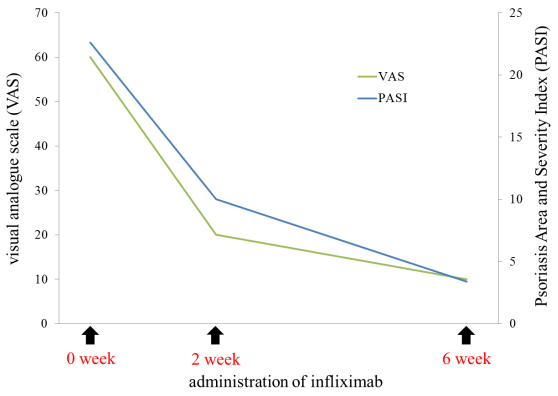

Figure 5. The time course of the changes of PASI of the cutaneous lesions and VAS of the arthritis during the treatment with infliximab, which was administered three times (0, second and, sixth week).

3. Discussion

Though the aetiology of psoriasis and psoriatic arthritis is multifactorial, one of the most likely pathogenic agents may be T cell (*2*). This suggestion is supported by many clinical studies for the treatment of psoriasis and psoriatic arthritis: e.g. the clinical efficacy of cyclosporin, a highly selective antagonist of T-cell proliferation and activation (*2*). Psoriasis has been regarded as the Th1-mediated disease like RA and Crohn disease (*2-5*). However, in the last few years, Th17, a new subset of CD4 T cells, has been identified, based on their production of IL-17 (*6*). There are many reports that indicate IL-17 is associated with the pathogenesis of psoriasis (*7*). In addition, it was reported that regulatory T cells (Treg), which suppress CD4 helper T cells, are impaired in many autoimmune diseases (*8*). Psoriatic Treg have also been found to defect the activity, which may result in the auto-reactive T cell activation and contribute to the pathogenesis for psoriasis (*9*). Taken together, in psoriasis and psoriatic arthritis, Th1 and Th17 should be predominant rather than Th2 and Treg, like RA.

On the other hand, although the change of immune system during pregnancy has not been fully clarified,

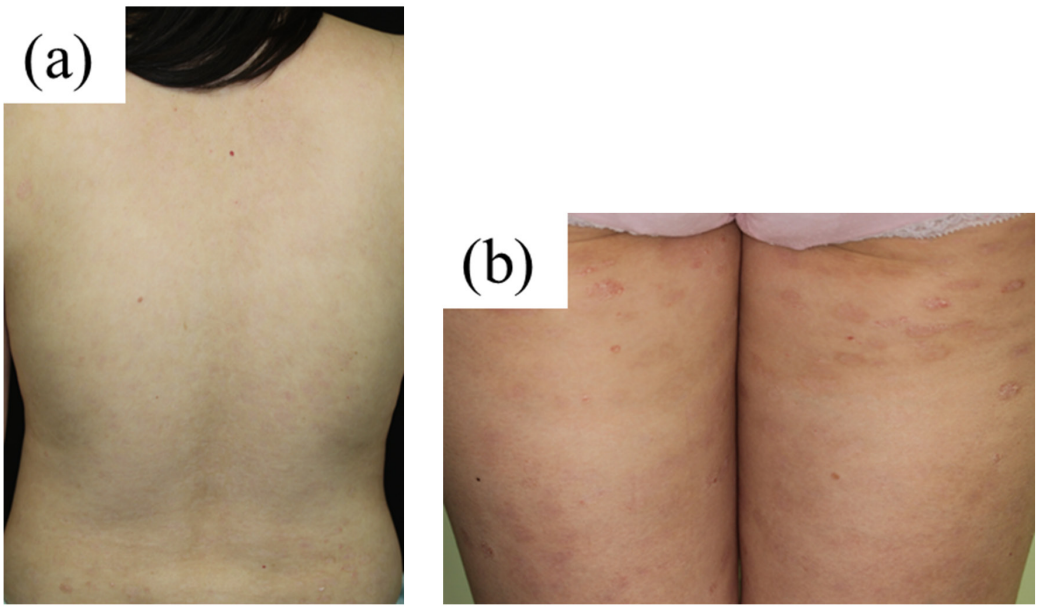

Figure 4. Macroscopic appearance of the back (a) and thighs (b) of the patient after three times of infliximab administration.

many studies have reported a predominant Th2/Treg-type immunity and a suppressed Th1/17-type immunity during normal pregnancy (*10*). These immunological changes seem to be necessary for successful pregnancy, because the predominance of Th1/17-type immunity over Th2/Treg-type immunity is observed in abortion patients (*10*). Estrogens and progesterone are known to inhibit Th1 immune responses including TNF-α and IL-12 production, while induce Th2 immune responses like IL-10 and IL-4 production (*11*). These hormones are significantly increased during pregnancy in comparison with the postpartum period. In addition, during pregnancy, Th1-type immunity is well controlled to avoid its overstimulation, probably due to the suppression by Treg, which are observed to increase in decidua (*11*). Furthermore, the level of IL-17 in normal pregnancy is lower than that in non-pregnancy, and Th17 is thought to be inhibited in the former condition (*12*). Taken together, in pregnancy, Th2/Treg-type immunity should be predominant over Th1/Th17-type immunity by the above changes in the hormones and cytokines, and the subsequent rebound of Th1/Th17 may occur after delivery.

The above notions suggest that immune tolerance may diminish in the postpartum period, which may alter the susceptibility to autoimmune diseases including RA. Actually, postpartum onset of RA by the Th1/Th17 activation has been well described (*13*). On the other hand, psoriasis is known to be one of the diseases which are improved during pregnancy (*14*). Furthermore, there is a very old report that states 6 of 20 psoriasis patients developed arthritis during postpartum period (*15*). Since then, however, there have been no reports describing similar cases. Our case is the second to suggest that the changes in immune balance after delivery may be the newly described trigger of arthritis in female patients with psoriasis. From this point of view, female patients should be followed-up carefully during postpartum period against the occurrence of arthritis.

Recent papers have shown that serum IL-17 level is reduced and Treg level is increased after infliximab treatment in psoriasis (*16,17*). As the limitation of the paper, because blood samples of the patient were not collected, we could not perform time course measurement of IL-17 levels and the number or activity of Treg before and during the treatment with infliximab, which may support our hypothesis. To confirm the immunologic mechanism in female patients with psoriatic arthritis during pre/postpartum period, further studies are needed in a large number of patients in the future.

References

1. Takahashi H, Nakamura K, Kaneko F, Nakagawa H, Iizuka H, Japanese Society for Psoriasis Research. Analysis of psoriasis patients registered with the Japanese Society for Psoriasis Research from 2002-2008. J Dermatol. 2011; 38:1125-1129.
2. Ciocon DH, Kimball AB. Psoriasis and psoriatic arthritis: separate or one and the same? Br J Dermatol. 2007; 157:850-860.
3. Jacob SE, Nassiri M, Kerdel FA, Vincek V. Simultaneous measurement of multiple Th1 and Th2 serum cytokines in psoriasis and correlation with disease severity. Mediators Inflamm. 2003; 12:309-313.
4. Berner B, Akça D, Jung T, Muller GA, Reuss-Borst MA. Analysis of Th1 and Th2 cytokines expressing CD4+ and CD8+ T cells in rheumatoid arthritis by flow cytometry. J Rheumatol. 2000; 27:1128-1135.
5. Parronchi P, Romagnani P, Annunziato F, Sampognaro S, Becchio A, Giannarini L, Maggi E, Pupilli C, Tonelli F, Romagnani S. Type 1 T-helper cell predominance and interleukin-12 expression in the gut of patients with Crohn's disease. Am J Pathol. 1997; 150:823-832.
6. Weaver CT, Harrington LE, Mangan PR, Gavrieli M, Murphy KM. Th17: An effector CD4 T cell lineage with regulatory T cell ties. Immunity. 2006; 24:677-688.
7. Li J, Li D, Tan Z. The expression of interleukin-17, interferon-γ, and macrophage inflammatory protein-3 α mRNA in patients with psoriasis vulgaris. J Huazhong Univ Sci Technolog Med Sci. 2004; 24:294-296.
8. Buckner JH. Mechanisms of impaired regulation by CD4(+)CD25(+)FOXP3(+) regulatory T cells in human autoimmune diseases. Nat Rev Immunol. 2010; 10:849-859.
9. Goodman WA, Cooper KD, McCormick TS. Regulation generation: The suppressive functions of human regulatory T cells. Crit Rev Immunol. 2012; 32:65-79.
10. Saito S, Nakashima A, Shima T, Ito M. Th1/Th2/Th17 and regulatory T-cell paradigm in pregnancy. Am J Reprod Immunol. 2010; 63:601-610.
11. Robinson DP, Klein SL. Pregnancy and pregnancy-associated hormones alter immune responses and disease pathogenesis. Horm Behav. 2012; 62:263-271.
12. Santner-Nanan B, Peek MJ, Khanam R, Richarts L, Zhu E, Fazekas de St Groth B, Nanan R. Systemic increase in the ratio between Foxp3+ and IL-17-producing CD4+ T cells in healthy pregnancy but not in preeclampsia. J Immunol. 2009; 183:7023-7030.
13. Ostensen M, Villiger PM. The remission of rheumatoid arthritis during pregnancy. Semin Immunopathol. 2007; 29:185-191.
14. Murase JE, Chan KK, Garite TJ, Cooper DM, Weinstein GD. Hormonal effect on psoriasis in pregnancy and post partum. Arch Dermatol. 2005; 141:601-606.
15. McHugh NJ, Laurent MR. The effect of pregnancy on the onset of psoriatic arthritis. Br J Rheumatol. 1989; 28:50-52.
16. Kagami S, Rizzo HL, Lee JJ, Koguchi Y, Blauvelt A. Circulating Th17, Th22, and Th1 cells are increased in psoriasis. J Invest Dermatol. 2010 ; 130:1373-1383.
17. Diluvio L, Romiti ML, Angelini F, Campione E, Rossi P, Prinz JC, Chimenti S, Lamioni A. Infliximab therapy induces increased polyclonality of CD4+CD25+ regulatory T cells in psoriasis. Br J Dermatol. 2010; 162:895-897.

(Received October 13, 2012; Revised December 30, 2013; Accepted January 31, 2014)

BST
BioScience Trends

Guide for Authors

1. Scope of Articles

BioScience Trends is an international peer-reviewed journal. BioScience Trends devotes to publishing the latest and most exciting advances in scientific research. Articles cover fields of life science such as biochemistry, molecular biology, clinical research, public health, medical care system, and social science in order to encourage cooperation and exchange among scientists and clinical researchers.

2. Submission Types

Original Articles should be well-documented, novel, and significant to the field as a whole. An Original Article should be arranged into the following sections: Title page, Abstract, Introduction, Materials and Methods, Results, Discussion, Acknowledgments, and References. Original articles should not exceed 5,000 words in length (excluding references) and should be limited to a maximum of 50 references. Articles may contain a maximum of 10 figures and/or tables.

Brief Reports definitively documenting either experimental results or informative clinical observations will be considered for publication in this category. Brief Reports are not intended for publication of incomplete or preliminary findings. Brief Reports should not exceed 3,000 words in length (excluding references) and should be limited to a maximum of 4 figures and/or tables and 30 references. A Brief Report contains the same sections as an Original Article, but the Results and Discussion sections should be combined.

Reviews should present a full and up-to-date account of recent developments within an area of research. Normally, reviews should not exceed 8,000 words in length (excluding references) and should be limited to a maximum of 100 references. Mini reviews are also accepted.

Policy Forum articles discuss research and policy issues in areas related to life science such as public health, the medical care system, and social science and may address governmental issues at district, national, and international levels of discourse. Policy Forum articles should not exceed 2,000 words in length (excluding references).

Case Reports should be detailed reports of the symptoms, signs, diagnosis, treatment, and follow-up of an individual patient. Case reports may contain a demographic profile of the patient but usually describe an unusual or novel occurrence. Unreported or unusual side effects or adverse interactions involving medications will also be considered. Case Reports should not exceed 3,000 words in length (excluding references).

News articles should report the latest events in health sciences and medical research from around the world. News should not exceed 500 words in length.

Letters should present considered opinions in response to articles published in BioScience Trends in the last 6 months or issues of general interest. Letters should not exceed 800 words in length and may contain a maximum of 10 references.

3. Editorial Policies

Ethics: BioScience Trends requires that authors of reports of investigations in humans or animals indicate that those studies were formally approved by a relevant ethics committee or review board.

Conflict of Interest: All authors are required to disclose any actual or potential conflict of interest including financial interests or relationships with other people or organizations that might raise questions of bias in the work reported. If no conflict of interest exists for each author, please state "There is no conflict of interest to disclose".

Submission Declaration: When a manuscript is considered for submission to BioScience Trends, the authors should confirm that 1) no part of this manuscript is currently under consideration for publication elsewhere; 2) this manuscript does not contain the same information in whole or in part as manuscripts that have been published, accepted, or are under review elsewhere, except in the form of an abstract, a letter to the editor, or part of a published lecture or academic thesis; 3) authorization for publication has been obtained from the authors' employer or institution; and 4) all contributing authors have agreed to submit this manuscript.

Cover Letter: The manuscript must be accompanied by a cover letter signed by the corresponding author on behalf of all authors. The letter should indicate the basic findings of the work and their significance. The letter should also include a statement affirming that all authors concur with the submission and that the material submitted for publication has not been published previously or is not under consideration for publication elsewhere. The cover letter should be submitted in PDF format. For example of Cover Letter, please visit http://www.biosciencetrends.com/downcentre.php (Download Centre).

Copyright: A signed JOURNAL PUBLISHING AGREEMENT (JPA) form must be provided by post, fax, or as a scanned file before acceptance of the article. Only forms with a hand-written signature are accepted. This copyright will ensure the widest possible dissemination of information. A form facilitating transfer of copyright can be downloaded by clicking the appropriate link and can be returned to the e-mail address or fax number noted on the form (Please visit Download Centre). Please note that your manuscript will not proceed to the next step in publication until the JPA Form is received. In addition, if excerpts from other copyrighted works are included, the author(s) must obtain written permission from the copyright owners and credit the source(s) in the article.

Suggested Reviewers: A list of up to 3 reviewers who are qualified to assess the scientific merit of the study is welcomed. Reviewer information including names, affiliations, addresses, and e-mail should be provided at the same time the manuscript is submitted online. Please do not suggest reviewers with known conflicts of interest, including participants or anyone with a stake in the proposed research; anyone from the same institution; former students, advisors, or research collaborators (within the last three years); or close personal contacts. Please note that the Editor-in-Chief may accept one or more of the proposed reviewers or may request a review by other qualified persons.

Language Editing: Manuscripts prepared by authors whose native language is not English should have their work proofread by a native English speaker before submission. If not, this might delay the publication of your manuscript in BioScience Trends.

The Editing Support Organization can provide English proofreading, Japanese-English translation, and Chinese-English translation services to authors who want to publish in BioScience Trends and need assistance before submitting a manuscript. Authors can visit this organization directly at http://www.iacmhr.com/iac-eso/support.php?lang=en. IAC-ESO was established to facilitate manuscript preparation by researchers whose native language is not English and to help edit works intended for international academic journals.

4. Manuscript Preparation

Manuscripts should be written in clear, grammatically correct English and submitted as a Microsoft Word file in a single-column format. Manuscripts must be paginated and typed in 12-point Times New Roman font with 24-point line spacing. Please do not embed figures in the text. Abbreviations should be used as little as possible and should be explained at first mention unless the term is a well-known abbreviation (*e.g.* DNA). Single words should not be abbreviated.

Title Page: The title page must include 1) the title of the paper (Please note the title should be short, informative, and contain the major key words); 2) full name(s) and affiliation(s) of the author(s), 3) abbreviated names of the author(s), 4) full name, mailing address, telephone/fax numbers, and e-mail address of the corresponding author; and 5) conflicts of interest (if you have an actual or potential conflict of interest to disclose, it must be included as a footnote on the title page of the manuscript; if no conflict of

interest exists for each author, please state "There is no conflict of interest to disclose"). Please visit Download Centre and refer to the title page of the manuscript sample.

Abstract: The abstract should briefly state the purpose of the study, methods, main findings, and conclusions. For article types including Original Article, Brief Report, Review, Policy Forum, and Case Report, a one-paragraph abstract consisting of no more than 250 words must be included in the manuscript. For News and Letters, a brief summary of main content in 150 words or fewer should be included in the manuscript. Abbreviations must be kept to a minimum and non-standard abbreviations explained in brackets at first mention. References should be avoided in the abstract. Key words or phrases that do not occur in the title should be included in the Abstract page.

Introduction: The introduction should be a concise statement of the basis for the study and its scientific context.

Materials and Methods: The description should be brief but with sufficient detail to enable others to reproduce the experiments. Procedures that have been published previously should not be described in detail but appropriate references should simply be cited. Only new and significant modifications of previously published procedures require complete description. Names of products and manufacturers with their locations (city and state/country) should be given and sources of animals and cell lines should always be indicated. All clinical investigations must have been conducted in accordance with Declaration of Helsinki principles. All human and animal studies must have been approved by the appropriate institutional review board(s) and a specific declaration of approval must be made within this section.

Results: The description of the experimental results should be succinct but in sufficient detail to allow the experiments to be analyzed and interpreted by an independent reader. If necessary, subheadings may be used for an orderly presentation. All figures and tables must be referred to in the text.

Discussion: The data should be interpreted concisely without repeating material already presented in the Results section. Speculation is permissible, but it must be well-founded, and discussion of the wider implications of the findings is encouraged. Conclusions derived from the study should be included in this section.

Acknowledgments: All funding sources should be credited in the Acknowledgments section. In addition, people who contributed to the work but who do not meet the criteria for authors should be listed along with their contributions.

References: References should be numbered in the order in which they appear in the text. Citing of unpublished results, personal communications, conference abstracts, and theses in the reference list is not recommended but these sources may be mentioned in the text. In the reference list, cite the names of all authors when there are fifteen or fewer authors; if there are sixteen or more authors, list the first three followed by *et al.* Names of journals should be abbreviated in the style used in PubMed. Authors are responsible for the accuracy of the references. Examples are given below:

Example 1 (Sample journal reference):
Inagaki Y, Tang W, Zhang L, Du GH, Xu WF, Kokudo N. Novel aminopeptidase N (APN/CD13) inhibitor 24F can suppress invasion of hepatocellular carcinoma cells as well as angiogenesis. Biosci Trends. 2010; 4:56-60.

Example 2 (Sample journal reference with more than 15 authors):
Darby S, Hill D, Auvinen A, *et al.* Radon in homes and risk of lung cancer: Collaborative analysis of individual data from 13 European case-control studies. BMJ. 2005; 330:223.

Example 3 (Sample book reference):
Shalev AY. Post-traumatic stress disorder: diagnosis, history and life course. In: Post-traumatic Stress Disorder, Diagnosis, Management and Treatment (Nutt DJ, Davidson JR, Zohar J, eds.). Martin Dunitz, London, UK, 2000; pp. 1-15.

Example 4 (Sample web page reference):
Ministry of Health, Labour and Welfare of Japan. Dietary reference intakes for Japanese. *http://www.mhlw.go.jp/houdou/2004/11/h1122-2a.html* (accessed June 14, 2010).

Tables: All tables should be prepared in Microsoft Word or Excel and should be arranged at the end of the manuscript after the References section. Please note that tables should not in image format. All tables should have a concise title and should be numbered consecutively with Arabic numerals. If necessary, additional information should be given below the table.

Figure Legend: The figure legend should be typed on a separate page of the main manuscript and should include a short title and explanation. The legend should be concise but comprehensive and should be understood without referring to the text. Symbols used in figures must be explained.

Figure Preparation: All figures should be clear and cited in numerical order in the text. Figures must fit a one- or two-column format on the journal page: 8.3 cm (3.3 in.) wide for a single column, 17.3 cm (6.8 in.) wide for a double column; maximum height: 24.0 cm (9.5 in.). Please make sure that the symbols and numbers appeared in the figures should be clear. Please make sure that artwork files are in an acceptable format (TIFF or JPEG) at minimum resolution (600 dpi for illustrations, graphs, and annotated artwork, and 300 dpi for micrographs and photographs). Please provide all figures as separate files. Please note that low-resolution images are one of the leading causes of article resubmission and schedule delays. All color figures will be reproduced in full color in the online edition of the journal at no cost to authors.

Units and Symbols: Units and symbols conforming to the International System of Units (SI) should be used for physicochemical quantities. Solidus notation (*e.g.* mg/kg, mg/mL, mol/mm^2/min) should be used. Please refer to the SI Guide www.bipm.org/en/si/ for standard units.

Supplemental data: Supplemental data might be useful for supporting and enhancing your scientific research and BioScience Trends accepts the submission of these materials which will be only published online alongside the electronic version of your article. Supplemental files (figures, tables, and other text materials) should be prepared according to the above guidelines, numbered in Arabic numerals (*e.g.*, Figure S1, Figure S2, and Table S1, Table S2) and referred to in the text. All figures and tables should have titles and legends. All figure legends, tables and supplemental text materials should be placed at the end of the paper. Please note all of these supplemental data should be provided at the time of initial submission and note that the editors reserve the right to limit the size and length of Supplemental Data.

5. Submission Checklist

The Submission Checklist will be useful during the final checking of a manuscript prior to sending it to BioScience Trends for review. Please visit Download Centre and download the Submission Checklist file.

6. Online Submission

Manuscripts should be submitted to BioScience Trends online at http://www.biosciencetrends.com. The manuscript file should be smaller than 5 MB in size. If for any reason you are unable to submit a file online, please contact the Editorial Office by e-mail at office@biosciencetrends.com.

7. Accepted Manuscripts

Proofs: Galley proofs in PDF format will be sent to the corresponding author via e-mail. Corrections must be returned to the editor (proof-editing@biosciencetrends.com) within 3 working days.

Offprints: Authors will be provided with electronic offprints of their article. Paper offprints can be ordered at prices quoted on the order form that accompanies the proofs.

Page Charge: Page charges will be levied on all manuscripts accepted for publication in BioScience Trends ($140 per page for black white pages; $340 per page for color pages). Under exceptional circumstances, the author(s) may apply to the editorial office for a waiver of the publication charges at the time of submission.

(*Revised February 2013*)

Editorial and Head Office:
Pearl City Koishikawa 603
2-4-5 Kasuga, Bunkyo-ku
Tokyo 112-0003 Japan
Tel: +81-3-5840-8764
Fax: +81-3-5840-8765
E-mail: office@biosciencetrends.com

BST
BioScience Trends

JOURNAL PUBLISHING AGREEMENT (JPA)

Manuscript No.:

Title:

Corresponding Author:

The International Advancement Center for Medicine & Health Research Co., Ltd. (IACMHR Co., Ltd.) is pleased to accept the above article for publication in BioScience Trends. The International Research and Cooperation Association for Bio & Socio-Sciences Advancement (IRCA-BSSA) reserves all rights to the published article. Your written acceptance of this JOURNAL PUBLISHING AGREEMENT is required before the article can be published. Please read this form carefully and sign it if you agree to its terms. The signed JOURNAL PUBLISHING AGREEMENT should be sent to the BioScience Trends office (Pearl City Koishikawa 603, 2-4-5 Kasuga, Bunkyo-ku, Tokyo 112-0003, Japan; E-mail: **office@biosciencetrends.com**; Tel: **+81-3-5840-8764**; Fax: **+81-3-5840-8765**).

1. Authorship Criteria

As the corresponding author, I certify on behalf of all of the authors that:
1) The article is an original work and does not involve fraud, fabrication, or plagiarism.
2) The article has not been published previously and is not currently under consideration for publication elsewhere. If accepted by BioScience Trends, the article will not be submitted for publication to any other journal.
3) The article contains no libelous or other unlawful statements and does not contain any materials that infringes upon individual privacy or proprietary rights or any statutory copyright.
4) I have obtained written permission from copyright owners for any excerpts from copyrighted works that are included and have credited the sources in my article.
5) All authors have made significant contributions to the study including the conception and design of this work, the analysis of the data, and the writing of the manuscript.
6) All authors have reviewed this manuscript and take responsibility for its content and approve its publication.
7) I have informed all of the authors of the terms of this publishing agreement and I am signing on their behalf as their agent.

2. Copyright Transfer Agreement

I hereby assign and transfer to IACMHR Co., Ltd. all exclusive rights of copyright ownership to the above work in the journal BioScience Trends, including but not limited to the right 1) to publish, republish, derivate, distribute, transmit, sell, and otherwise use the work and other related material worldwide, in whole or in part, in all languages, in electronic, printed, or any other forms of media now known or hereafter developed and the right 2) to authorize or license third parties to do any of the above.

I understand that these exclusive rights will become the property of IACMHR Co., Ltd., from the date the article is accepted for publication in the journal BioScience Trends. I also understand that IACMHR Co., Ltd. as a copyright owner has sole authority to license and permit reproductions of the article.

I understand that except for copyright, other proprietary rights related to the Work (*e.g.* patent or other rights to any process or procedure) shall be retained by the authors. To reproduce any text, figures, tables, or illustrations from this Work in future works of their own, the authors must obtain written permission from IACMHR Co., Ltd.; such permission cannot be unreasonably withheld by IACMHR Co., Ltd.

3. Conflict of Interest Disclosure

I confirm that all funding sources supporting the work and all institutions or people who contributed to the work but who do not meet the criteria for authors are acknowledged. I also confirm that all commercial affiliations, stock ownership, equity interests, or patent-licensing arrangements that could be considered to pose a financial conflict of interest in connection with the article have been disclosed.

Corresponding Author's Name (Signature):

Date: